

University of Windsor

## Scholarship at UWindor

---

Electronic Theses and Dissertations

Theses, Dissertations, and Major Papers

---

2006

### Petrologic and geochemical attributes of dolomite recrystallization: An example from the Mississippian Pekisko Formation, west-central Alberta.

JoAnn Adam  
*University of Windsor*

Follow this and additional works at: <https://scholar.uwindsor.ca/etd>

---

#### Recommended Citation

Adam, JoAnn, "Petrologic and geochemical attributes of dolomite recrystallization: An example from the Mississippian Pekisko Formation, west-central Alberta." (2006). *Electronic Theses and Dissertations*. 3075.

<https://scholar.uwindsor.ca/etd/3075>

This online database contains the full-text of PhD dissertations and Masters' theses of University of Windsor students from 1954 forward. These documents are made available for personal study and research purposes only, in accordance with the Canadian Copyright Act and the Creative Commons license—CC BY-NC-ND (Attribution, Non-Commercial, No Derivative Works). Under this license, works must always be attributed to the copyright holder (original author), cannot be used for any commercial purposes, and may not be altered. Any other use would require the permission of the copyright holder. Students may inquire about withdrawing their dissertation and/or thesis from this database. For additional inquiries, please contact the repository administrator via email ([scholarship@uwindsor.ca](mailto:scholarship@uwindsor.ca)) or by telephone at 519-253-3000ext. 3208.

**Petrologic and geochemical attributes of dolomite  
recrystallization: an example from the Mississippian Pekisko  
Formation, west-central Alberta**

by

JoAnn Adam

A Thesis  
Submitted to the Faculty of Graduate Studies and Research  
through the Department of Earth Sciences  
in Partial Fulfillment of the Requirements for  
the Degree of Master of Science at the  
University of Windsor.

Windsor, Ontario, Canada

2005

© 2005 JoAnn Adam



Library and  
Archives Canada

Bibliothèque et  
Archives Canada

Published Heritage  
Branch

Direction du  
Patrimoine de l'édition

395 Wellington Street  
Ottawa ON K1A 0N4  
Canada

395, rue Wellington  
Ottawa ON K1A 0N4  
Canada

*Your file* *Votre référence*  
*ISBN: 978-0-494-17060-1*  
*Our file* *Notre référence*  
*ISBN: 978-0-494-17060-1*

**NOTICE:**

The author has granted a non-exclusive license allowing Library and Archives Canada to reproduce, publish, archive, preserve, conserve, communicate to the public by telecommunication or on the Internet, loan, distribute and sell theses worldwide, for commercial or non-commercial purposes, in microform, paper, electronic and/or any other formats.

The author retains copyright ownership and moral rights in this thesis. Neither the thesis nor substantial extracts from it may be printed or otherwise reproduced without the author's permission.

**AVIS:**

L'auteur a accordé une licence non exclusive permettant à la Bibliothèque et Archives Canada de reproduire, publier, archiver, sauvegarder, conserver, transmettre au public par télécommunication ou par l'Internet, prêter, distribuer et vendre des thèses partout dans le monde, à des fins commerciales ou autres, sur support microforme, papier, électronique et/ou autres formats.

L'auteur conserve la propriété du droit d'auteur et des droits moraux qui protègent cette thèse. Ni la thèse ni des extraits substantiels de celle-ci ne doivent être imprimés ou autrement reproduits sans son autorisation.

---

In compliance with the Canadian Privacy Act some supporting forms may have been removed from this thesis.

Conformément à la loi canadienne sur la protection de la vie privée, quelques formulaires secondaires ont été enlevés de cette thèse.

While these forms may be included in the document page count, their removal does not represent any loss of content from the thesis.

Bien que ces formulaires aient inclus dans la pagination, il n'y aura aucun contenu manquant.

  
**Canada**

**ABSTRACT**

Carbonates of the Pekisko Formation are important reservoir rocks in west-central Alberta, especially in fields along the Pekisko subcrop edge. They represent a transgressive-regressive carbonate ramp sequence comprised of upward shallowing facies, which subsequently underwent extreme erosion leading to the development of karst topography. Lithofacies include grainstones, wackestones/packstones, mudstones, intraclast breccia mudstones and dolostones. Several generations of calcite cementation and dolomitization are the result of very complex diagenetic changes. Calcite cements include: isopachous, drusy mosaic, pendant/meniscus, blocky, syntaxial, fibrous and equant/prismatic. Five dolomite types have been identified: pervasive, dissolution seam-associated, planar void-filling, selective and saddle. Consequently, diagenetic alteration mainly by dolomitization has affected most of the carbonate facies.

Pervasive dolomite is the most important and abundant type of dolomite in the Pekisko carbonates. It replaced early calcite phases prior to early chemical compaction and forms the dolostone units. These units contain the best reservoir porosities in the formation. Geochemical analyses suggest a formation from mixed meteoric-marine fluids. Dissolution seam-associated dolomite is a relatively minor phase occurring exclusively in grainstones during early chemical compaction in association with dissolution seams. Void-filling dolomite occurs as relatively clear euhedral cement occluding vugs and molds within dolostone intervals in minor amounts. During intermediate burial, selective dolomitization of several grains, matrix and cement occurred in grainstones and dolostones. The covariant depletion trend revealed by stable isotope values marks a departure from the postulated Mississippian dolomite and represents precipitation from a mixed fluid and/or recrystallization. Saddle dolomite was the last phase to precipitate during deeper burial. Petrographically, it is associated with late chemical compaction and secondary anhydrite and it is isotopically much more depleted than other dolomite phases which implies precipitation from more saline fluids at elevated temperatures. Recrystallization and neomorphism has affected all phases in the Pekisko carbonates. Evidence for recrystallization in pervasive dolomite includes: increasing crystal size, anhedral crystals, zonations with etched interfaces, dedolomitization, depletion in both stable isotopes and radiogenic strontium isotope ratios.

I'd like to dedicate this thesis to Scott who encouraged and pushed me more than anyone throughout the process.

## **ACKNOWLEDGEMENTS**

I would first like to thank my supervisor Dr. I. S. Al-Aasm for his guidance throughout the course of my studies.

Dr. Jeff Packard is thanked for the time involved in collecting well data and for giving me a refresher on how to proceed with my core sampling and analysis. I thank Melissa Price for all of her help with the stable isotopes and several other miscellaneous things. My gratitude goes out to Daniel Rivas for answering my millions of questions during my first year. I really appreciated the good conversations, companionship and encouragement from Samantha Raymus. I would also like to thank Denis Tetreault for all of his advice and good conversations. Sharon Horne is also thanked for answering my many questions.

I'd also like to thank my mom, my dad and my sister for encouraging and listening to me when times were a little tough. Lastly, I thank Scott Bland for making me laugh when I had a bad day, encouraging me when I just wanted to stop, pushing me to do my best and just for being there for me.

## TABLE OF CONTENTS

<b>ABSTRACT .....</b>	<b>iii</b>
<b>DEDICATION .....</b>	<b>iv</b>
<b>ACKNOWLEDGEMENTS .....</b>	<b>v</b>
<b>LIST OF FIGURES .....</b>	<b>ix</b>
<b>LIST OF PLATES .....</b>	<b>x</b>
<b>CHAPTER I: INTRODUCTION .....</b>	<b>1</b>
1.1 Purpose of Study .....	1
1.2 Previous Studies .....	3
1.3 Methods of Study .....	5
<b>CHAPTER II: REGIONAL FRAMEWORK.....</b>	<b>8</b>
2.1 Regional Geology.....	8
2.2 Stratigraphy .....	8
2.2.1 Banff Formation .....	10
2.2.2 Pekisko Formation .....	10
2.2.3 Shunda Formation .....	11
2.2.4 Turner Valley Formation .....	11
2.3 Structural History.....	11
<b>CHAPTER III: SEDIMENTOLOGY OF THE PEKISKO FORMATION.....</b>	<b>15</b>
3.1 Introduction.....	15
3.2 Facies.....	15
3.2.1 Grainstone facies.....	17
3.2.1.1 <i>Crinoidal grainstones</i> .....	17
3.2.1.2 <i>Oolitic/Bioclastic grainstones</i> .....	18
3.2.1.3 <i>Peloidal grainstones</i> .....	18
3.2.2 Wackestone and packstone facies.....	19
3.2.3 Mudstone facies.....	19
3.2.4 Intraclast breccia mudstone facies .....	19
3.2.5 Dolostone facies .....	20
3.3 Depositional Model.....	23
<b>CHAPTER IV: DIAGENESIS OF THE PEKISKO FORMATION.....</b>	<b>27</b>
4.1 Introduction.....	27
4.2 Micritization .....	27
4.3 Compaction .....	28
4.3.1 Mechanical compaction .....	28
4.3.2 Chemical compaction.....	29
4.4 Calcite cementation.....	32
4.4.1 Isopachous rinds.....	32
4.4.2 Drusy mosaic calcite.....	35
4.4.3 Pendant/Meniscus calcite .....	35
4.4.4 Blocky calcite .....	35
4.4.5 Syntaxial calcite .....	35
4.4.6 Fibrous calcite.....	36

4.4.7 Bladed prismatic to equant calcite.....	36
4.5 Neomorphism and neomorphic spar.....	36
4.6 Dolomitization.....	37
4.6.1 Pervasive dolomite.....	37
4.6.2 Dissolution seam-associated dolomite.....	38
4.6.3 Planar void-filling dolomite.....	38
4.6.4 Selective dolomite.....	38
4.6.5 Saddle dolomite.....	41
4.7 Silicification.....	41
4.8 Sulphide mineralization.....	42
4.9 Dissolution.....	42
4.10 Pyrobitumen.....	45
4.11 Fracturing.....	45
<b>CHAPTER V: PALEOEXPOSURE EVIDENCE IN THE PEKISKO FORMATION .....</b>	<b>46</b>
5.1 Introduction.....	46
5.2 Evidence of paleoexposure.....	47
<b>CHAPTER VI: GEOCHEMISTRY OF THE PEKISKO FORMATION.....</b>	<b>51</b>
6.1 Introduction.....	51
6.2 Isotopes.....	51
6.2.1 Stable isotope theory.....	51
6.2.2 Stable isotopes in carbonate diagenesis.....	52
6.2.3 Carbon and oxygen isotope results.....	53
6.2.3.1 Calcite components.....	53
6.2.3.2 Dolomite.....	54
6.2.4 Strontium isotopes.....	55
6.2.5 Strontium isotope results.....	57
6.3 Elemental analysis.....	59
6.3.1 Elemental theory.....	59
6.3.2 Calcium and Magnesium: dolomite stoichiometry.....	60
6.3.3 Iron and Manganese.....	61
6.3.3.1 Calcite.....	62
6.3.3.2 Dolomite.....	62
6.3.4 Strontium.....	62
6.3.4.1 Calcite.....	62
6.3.4.2 Dolomite.....	63
6.4 Fluid inclusions.....	63
6.4.1 Fluid inclusion theory.....	63
6.4.2 Fluid inclusion results.....	64
<b>CHAPTER VII: POROSITY OF THE PEKISKO FORMATION.....</b>	<b>65</b>
7.1 Introduction.....	65
7.2 Primary porosity.....	66
7.3 Secondary porosity.....	66
7.4 Relationship between porosity and permeability.....	70
7.5 Diagenetic controls on porosity evolution.....	71
<b>CHAPTER VIII: DISCUSSION AND INTERPRETATION OF DIAGENESIS .....</b>	<b>75</b>
8.1 Introduction.....	75
8.2 Micritization.....	75
8.3 Calcite cementation.....	75
8.3.1 Isopachous rinds.....	77
8.3.2 Drusy mosaic calcite.....	77
8.3.3 Blocky calcite.....	78
8.3.4 Syntaxial calcite.....	80



8.3.5 Fibrous calcite .....	81
8.3.6 Bladed prismatic to equant calcite .....	84
8.4 Neomorphism and neomorphic spar .....	84
8.5 Silicification.....	85
8.6 Sulphide mineralization .....	87
8.7 Dissolution .....	87
8.8 Lithofacies and dolomitization .....	88
8.9 Mechanisms of Dolomitization .....	89
8.9.1 Pervasive dolomite.....	89
8.9.2 Dissolution seam-associated dolomite .....	96
8.9.3 Void-filling dolomite.....	96
8.9.4 Selective dolomite.....	97
8.9.5 Saddle dolomite .....	97
8.10 Dolomite recrystallization in the Pekisko Formation .....	98
8.11 Diagenetic Model.....	101
<b>CHAPTER IV: CONCLUSIONS .....</b>	<b>108</b>
<b>REFERENCES .....</b>	<b>111</b>
<b>APPENDIX I: WELL LOCATIONS.....</b>	<b>119</b>
<b>APPENDIX II: THIN SECTION DESCRIPTIONS .....</b>	<b>120</b>
<b>APPENDIX III: GEOCHEMICAL RESULTS .....</b>	<b>145</b>
<b>VITA AUCTORIS.....</b>	<b>149</b>

## LIST OF FIGURES

<b>Figure</b>		
<b>1.1</b>	Location map of study area	2
<b>2.1</b>	Stratigraphy of the Rundle Group	9
<b>2.2</b>	Structural elements of Alberta in the Carboniferous	14
<b>3.1</b>	Cross-section A' – A''	16
<b>3.2</b>	Carbonate ramp depositional model for the Pekisko Formation	25
<b>3.3</b>	General lithology of the Pekisko Formation	26
<b>6.1A</b>	Carbon and oxygen stable isotopic compositions for calcite	56
<b>6.1B</b>	Carbon and oxygen stable isotopic compositions for dolomite phases	56
<b>6.2</b>	$^{87}\text{Sr}/^{86}\text{Sr}$ versus oxygen isotope compositions	58
<b>7.1A</b>	Porosity versus permeability plot for the various porosity types	72
<b>7.1B</b>	Porosity versus percentage of dolomite for the same porosity types	72
<b>8.1</b>	Paragenetic sequence of events for carbonates	76
<b>8.2</b>	Fluid oxygen isotope composition versus formation temperature	82
<b>8.3A</b>	Sr versus Fe concentrations for calcite components	83
<b>8.3B</b>	1000 Sr/Ca versus Mn concentrations for dolomite and calcite phases	83
<b>8.4A</b>	Stable carbon and oxygen isotope distribution for pervasive dolomites	94
<b>8.4B</b>	$^{87}\text{Sr}/^{86}\text{Sr}$ versus oxygen isotope compositions of calcite and dolomite	94
<b>8.5A</b>	Sr versus Mn concentrations for fine and coarse pervasive dolomites	95
<b>8.5B</b>	Sr versus Fe concentrations for fine and coarse pervasive dolomites	95

## LIST OF PLATES

### Plates

<b>A</b>	Lithofacies	21
<b>B</b>	Mechanical and chemical compaction	30
<b>C</b>	Calcite phases	33
<b>D</b>	Dolomite phases	39
<b>E</b>	Silicification and pyritization	43
<b>F</b>	Karstification	49
<b>G</b>	Porosity	68
<b>H</b>	SEM porosity	73
<b>I</b>	Dolomite recrystallization	103
<b>J</b>	SEM dolomite recrystallization	105

## CHAPTER I INTRODUCTION

### 1.1 Purpose of Study

Mississippian carbonates of the Pekisko Formation are important reservoir rocks in west-central Alberta, especially in fields along the Pekisko subcrop edge. Collectively they yield approximately 20.8% of the basin's marketable gas reserves and 14.4% of recoverable oil reserves (Podruski et al., 1988). Diagenetic alteration mainly through dolomitization has affected most of the carbonate facies.

The purpose of this study is to examine samples collected from cores of the Pekisko Formation between townships 36 to 60 and ranges 5w5 to 20w5 (Figure 1.1) using petrographic and geochemical techniques. These will help to reconstruct the formation and recrystallization history of the dolomites as well as the porosity evolution of the Pekisko Formation over a vast area. The primary objectives of this study are as follows:

- (1) To ascertain if within the pervasive dolomites, there is a change in geochemical, petrographic or crystallographic characteristics as one moves away from the subcrop edge. If there is, can the variation be explained by flow of diagenetic fluids regulated by the unconformity surface?
- (2) To deduce whether or not the grainstone and mudstone facies were dolomitized by the same brine during the same flow event and to determine the occurrence, distribution and timing of different dolomite phases and other diagenetic events.
- (3) To determine the influence the original substrate has had on the present dolomite fabric (i.e. is the dolomite selective?).
- (4) To identify the relationship between dolomitization and porosity development.
- (5) To establish a geochemical model for the Pekisko dolomites and diagenetic fluids.

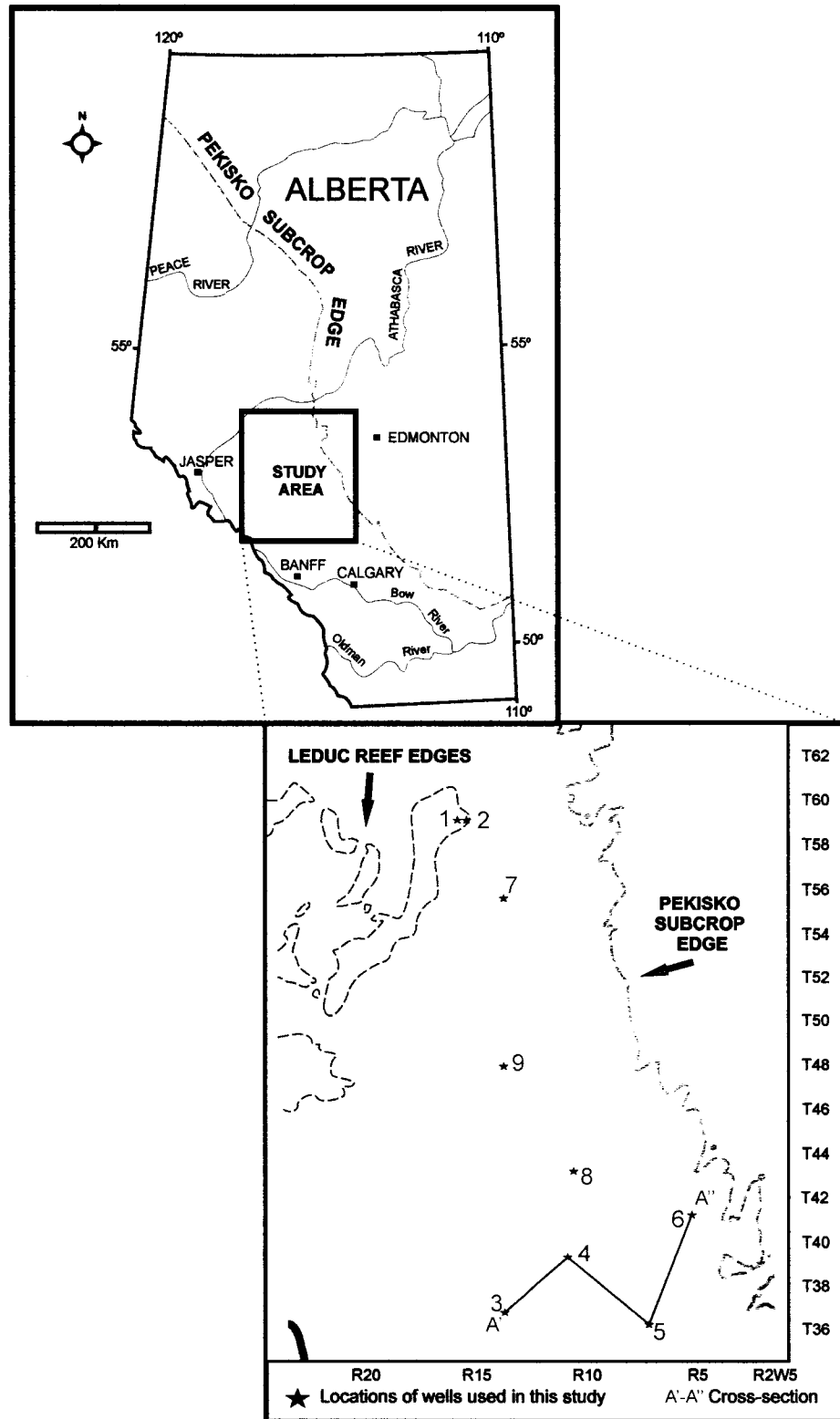


**Figure 1.1** Location map of study area showing the subcrop edge. Wells studied are numbered 1 through 9 along the subcrop edge (modified from Speranza 1984).

## 1.2 Previous Studies

There have been several published papers on the Mississippian of the Western Canada Sedimentary Basin (WCSB) pertaining to the Rundle group. Warren (1927) was the first to describe the Rundle limestone and classified it as a formation. Later, Douglas (1953) established the Rundle Formation as a group and named the formations within it, namely the Shunda, Pekisko and Banff. In the late 1950's and 1960's, researchers began to publish detailed descriptions of the stratigraphy and sedimentology of the Pekisko Formation. Illing (1959) recognized distinct oscillations of sedimentary environments within the Pekisko and Middleton (1963) described sedimentary facies variations and recognized channels filled with carbonate sand. Macqueen and Bamber (1967) correlated the Pekisko, Shunda and Turner Valley formations in the east to the Livingstone formation to the west. Structural elements have been studied by Procter and Macauley (1968) and O'Connell (1990). However the reader is referred to Richards et al. (1994) who has supplied the best and most detailed reconnaissance of the Mississippian's structural history.

In the early 1980's there was a resurgence of studies on the Mississippian succession of the WCSB. Bamber et al. (1980, 1981) described facies relationships at the Mississippian carbonate platform margin and elaborated on the stratigraphy and sedimentology at Moose Mountain in Alberta. Just recently, a few studies have looked at the reservoir properties of the Pekisko and the surrounding lithofacies. These have been discussed in detail by Hopkins (1997) for the Medicine River field, as well as porosity and permeability studies related to reservoir quality. He proposed three reservoir dolomite lithofacies: medium and coarse-crystalline dolostone, dolomudstone and the undolomitized host limestone. Furthermore, two dolomitizing phases affecting the rocks are proposed, an early and a late dolomite. Later, Hopkins (1999), again studying the Medicine River field, described porous facies and evaluated the role paleokarst had in enhancing porosity. He described a fourth facies, fenestral mudstone, present at the very top of the sequence. A third very recent publication by Hopkins (2004) focused on the Medicine River Pekisko pool E specifically. In this study, Hopkins evaluated the geometry of the dolomite body within this pool and revealed that it is constrained within the lower-porosity

limestones. Unlike his previous studies he provided some geochemical results. He suggested that the precipitation of most of the dolomite originated from early Carboniferous seawater or modified seawater. Other works include that of Hrabí and Lawton (2001) and Williams (2005). Hrabí and Lawton (2001) evaluated Pekisko porosity through seismic modeling. They concluded that the amplitude anomaly on the seismic data might be from the development of porosity. Williams (2005) analyzed the paleokarst development in the Pekisko (specifically in the Gilby-Wilson Creek-Minnehik area) and its impact on the reservoirs we have today and suggested multiple karsting events. The first occurred from the Pennsylvanian to earliest Jurassic, when a warm humid climate promoted rapid and deep karsting. The second event occurred from the late Jurassic to early Cretaceous and represented the most extensive karsting. Recently Al-Aasm (2000) looked at the chemistry and isotopic signatures of Mississippian dolomites in different formations throughout the Western Canada Sedimentary Basin. Two types of dolomite were observed: an early microcrystalline dolomite and a pervasive mesodolomite. For the Pekisko Formation at Sylvan Lake, mean isotopic values were:  $\delta^{18}\text{O} = -2.08\text{‰}$  and  $\delta^{13}\text{C} = +2.67\text{‰}$  for the microcrystalline dolomite and  $\delta^{18}\text{O} = -1.92\text{‰}$  and  $\delta^{13}\text{C} = +2.34\text{‰}$  for the pervasive mesodolomite. The microcrystalline dolomite and pervasive mesodolomite are stoichiometric and in the Sylvan lake area have low strontium values. Generally higher Mn concentrations are observed in mesodolomites than in microcrystalline dolomites. Al-Aasm (2000) concluded that the recrystallization of dolomite began early and continued during burial. Furthermore, similar carbonates with similar depositional environments in the basin yielded very different results reflecting the changes in tectonics, fluids and burial. For the Pekisko Formation, microcrystalline dolomite recrystallized in a meteoric water-dominated system. On the other hand, mesodolomites were formed during deeper burial from basinal fluids.

Within the last decade or so, there have been several theses focused on different attributes of the Pekisko Formation. The thesis by Speranza (1984) focused on the sedimentation and diagenesis of the Pekisko in Canyon Creek, Alberta. He investigated the petrography, oxygen and carbon isotopic signatures and total organic carbon of limestones and dolomites. Speranza suggested that there was a heavy to light isotope evolution from Moose

Mountain to Twining Field (SW to NE) supported by stratigraphic and petrologic textural evidence. Kirkby (1994) compared and contrasted the reservoir development and growth of Waulsortian mounds of the Pekisko Formation of west-central Alberta with the Lake Valley Formation of New Mexico. The two formations have similar growth patterns that have undergone different diagenesis. More recently Reid (1998) looked at the sedimentation, diagenesis and paleokarst of the Pekisko Formation in the Twining Field. In this area two dolomite types are described as a more abundant scattered dolomite within mudstones and pervasive dolomite in wackestones. Also observed are five periods of erosion whereby karsting occurred due to the pre-Cretaceous exposure period, based on the petrography of cavity fill. Kreitner (1999) studied the Pekisko Formation in the Gilby, Wilson Creek and Minnehik-Buck Lake oil fields focusing on the facies, diagenesis and depositional environments of the area. Three distinct lithofacies based on fossil content were as follows: bryozoan-pelmatozoan, peloidal-skeletal and ooid-skeletal. These were interpreted to be deposited on a carbonate platform during two transgressive- regressive cycles. Diagenetic processes include micritization, compaction, cementation, dolomitization, dissolution and neomorphism. Most recently Fattahi (2001) studied the sedimentology and paragenetic evolution of the Pekisko Formation in the Minnehik-Buck lake field using various methods such as oxygen and carbon stable isotopes, SEM, fluid inclusion analysis, X-ray diffraction and porosity/permeability studies.

### **1. 3 Methods of Study**

In August of 2003, seven cored wells from the Pekisko Formation of west-central Alberta were described and sampled at the Energy and Utilities Board (EUB) core research centre in Calgary, Alberta. Later, in January of 2005, two more wells were described and sampled to attain a greater coverage of the study area. In order to satisfy the objectives of this study, it was important to select wells that would be representative of a large area progressively away from the subcrop edge. Since several studies have already been conducted along the zero edge, only one well at the subcrop edge (outside of these previously studied fields) was selected for this study. The results attained by these previous studies will serve as useful references to support



conclusions reached by this study. Wells which contained the greatest dolomitized thicknesses were preferentially chosen. Several wells were previously subjected to whole rock permeability, porosity and grain density measurements by the IHS Energy Group. As this data has important implications for this study, wells were also selected based on the availability of this information. Samples and photographs were taken from all nine of the selected wells (3-28-59-15w5, 10-23-59-15W5, 12-11-37-14W5, 8-27-39-11W5, 12-28-36-7W5, 16-27-41-5W5, 10-04-56-13w5, 9-29-43-10w5 and 16-18-48-13w5). The rocks were sampled along lithofacies contacts, within representative sections and in zones containing distinct diagenetic and depositional features. There are a total of 89 samples of which 84 were thin sectioned and stained with a mixture of Alizarin Red-S and Potassium Ferricyanide according to the procedure of Dickson (1965). This procedure provides distinctions between ferroan and non-ferroan calcite and dolomite, through the following color variations: ferroan dolomite, blue; non-ferroan dolomite, no colour; ferroan calcite, purple and non-ferroan calcite, red to pink. Thin sections were examined under a standard petrographic microscope to observe textural relationships and diagenetic fabrics. Fluorescence characteristics of samples were examined using a Nikon EPI Fluorescence attachment connected to a petrographic microscope. This method was used to show zonations within dolomite and calcite crystals through varying degrees of brightness, to distinguish dolomite from calcite portions and reveal textural relationships and precursor fabrics not seen under plane polarized light. Cathodoluminescence microscopy (CL) was carried out using a Technosyn cold cathodoluminescence stage with a 12-18 kV beam and a gun current intensity of 400-430 $\mu$ A.

Oxygen and carbon isotope extractions were performed at the University of Windsor for calcite and dolomite using the chemical separation method of Al-Aasm et al. (1990). Powdered samples of calcite and dolomite were obtained using a microscope mounted drill assembly. The samples were reacted in vacuo with 100% pure phosphoric acid for at least 4 hours at 50°C for dolomite and 25°C for calcite. The extracted CO<sub>2</sub> gas was analyzed for isotopic ratios on a Thermo Finnigan Delta Plus Ion Ratio Mass Spectrometer (IRMS) at the University of Windsor. The values of carbon and oxygen isotopes are reported in per mil (‰) relative to the VPDB (Vienna PeeDee Belemnite) standard. Precision was 0.02 ‰ for  $\delta^{13}\text{C}$  and 0.04 ‰ for  $\delta^{18}\text{O}$ .

Strontium isotopes were measured for 15 dolomite and calcite samples on a Micromass Sector 54 Thermal Ionization Mass Spectrometer at the University of Alberta in Edmonton. The strontium is measured by Faraday collectors in multi-dynamic mode using a single rhenium filament and a tantalum activator. The standard used was the NIST Standard Reference Material (SRM) 987 Strontium isotope standard. All  $^{87}\text{Sr}/^{86}\text{Sr}$  ratios are presented relative to a value of 0.710245 for this accepted standard. The long-term measured value for SRM987 is 0.71026 +/- 0.000015 (1 SD).

Major, minor and trace element analyses were performed on 28 dolomite and calcite samples by digesting them with 5%  $\text{HNO}_3$  then measuring the solutions using a Thermo Jarrell Ash Inductively Coupled Plasma Optical Emission Spectrophotometer (ICP-OES) at the Great Lakes Institute of Environmental Research (GLIER) in Windsor. Liquid samples are introduced into the ICP-OES via a Meinhard concentric glass nebulizer and a cyclonic spray chamber. The standard used was an 88b dolomitic limestone. Method detection limits were 547 ppm for Ca, 74.13 ppm for Mg, 4.42 ppm for Fe, 0.6162 ppm for Mn, 16.27 ppm for K and 1.715 ppm for Sr.

Scanning electron microscope (SEM) analysis consists of the nondestructive magnification of surfaces (50X up to 100,00X or more) by bombarding a sample with electrons causing three-dimensional effects by luminescence (Lewis and McConchie, 1994). Four polished slabs were etched with 30% HCl for 10-15 seconds (Jones, 2005), plated with gold and examined under a JEOL JSM-5800 LV scanning electron microscope (SEM) to study fine diagenetic features such as dolomite crystal habits, microstructures, microporosity and recrystallization textures.

## **CHAPTER II REGIONAL FRAMEWORK**

### **2.1 Regional Geology**

The Mississippian succession of the Western Canada Sedimentary Basin forms two major sinuous lithofacies belts deposited on the western margin of the downwarped and downfaulted ancestral North American plate (Richards et al., 1994). The eastern facies are represented by thick platform carbonates and thin basinal shales make up the western facies. These facies belts extend from southern Alberta and British Columbia to the northern Yukon Territory and cut obliquely across the northwest direction of the eastern cordillera (Bamber et al., 1980). The original depositional slope of the carbonate platform was very low and the shallow water deposits grade westward into deep basinal rocks (Bamber et al., 1980). Overall the Mississippian succession represents a second-order regression. However, in southwestern Alberta the Mississippian interval records a series of stacked smaller-scale transgressive and regressive carbonate cycles. Stratigraphic relationships for west-central Alberta are summarized in Figure 2.1.

### **2.2 Stratigraphy**

The Mississippian consists mainly of basinal shales, siltstones, spiculites, radiolarian cherts and argillaceous carbonates of the Exshaw and Banff formations unconformably overlain by carbonates of the Rundle Group with minor amounts of terrigenous clastics (Bamber et al., 1980). The Mississippian succession has been progressively removed further north- and eastward due to post-Mississippian erosion. The resulting subcrop edges are overlain by Jurassic and Cretaceous siliciclastics (Hopkins, 1999). As a result most of the Mississippian oil and gas reserves in Alberta are in subcrop or erosional traps (Procter and Macauley, 1968). The Rundle Group consists of three formations; the Pekisko, the Shunda and the Turner Valley formations deposited in a ramp setting. The Rundle Group is an upward shallowing facies indicative

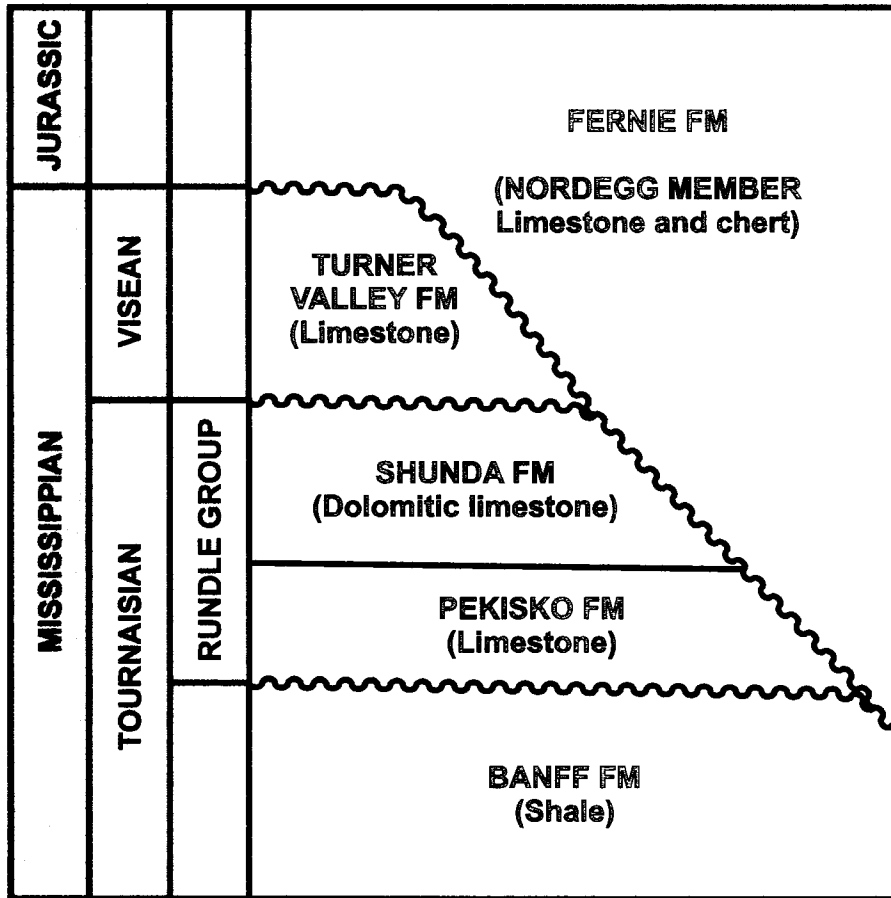


**Figure 2.1** Stratigraphy of the Rundle Group in West-Central Alberta, Canada (modified from Richards et al. 1994).

of major regression at that time (Bamber et al., 1980). Laterally westward, the Rundle Group grades into the Livingstone Formation. The eastern succession of the Rundle Group consists of peritidal facies whereby western facies are open marine (Macqueen and Bamber, 1967). Peritidal facies include mudstones, wackestones and packstones made up of non-skeletal grains such as peloids, intraclasts and ooids. Open marine facies include, echinoderm and bryozoan grainstones to packstones. The Pekisko/Shunda sequence formed during the latest middle Tournaisian transgression and represents a third order transgressive/regressive cycle initiated by eustatic and tectonic sea level fluctuations (Richards et al., 1994). Overall the succession is comprised of upward-shallowing facies, which was subsequently eroded during several stages leading to the development of karst topography. Approximately 50 km southwest of Calgary, the Mississippian succession including the Rundle Group is well exposed. No Mississippian strata beyond the Rundle are exposed at this location; instead they are disconformably overlain by the Jurassic Fernis Formation (Bamber et al., 1981).

### **2.2.1 Banff Formation**

The Banff Formation is separated from the Pekisko Formation by an erosional transgressive unconformity surface (Bamber et al., 1981). The Banff Formation is a shallowing up sequence of argillaceous shales, laminites and silty dolostones deposited in prograding ramp to basin settings (Beauchamp et al., 1986). Along the subcrop edge the clastics of the Cretaceous Nordegg Formation directly overlie the Banff Formation. Here the Banff Formation indicates deposition within transitional basinal to shelf environments (Bamber et al., 1981).

### **2.2.2 Pekisko Formation**

The Pekisko Formation is dominantly thick bedded and cliff forming. It consists of echinoderm grainstones, minor ooid and peloid grainstones, intraclast mudstones and local dolomitization. The Formation is part of the Rundle Group which includes the later Shunda Formation. It is conformably overlain by the laminites and dolomudstones of the Shunda

Formation away from the subcrop edge and unconformably overlain by Jurassic and Cretaceous siliciclastics closer to the erosional edge. According to Bamber et al. (1981) the Pekisko is dominantly echinoderm-bryozoan grainstones with minor amounts of ooid grainstones and local dolomitization. They also point out that in contrast, the Shunda Formation contains lime packstones to mudstone rich in calcispheres with a birds-eye fabric. The Pekisko Formation is comprised of a transgressive-regressive carbonate platform sequence. It extends from the southwestern portion of the district of Mackenzie, southward through Alberta, southeast to British Columbia to Montana and into northern Wyoming. The Pekisko consists predominantly of grainstones deposited as high energy barrier shoals in an open marine environment (Bamber et al., 1981). Thin beds of dolomudstone and chert are fairly common.

### **2.2.3 Shunda Formation**

The recessively weathered Shunda Formation has birds-eye structures and consists mainly of peloidal mudstones to packstones interbedded with dolomudstones deposited in intertidal to hypersaline environments. Dolomitization is more persistent in this formation with interbeds of microcrystalline dolomite.

### **2.2.4 Turner Valley Formation**

The weather resistant Turner Valley Formation is thick bedded and is composed of echinoderm-bryozoan packstones to grainstones with minor amounts of dolomite (Bamber et al., 1980). This Formation is the beginning of the next transgressive/regressive cycle.

## **2.3 Structural History**

During the Carboniferous in the Western Canada Sedimentary Basin, the major tectonic elements were the Prophet Trough, the Peace River Embayment, the cratonic platform, the Williston Basin and the Yukon Fold Belt (Figure 2.2; Richards et al., 1994). The Prophet Trough

developed in the Late Devonian to Early Carboniferous and continued to develop into the Late Cretaceous. The trough contains the thickest Carboniferous sections in western Canada. In southern-most Canada, the Prophet Trough is characterized by a thinner Carboniferous succession. During the Late Famennian to Tournaisian a hinge zone formed between the Prophet Trough and the cratonic platform causing water depths and sedimentation rates to increase basin-ward or westward. Along the western rim of the Prophet Trough, volcanism, granitic plutonism, faulting and folding prevailed during the Late Devonian to Early Carboniferous (Richards et al., 1994).

The Peace River Embayment was a broad, fault controlled opening into the western cratonic platform that opened into the Prophet Trough (Richards et al., 1994). It contained an extensive central graben system and a thick Carboniferous interval. The cratonic platform contained the Williston Basin and many arches. It extended from the northern U.S.A. to the Yukon Fold Belt (Richards et al., 1994). In the Tournaisian, the Williston Basin was part of an extensive embayment connected to the Prophet Trough and the Antler Foreland Basin by a broad seaway. During the Carboniferous the Western Canada Sedimentary Basin was divided into the western assemblage (west of the Rocky Mountains) and an eastern assemblage. The western assemblage was deposited on the western rim of the Prophet Trough (Richards et al., 1994). For this study the eastern assemblage is of greater importance. Contained within this assemblage are the Banff, Rundle and Mattson assemblages consisting of platform to ramp carbonates. Tournaisian to Upper Viséan in age, the Rundle assemblage is comprised of the Rundle Group and the Upper Madison Group. The Rundle Group which contains the Pekisko Formation extends from the district of Mackenzie into south-eastern British Columbia. The Pekisko is present in successions both within and extending north and south of the Peace River Embayment. The Rundle assemblage represents a shallowing upward succession consisting of carbonate platform lithofacies with subordinate carbonate ramp lithofacies and basinal to supratidal siliciclastics (Richards et al., 1994). The most prominent structures in the basin were caused by thrusting and faulting during the Laramide Orogeny, resulting in 200 km of shortening in a west to east progression (McMechan and Thompson, 1989).

There have been three major phases of tectonism observed in the Upper Devonian and Carboniferous. The first phase took place during the latest Devonian and continued into the Late Tournaisian and consisted of block faulting in the Peace River Embayment. This compression-related tectonism caused intraplate shearing that resulted in the development of north-east striking normal faults (Richards et al., 1994). In the Late Tournaisian to Early Visean a transitional period followed that allowed for moderate subsidence rates and a basinward progradation of shallow water carbonates. During the Late Visean to Late Serpukhovian, a second tectonic phase occurred causing extension in the Peace River Embayment and towards the north-west. This extension generated substantial subsidence and block faulting (Richards et al., 1994). The third and final tectonic phase coincided with the collision of Euramerica with Gondwana during the Late Serpukhovian to Permian. At this time, subsidence rates were moderate to low and episodes of broad epirogenic uplift were accompanied by deep subaerial erosion (Richards et al., 1994).



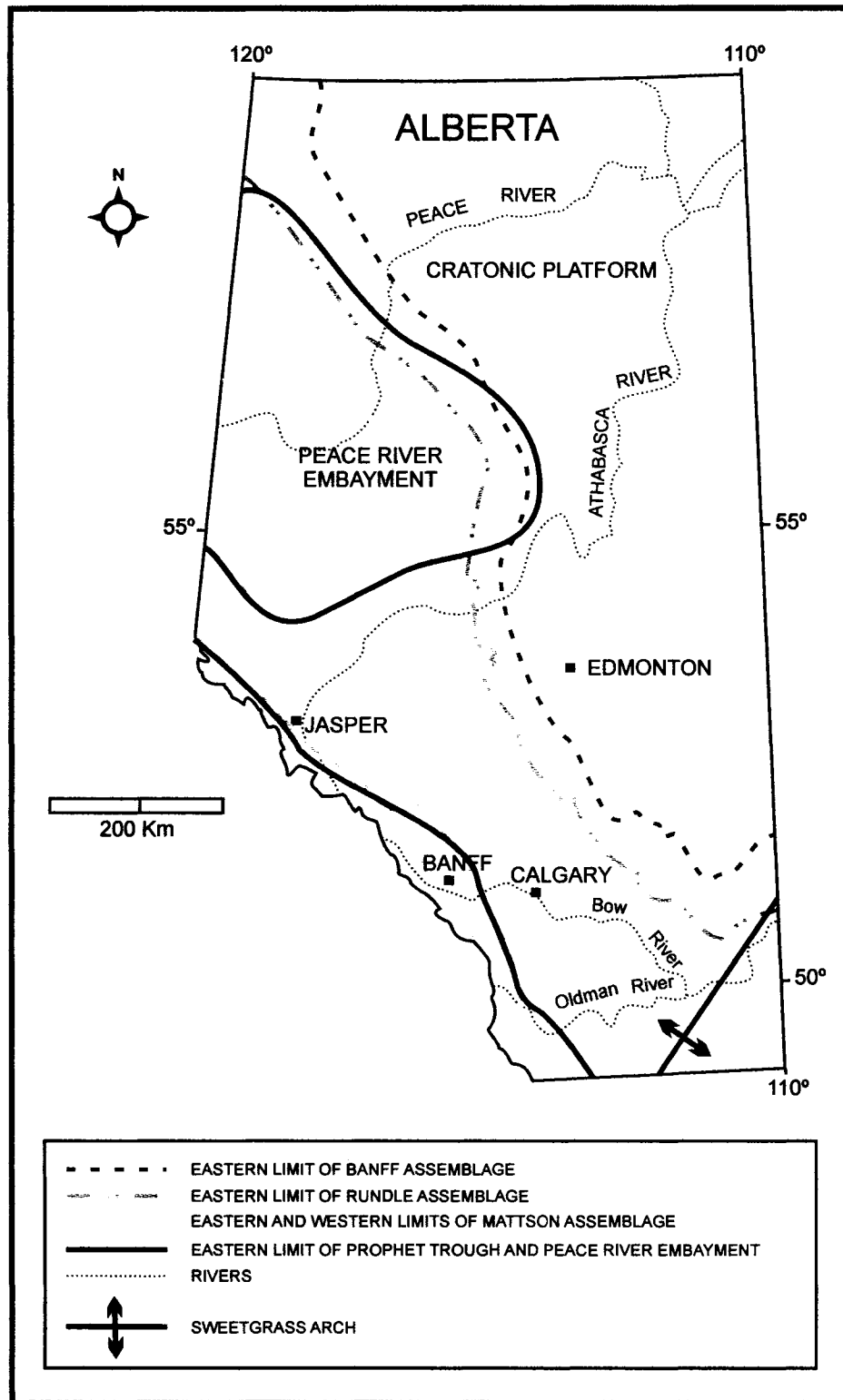


**Figure 2.2** Structural elements of Alberta in the Carboniferous (modified from Richards et al. 1994).

## CHAPTER III

### SEDIMENTOLOGY OF THE PEKISKO FORMATION

#### 3.1 Introduction

The sedimentology of the Pekisko Formation will be described and discussed using the concept of facies analysis. A facies is defined as a body of rock that possesses specific characteristics (Reading, 1986). These characteristics include colour, composition, bedding, texture, fossils and sedimentary structures. The term lithofacies will be used here because emphasis is on the chemical and physical characteristics of the rock. Based on the lateral and vertical distributions of the facies defined, a depositional model will also be established.

#### 3.2 Facies

Pekisko facies were identified by a combination of core examination and petrographic observations. Figure 3.1 shows the distribution of lithofacies with an emphasis on dolostones across wells 3 to 6 away from the subcrop. The location of the cross-section is marked as A' to A" on the location map of Figure 1.1. In this study pervasive dolomitization has in some cases obliterated precursor fabrics; therefore facies were identified primarily from limestones and dolomitic limestones. The limestone classification employed here is that of Dunham (1962) as modified by Embry and Klovan (1972). Lithofacies identified in the Pekisko Formation include: grainstone, wackestone/packstone, mudstone, intraclast breccia mudstone and dolostone. These facies have been further subdivided into subfacies as will be discussed below. Chert nodules and thin beds also occur throughout the different facies in some wells but are a minor constituent.

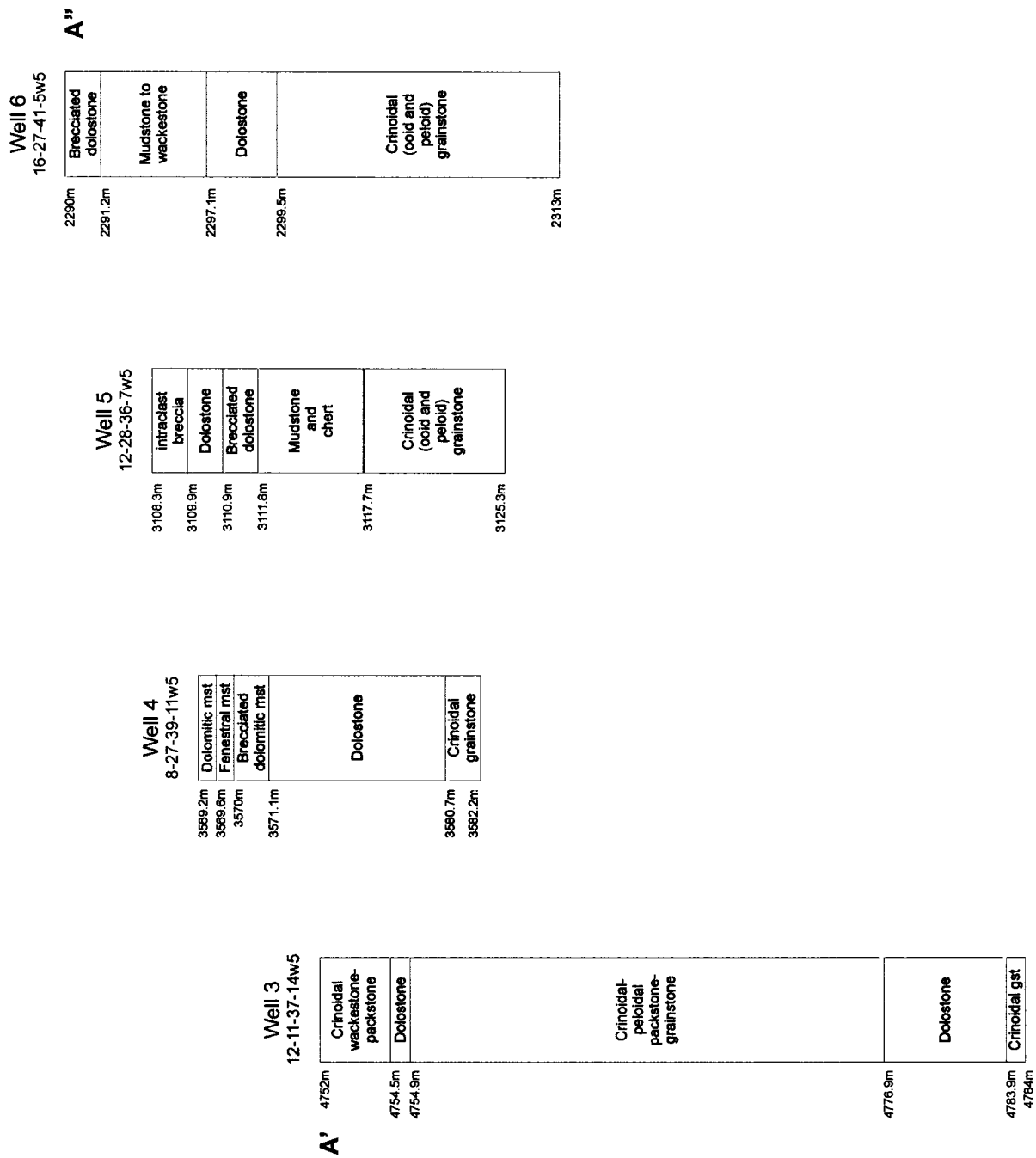


**Figure 3.1** Cross-section A' - A'' from Figure 1.1 showing the distribution of lithofacies in wells progressively away from the subcrop edge. The dotted lines mark the edges of the dolomite body (grey in sections).

### **3.2.1 Grainstone facies**

In hand sample grainstones are light to medium brown or beige to grey in colour. Samples with bedding normally consist of thin and wavy laminations. Skeletal and non-skeletal components present in approximate decreasing order of abundance are: crinoids, brachiopods, peloids, ooids, bryozoans, corals, mollusks, ostracods, gastropods and algae. Several broken bioclast fragments of unidentified species are also present. The grainstones have low porosity since much of the primary interparticle, intraparticle and moldic porosity has been occluded by calcite cement. Most of the grainstones are moderately to highly compacted, suggesting that that they were not well cemented early in the diagenetic history of the Pekisko Formation. However some grainstones, as will be described below, show little to no compaction indicating early cementation prior to diagenesis. Dolomite is present in minor amounts in this facies, usually selectively replacing crinoid centers or the matrix surrounding the grains. The grainstone facies are present in wells 2, 3, 4, 5, 6 and 8. Three grainstone subfacies have been identified in the Pekisko Formation; crinoidal, oolitic/bioclastic and peloidal.

#### **3.2.1.1 Crinoidal grainstones**

Crinoidal grainstones are the most abundant subfacies present in the cores studied (Plate A-6). They are well sorted and contain vertical, horizontal and oblique cross-sections of crinoidal fragments with associated syntaxial overgrowths in many cases. Most fragments are twinned and many are flattened from mechanical compaction. Grain contacts are sutured, concave or pointed. Porosity is very low due to the highly compacted nature of the grains. When porosity is observed, however, it is usually inter- or intraparticle. In this subfacies dolomite is present within the cores of crinoids in very minor amounts in the order of a few percent. Because the interparticle space contained more mud than cement a rigid framework did not develop which allowed for the physical compaction of the sediments.

### **3.2.1.2 Oolitic/Bioclastic grainstones**

Oolitic grainstones are moderately sorted and are a very rare subfacies present in wells 5 and 6 only (Plate A-8). In well 6, this subfacies appears to have been cemented early by marine calcite cements. Grains show some point contacts however most grains are not touching. The nuclei of the ooids vary greatly and include crinoids, brachiopods, fossil fragments and aggregate grains. The concentric rims are in some instances partially dolomitized by microdolomite. Other than a few microstylolites, this facies seems to have been relatively unaltered by compaction. In contrast to this, the ooid grainstone present in well 5 has been greatly altered. Most ooids have been leached out and the remaining molds have been filled with blocky calcite cement. The interparticle calcite matrix on the other hand has been selectively replaced by dolomite.

The bioclastic grainstones are poorly sorted and contain mostly ooids, peloids and crinoids and the fossils listed in crinoidal grainstones in minor amounts. Due to mechanical compaction, crinoids are often flattened and display twinning whereas other allochems are broken. Interpenetrating fabrics are common as in the above subfacies. Some of the peloids are of faecal origin but others represent complete to partial micritization of fossils. This subfacies is almost always oil stained and has a strong odour indicating that the pore system was well interconnected prior to compaction allowing for the infiltration of petroleum rich fluids. This facies was observed in wells throughout the study area.

### **3.2.1.3 Peloidal grainstones**

Peloidal grainstones are well sorted and represent a minor subfacies in the Pekisko Formation occurring only in well 2 (Plate A-3). The interparticle pores are filled with sparry calcite cement. Brachiopods and ostracods are present in minor amounts and in some instances are broken from compactional stress. As discussed in the previous subfacies the peloids are believed to be of faecal origin and some are due to micritization of fossils. In hand sample, peloidal grainstones have wavy laminations to bedding (1-3 cm).

### **3.2.2 Wackestone and packstone facies**

In hand sample this lithofacies is medium to dark grey in colour. It contains the following allochems in approximate decreasing order; brachiopods, ostracods, calcispheres, crinoids and fossil fragments. Most of these fossils are mechanically broken and crinoids display twinning. This facies is relatively non-porous with a dominantly muddy matrix. Pre-existing pores have been filled by calcite cement. These pores may have been the conduits for dolomitizing fluids as there is a presence of scattered dolomite in minor amounts (<15%). The wackestone to packstone facies occur as intervals between dolomitic facies or overlying breccia facies and are observed in minor amounts in wells 2, 3, 6 and 9.

### **3.2.3 Mudstone facies**

The mudstone facies are relatively minor in the Pekisko Formation. This lithofacies is generally light to dark brown in colour and is often associated with light beige to grey chert. The majority of the samples have parallel to wavy laminations or beds. Fossils are generally rare in this facies but where present they include calcispheres and ostracods. There are a few instances of fenestral porosity in wells 2 and 4 that have been occluded by calcite cement. Also present, only in wells 4 and 6, are minor amounts of calcite cement filled nodules. The mudstones of wells 2 and 5 are all associated with chert beds or nodules. The chert intervals reveal an abundance of tiny relict fossils that are too altered to recognize. However in one sample (well 5), chert nodules have preserved the precursor oolitic or crinoidal grainstone facies fabric.

### **3.2.4 Intraclast breccia mudstone facies**

The intraclast breccia facies was found in close association with the mudstone to peloidal packstone to grainstone facies. It is most often composed of angular to subangular clasts suspended in a calcite or partially dolomitized calcite cement matrix. Another common occurrence of authigenic quartz crystals and chalcedony is within the breccias matrix where it is observed

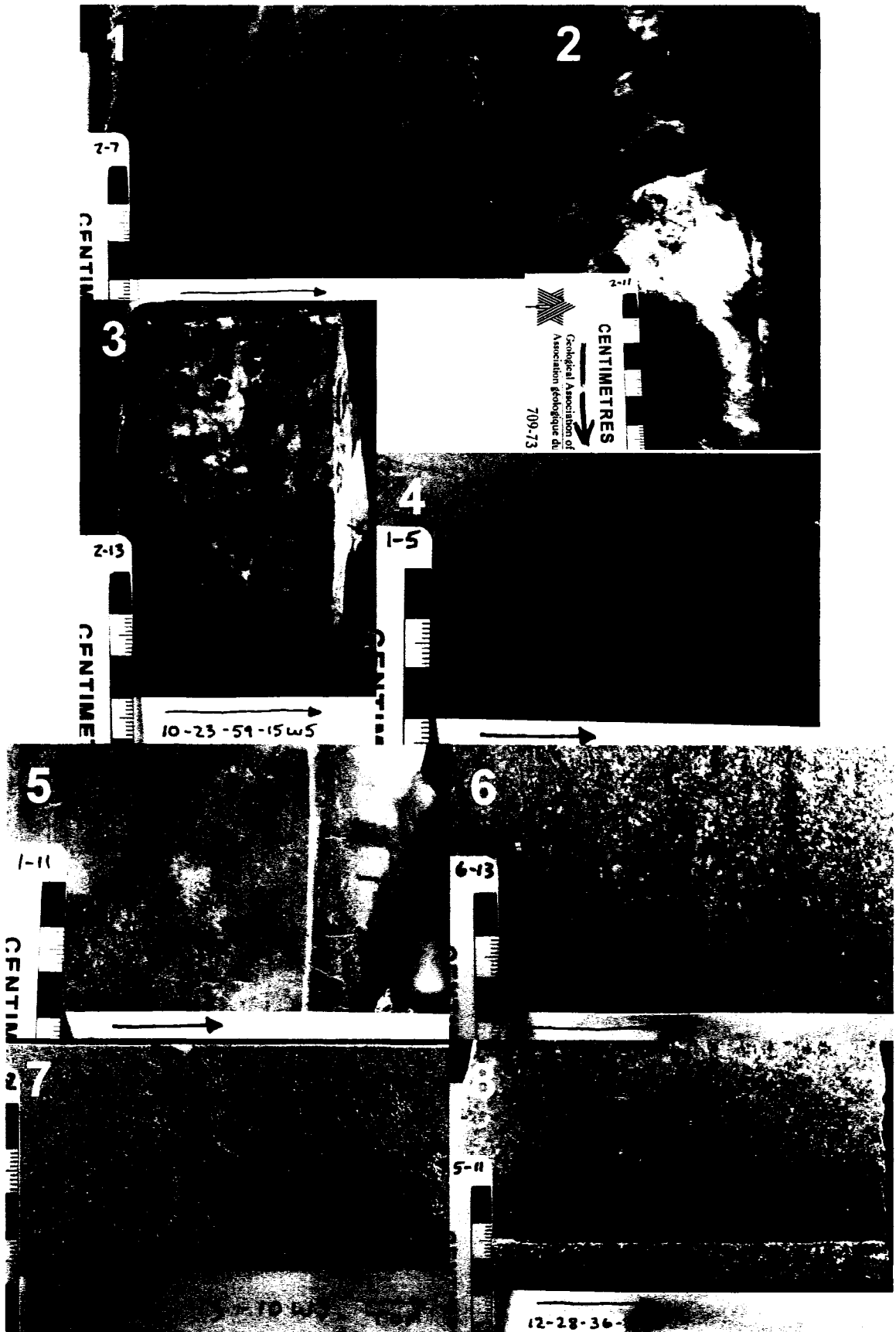
replacing both calcite and dolomite (wells 2 and 5). In some instances the precursor facies has been completely dolomitized (wells 1, 4, 5, 6 and 7 – Plate A-4). For undolomitized samples, most clasts are composed of a mudstone which is massive to laminated and sometimes contains dissolution seams. There is only one example of a brecciated peloidal grainstone in well 2 (Plate A-2). In hand sample the intraclast breccias are medium grey-brown in colour. The breccias of the Pekisko Formation have been classified using the schemes of Morrow (1982) and Kosa et al. (2003). The breccias within the wells mentioned above are cemented chaotic (angular) breccias that developed through solution collapse (Kosa et al., 2003). According to Morrow's (1982) classification scheme these breccias are categorized as cemented mosaic to rubble packbreccias. The cemented nature of the breccias denotes voids filled with chemically precipitated minerals. A cement matrix is the most common feature in diagenetic breccias formed from solution collapse (Taylor et al., 1975).

### **3.2.5 Dolostone facies**

The dolostone facies in this study are classified as units that have been completely dolomitized. These units include dolostones whose precursor lithofacies is unknown as well as dolostones which were likely grainstones, packstones or mudstones (Plate A-5). Dolostone facies are usually light to dark grey or brown. In wells 1 and 7, dolomite has pervasively dolomitized the entire interval. Crinoid pseudomorphs and ghost fossils are apparent but the original precursor fabric and associated facies remain difficult to discern. Also apparent in this facies are wavy laminations and cross-bedding. In terms of porosity, this facies is very porous and has vuggy, moldic and intercrystalline porosity types (Plate A-7). Dolostones within wells 3, 6, 8 and 9 consist of relatively thin beds sandwiched between wackestone/packstone and grainstone facies. It is also important to note that oil stained dolostones were only found in well 6, closest to the Pekisko subcrop edge.

**PLATE A**






### 3.3 Depositional Model

The depositional model for the Pekisko Formation is based on the vertical and lateral distribution of the lithofacies identified and their fossil assemblages. This information characterizes deposition in the inner ramp portion of a carbonate ramp and is illustrated in Figure 3.2. The general lithology of the Pekisko Formation is shown in Figure 3.3 with the associated depositional environments. The inner ramp is subdivided into five environments. Landward these environments include: the crinoid shoal, the ooid shoal, the lagoon and back barrier, the tidal flat and the sabkha. Crinoid grainstone shoals are the deepest facies found within the inner ramp in the Pekisko Formation and they require higher energy and nutrient rich water for growth (Martindale and Boreen, 1997). This environment is characterized by a low diversity and a high abundance of fossils that are massive to cross bedded and have syntaxial cements occluding pore spaces. The fossiliferous grainstones represent deposition along ooid shoals and in a transitional zone where they interfinger with crinoidal facies. Grainstones indicate shallower, warmer water environments where energy levels are still high. The ooid grainstones also form in ooid shoals that act as barriers restricting circulation in the lagoon and back barrier environments landward. These types of grainstones formed as a result of water agitation along the shore through wave action. The peloidal grainstones were deposited under much quieter conditions in the shallow lagoon or back barrier environment. The presence of micrite rims around bioclasts indicates deposition in water depths of less than 20m (Swinchett, 1969; Budd and Perkins, 1980). The wackestone to packstone lithofacies accumulated within the transitional zone between the deeper back barrier peloidal grainstones and the shallower lagoonal mudstone facies. Fossils have become significantly sparser within this facies with respect to the seaward grainstones. This marks a change in depositional environment to much shallower, quieter waters with episodic wave action during storm events that resulted in broken fossil fragments. The mudstone facies are rare but in some cases display fenestral fabrics, some laminations, chert beds and nodules, dolomitization and few fossils. These were deposited in a partially restricted low energy environment landward of the deeper back barrier to lagoon and bordering the shallower lagoon and peritidal environment. They may have also been subjected to periodic normal marine

incursions as suggested by Martindale and Boreen (1997). The intraclast breccia mudstones and dolostones represent deposition in a sabkha-type environment or are the result of paleoexposure leading to karstification. Some of the dolostones are bedded and in some instances contain secondary anhydrite nodules and laminations. Others are brecciated and cemented together by blocky calcite possibly of later meteoric origin. The erosion of more deeply buried sediment will produce more consolidated clasts that preserve their shape better when redeposited (Boggs, 1992). Most of the clasts observed here were well preserved, fitted and intact. If not formed through paleoexposure, then the likeliest scenario was that high energy water (normal wave, storm wave or currents) eroded seaward lagoonal sediments and carried them landward to be redeposited (Boggs, 1992). The entire carbonate ramp from the basinal environment to the sabkha represents a transition from cool water to warm water described as temperature stratification by Martindale and Boreen (1997).

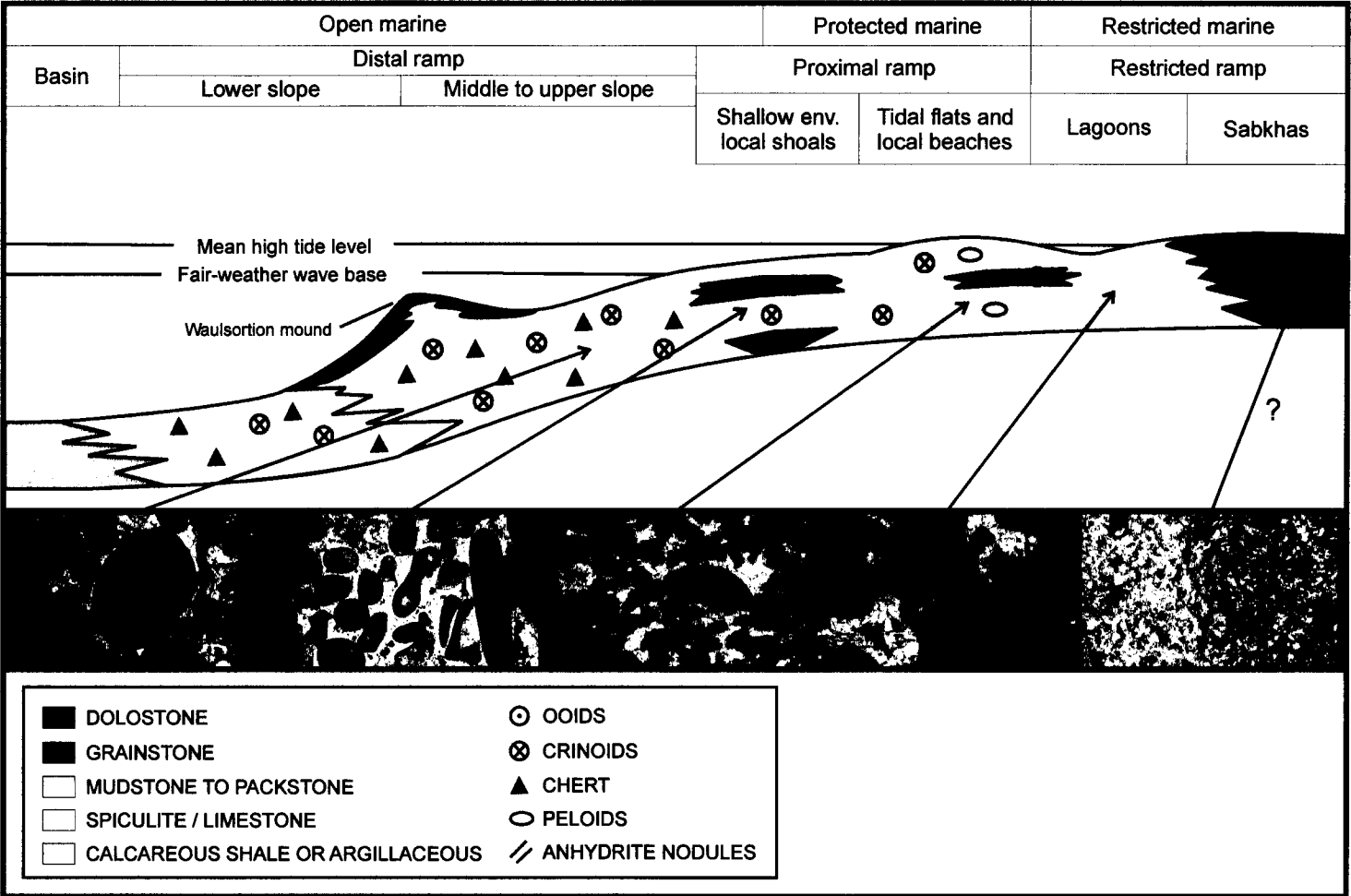


**Figure 3.2** Carbonate ramp depositional model for the Pekisko Formation (modified from Richards et al. 1994)

	Lithofacies	Depositional environment
Shallowing up 	Dolostone (some brecciated)	Sabkha
	Mudstone to wackestone (fenestral, bioclastic, chert)	Lagoon
	Peloidal and bioclastic packstone to wackestone (brecciated at top, some chert beds)	Tidal flats / lagoon
	Oolitic/mixed grainstone	Ooid/mixed grain shoals
	Crinoidal (ooid, peloids) grainstone	Crinoid shoals
	Dolostone	
	Crinoidal grainstone	

**Figure 3.3** General lithology of the Pekisko Formation in the study area with associated depositional environments.

## **CHAPTER IV**

### **DIAGENESIS OF THE PEKISKO FORMATION**

#### **4.1 Introduction**

Diagenesis includes all of the chemical, physical and biological changes (excluding weathering) that sediments undergo from the time they are deposited until metamorphism at elevated temperatures and/or pressures (Tucker and Wright, 1990; Blatt and Tracey, 1996).

During the process of diagenesis, carbonates are affected by many physical changes that can be observed petrographically and chemical changes that can be traced by geochemical analysis. The diagenetic history of the Pekisko carbonates is very complex and includes early shallow marine through to late deep burial environments. The most important changes that occurred in the Pekisko Formation were cementation, compaction, porosity evolution, dolomitization and recrystallization. Some of the diagenesis was facies-controlled and/or fabric selective, however also important in determining diagenetic pathways was the tectonic evolution of the basin. The Jurassic paleoexposure surface also played an important role in later dolomite formation and recrystallization.

Diagenetic modifications in this study were identified using standard petrography, ultraviolet fluorescence and cathodoluminescence analyses.

#### **4.2 Micritization**

A micrite (microcrystalline calcite) envelope forms from boring organisms such as endolithic algae and fungi infesting the whole surface of the grain (Bathurst, 1966; Boggs, 1992). The resulting borings then get filled in by micrite. More extensive boring will result in complete micritization forming a peloid type of grain. In the Pekisko Formation, micritization was the first diagenetic event to affect the limestone (Plate C-1 and 2). Especially seen in the grainstone facies, most envelopes are observed on crinoids, brachiopods, bryozoans, calcispheres, foraminifers and ostracods (Plate C-6). Several brachiopods and ostracods that have remained attached have no rims but are filled with a calcitic mud. Many other grains have been partially to

fully micritized forming the peloidal grains observed. Micritization is quite an extensive process seen in wells 2, 3, 4, 5, 6, 8 and 9. Foraminifera and calcispheres seem to have preferentially altered to peloids and shell fragments have envelopes. Since micritization is formed by organic degradation it is interpreted to be of early diagenetic origin.

### **4.3 Compaction**

Several compactional features are present within the Pekisko Formation as a result of overburden pressure and subsequent reduction in bed thickness. Diagenetic compactional processes include mechanical (physical) and chemical compaction.

#### **4.3.1 Mechanical compaction**

There are several effects of mechanical compaction present in the Pekisko Formation. These features include grain packing, grain reorientation and grain deformation and/or breakage. Both grain packing and reorientation accompany the dewatering process during early burial and continue until a grain supported fabric is established (Choquette and James, 1987). Unless sediments have been cemented early, compaction will cause a significant decrease in initial porosity and a thinning of beds. Porosity loss may be as little as 10% to as much as 40% (Boggs, 1992). With increasing overburden pressures porosity reduction continues to occur with deeper burial. These stresses result in grain deformation by brittle fracturing and breakage or by ductile or plastic deformation. Based on experiments, Shinn and Robin (1983) concluded that the greatest compactional effects were at pressures equivalent to < 305 m (1000 ft). At burial depths of 100 m this compaction can cause a reduction in depositional thicknesses by 50%. In the Pekisko Formation, especially within the grainstones facies, several grains show evidence of mechanical compaction where many are broken, aligned and deformed (Plate B-1). Plate B-2 shows a crinoid that has been flattened and become twinned as a result of mechanical compaction. The crinoidal grainstone facies may have initially been deposited as a wackestone to packstone, but with increasing compaction was altered to grainstone facies. The ooid and

peloidal facies show little evidence of mechanical compaction. The lack of compaction textures may be due to the early calcite cementation of these sediments.

#### **4.3.2 Chemical compaction**

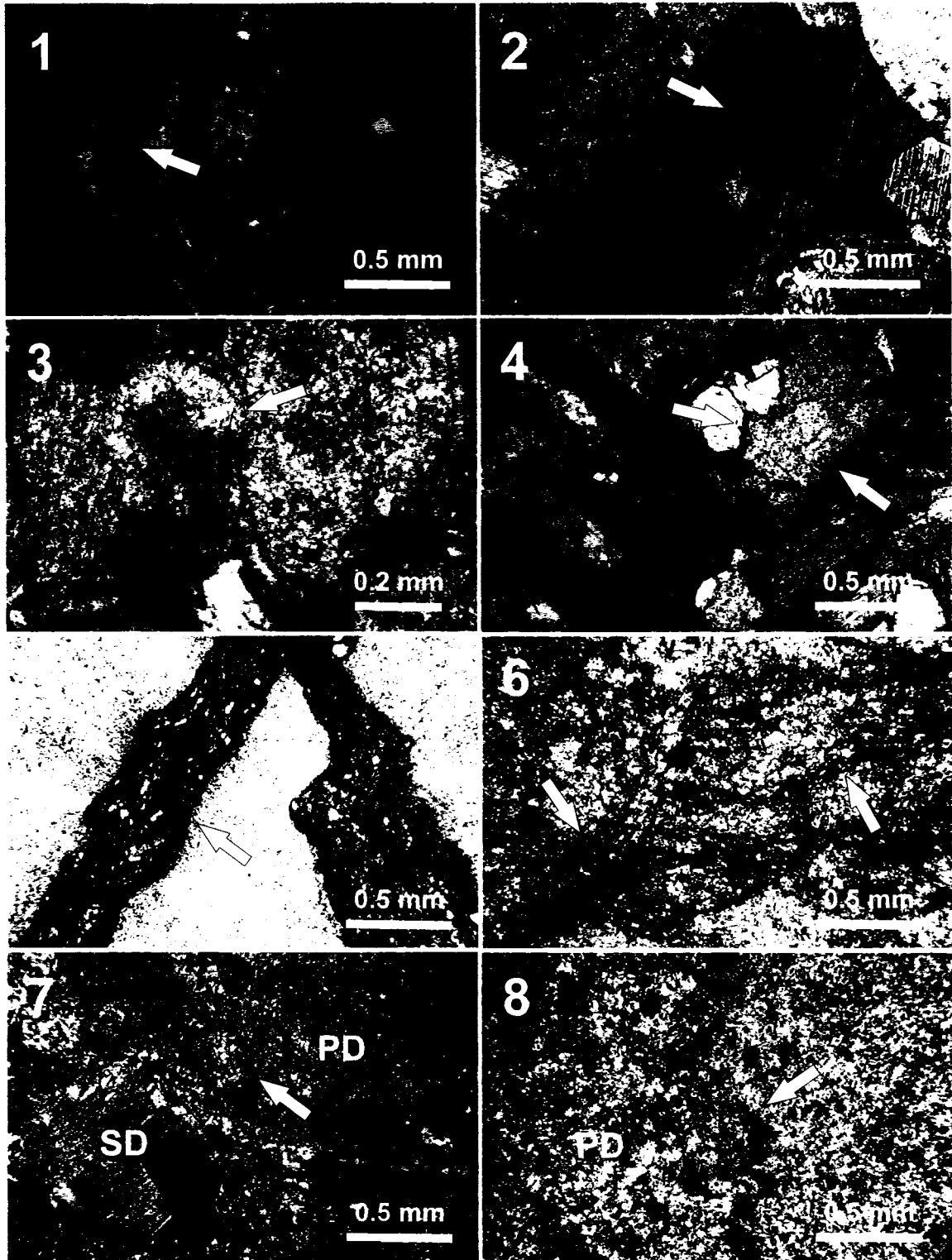
Several factors influence chemical compaction, such as; burial depth, tectonic stress, mineralogy, the presence of insolubles, pore water composition and elevated pore pressures (Choquette and James, 1987; Feazel and Schatzinger, 1985; Boggs, 1992). Once mechanical compaction has established a stable grain framework, chemical compaction then begins when load or tectonic stresses can be transmitted from grain to grain (Boggs, 1992). Authors have suggested that pressure solution can occur at depths < 200m, to as much as 1500 m due to carbonate mineralogy (Moore, 1989). The calcite mineral is dissolved and its ions released into solution where they can be reprecipitated locally as calcite cement or stay in pore waters and be transported to distant sites (Boggs, 1992). Effects of chemical compaction in the Pekisko carbonates include: stylolites, dissolution seams, sutured contacts and fitted fabrics.

Dissolution seams are undulose, anastomosing seams that are made up of insoluble residues such as clays and organics which are usually laterally continuous on a core scale (Plate B-6). Also apparent are seams formed in the shape of rings, usually adjacent to anastomosing seams (Plate B-7). These occur in wells 2 through to 6 usually within the dolostone facies indicating formation at a depth of at least 300 m (Dunnington, 1967). In well 2 the seams are thick and contain many tiny quartz crystals that remained insoluble (Plate B-5).

Stylolites have a sutured surface, characterized by a jagged surface of interpenetrating columns made up of a variable accumulation of insoluble residue along the surface. They are most often oriented parallel to bedding but also form perpendicular to bedding. In the Pekisko they have high to low amplitudes and occur vertically only in the dolostone facies. Horizontal stylolites are apparent in all wells and facies. Often associated with the stylolites is fibrous calcite cement (Plate C-8).



**PLATE B**



These stylolites sometimes form along facies or vein boundaries and in some instances crosscut dissolution seams (Plate B-6). For instance in well 1 a stylolite has formed along the contact between dolostone and a chert bed (Plate B-8).

Fitted fabrics occur only in wells 3, 4 and 5 and are defined as nonparallel and reticulated resulting in the creation of nodular fabric (Wanless, 1979; Buxton and Sibley, 1981 and Boggs, 1992). This fabric occurs within dolostones and highly compacted grainstones (Plate B-4). Sutured seams are common in the Pekisko grainstones in wells 3, 4 and 6 (Plate B-3). These seams are merely microstylolites forming at interpenetrating grain contacts.

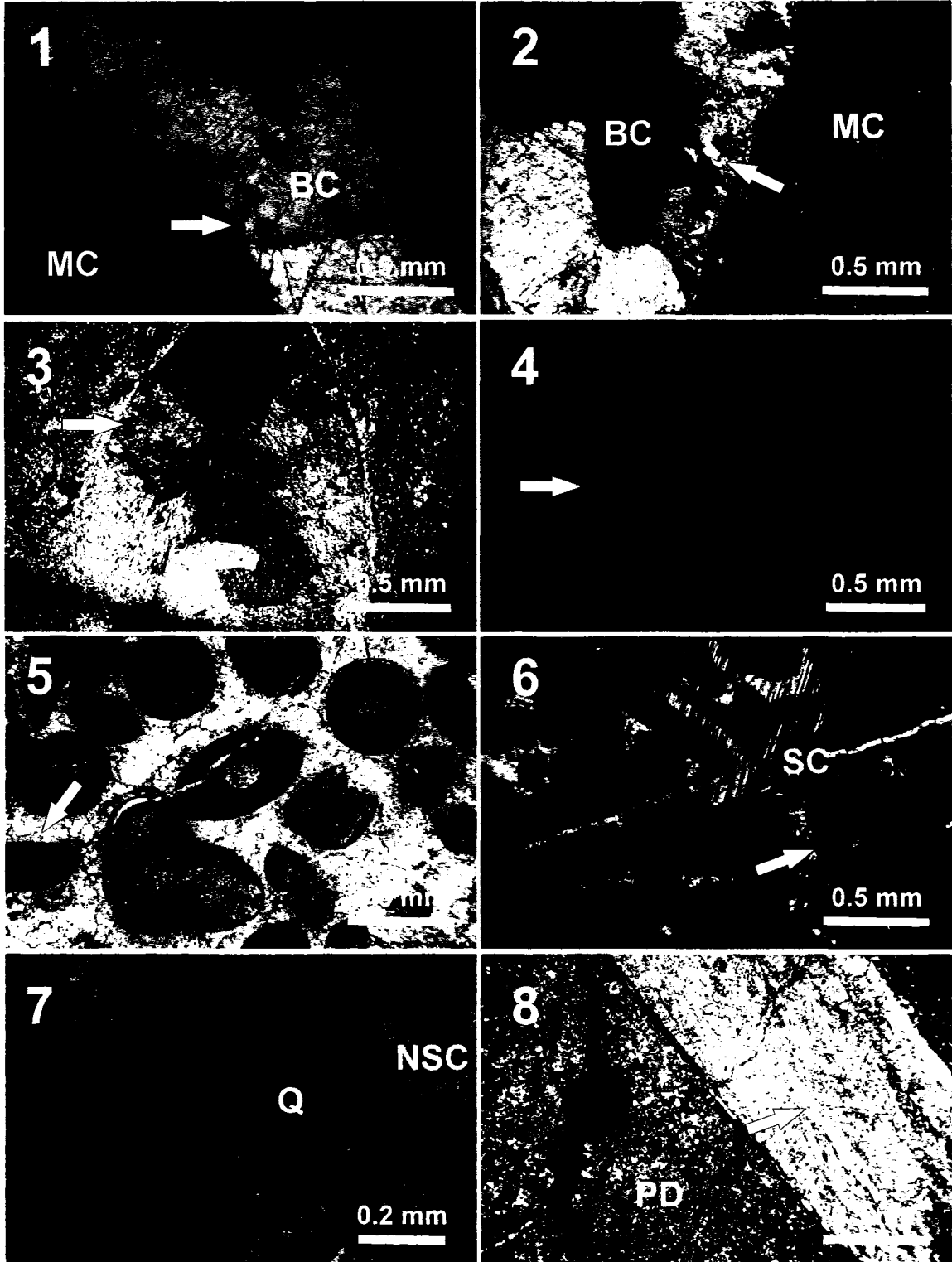
#### **4.4 Calcite cementation**

Calcite cementation has occurred throughout the diagenetic history of the Pekisko carbonates, occluding early to late porosity. Depending on the diagenetic environment, the precipitated calcite cement will have a variety of textures. These textures are largely dependant on the composition of pore fluids precipitated from various environments. Petrographically, seven distinct calcite cement types have been identified. These include, in order of formation: isopachous, drusy mosaic, pendant/meniscus, blocky I, syntaxial, fibrous, blocky II, bladed and blocky III.

##### **4.4.1 Isopachous rinds**

This cement occurs only within the well 6 ooid grainstones of the Pekisko Formation in very minor amounts. It consists of relatively clear, non-ferroan, non-luminescent or fluorescent fibrous crystals that are 30 $\mu$ m in size. This cement forms thin rinds around ooids that predates compaction which may indicate that they formed just after deposition on the surface (Plate C-5).

**PLATE C**



#### **4.4.2 Drusy mosaic calcite**

This cement occurs as clear, non-ferroan crystals ranging in size from 40 to 110 $\mu$ m. It is found occluding interparticle porosity in grainstone facies where it is relatively non-luminescent or fluorescent (Plate C-5). The cement is also highly zoned and luminescent in some instances where it fills articulated ostracods, brachiopods, gastropods and calcispheres (Plate C-3 and 4).

#### **4.4.3 Pendant/Meniscus calcite**

These cements occur in very minor amounts in wells 1 and 3 of the Pekisko Formation. The crinoidal grainstones are the only lithofacies which contain pendant cements. The grainstones are well compacted and grains have reoriented themselves during packing such that pendant cements are not all showing the same gravitational direction (Plate F-5). Meniscus cements are common between grains that have not been overly compacted as well as between some clasts in intraclast breccia dolostones. However where present in breccias, the meniscus cement has been replaced by selective dolomite (Plate F-6). These cements are non-fluorescent or luminescent and are non-ferroan.

#### **4.4.4 Blocky calcite**

This is the most common form of calcite cementation found as fracture and void filling cement within dolostone facies, but also appears within mudstone to wackestone facies (Plate C-1 and 2). Blocky crystals are very large (~ 0.5 mm), clear, with few inclusions, non-ferroan and show dull to bright luminescent and fluorescence. This cement occurs throughout the diagenetic history of the Pekisko Formation as blocky calcites I, II and III.

#### **4.4.5 Syntaxial calcite**

This cement is highly twinned, non-ferroan, non-luminescent or fluorescent and relatively cloudy occurring only in the crinoidal grainstone facies of wells 3 and 6. Syntaxial cements are

seen as overgrowths on many crinoids and engulf many surrounding grains (Plate C-6). In many instances it is twinned indicating that it has been subjected to mechanical strain. Petrographic evidence shows that the cement predates mechanical compaction.

#### **4.4.6 Fibrous calcite**

This cement occurs only within wells 3 and 9 of the Pekisko. It is found in dolostones and grainstones associated with chemical compaction, specifically with stylolites (Plate C-8). This cement is made up of dirty, long and thin adjacent blades of calcite crystals that are non-ferroan and non-fluorescent or luminescent. They are highly fractured and inclusion rich.

#### **4.4.7 Bladed prismatic to equant calcite**

These cements occur in wells 2, 4 and 6 of the Pekisko Formation. They are 50 – 250  $\mu\text{m}$  equant (Plate C-1) to prismatic (Plate C-2) crystals that are relatively clear, non-ferroan and non-luminescent or fluorescent. They are usually present along the edges of veins and breccia fractures which have later been filled by blocky cements within mudstone to wackestone facies but also occur in grainstones in minor amounts.

### **4.5 Neomorphism and neomorphic spar**

Neomorphism is the term used to cover all transformations between one mineral and itself or a polymorph. Therefore this term encompasses the polymorphic transformation of aragonite to calcite, alteration of Mg-calcite to calcite and recrystallization (Folk, 1965; Boggs, 1992). In the Pekisko Formation the two types of neomorphism observed are called aggrading neomorphism whereby carbonate minerals increase in crystal size from micrite to spar and degrading neomorphism resulting in a decrease in crystal size. Crystals usually appear cloudy and often show relicts of the precursor fabric within them (e.g. peloids). However the precursor

fabric is completely destroyed in most cases. A distinguishing feature of neomorphism from other calcite cement is the variability in the sizes of crystals adjacent to each other (Plate C-7).

#### **4.6 Dolomitization**

Dolomitization is the most important process affecting all carbonates of the Pekisko Formation to varying degrees. Since porosity is related to dolomite intervals it is important to understand the distribution, timing and mechanism(s) of dolomitization, especially in relation to reservoir potential and future exploration. Petrographically, five types of dolomite have been described for the Pekisko Formation, from oldest to youngest: (1) pervasive dolomite, (2) dissolution seam-associated dolomite, (3) planar void-filling dolomite, (4) selective dolomite and (5) non-planar void-filling or saddle dolomite. The textural classification of these dolomites are partially based on the schemes of Gregg and Sibley (1984), Sibley and Gregg (1987) and reprinted by Boggs (1992). The white card techniques of Folk (1987) were used to attempt to distinguish precursor fabrics destroyed by pervasive dolomite with varying degrees of success. Fluorescence microscopy techniques (Dravis and Yurcwicz 1985) were also used. The preceding sections describe all dolomite phases present in the Pekisko Formation; however, although these phases are described separately, some are genetically related and represent a continuum of the dolomitization process and recrystallization.

##### **4.6.1 Pervasive dolomite**

Pervasive dolomite is the dominant type of dolomite in the Pekisko Formation observed in all wells. Individual crystals range in size from 15-50  $\mu\text{m}$  for fine pervasive dolomite and 50-220  $\mu\text{m}$  for coarse pervasive dolomite with euhedral to anhedral textures. In some cases, usually in coarser samples, fluorescence microscopy reveals dull brown cores and bright yellow rims. CL studies show bright red cores and duller red rims in coarser pervasive dolomite (Plate D-2) and dull homogeneous CL in finer samples (Plate D-6). Both these methods show that some of the crystal boundaries are etched. This dolomite occurs primarily in mud-supported facies, but white



card observations of fossil relicts in some samples indicate a bioclastic precursor. Coarser pervasive dolomite intervals also have higher moldic and vuggy porosities (Plate D-1, 5 and 8). Pervasive dolomite is an early diagenetic product and is the dominant type of dolomite in the Pekisko Formation.

#### **4.6.2 Dissolution seam-associated dolomite**

Dissolution seam-associated dolomite (DSAD) occurs as 10-50  $\mu\text{m}$  crystals with a euhedral fabric associated exclusively with chemical compaction features (Plate D-7). DSAD is also non-fluorescent and non-luminescent. It is most commonly found in the grainstone facies and formed early, penecontemporaneously with early chemical compaction.

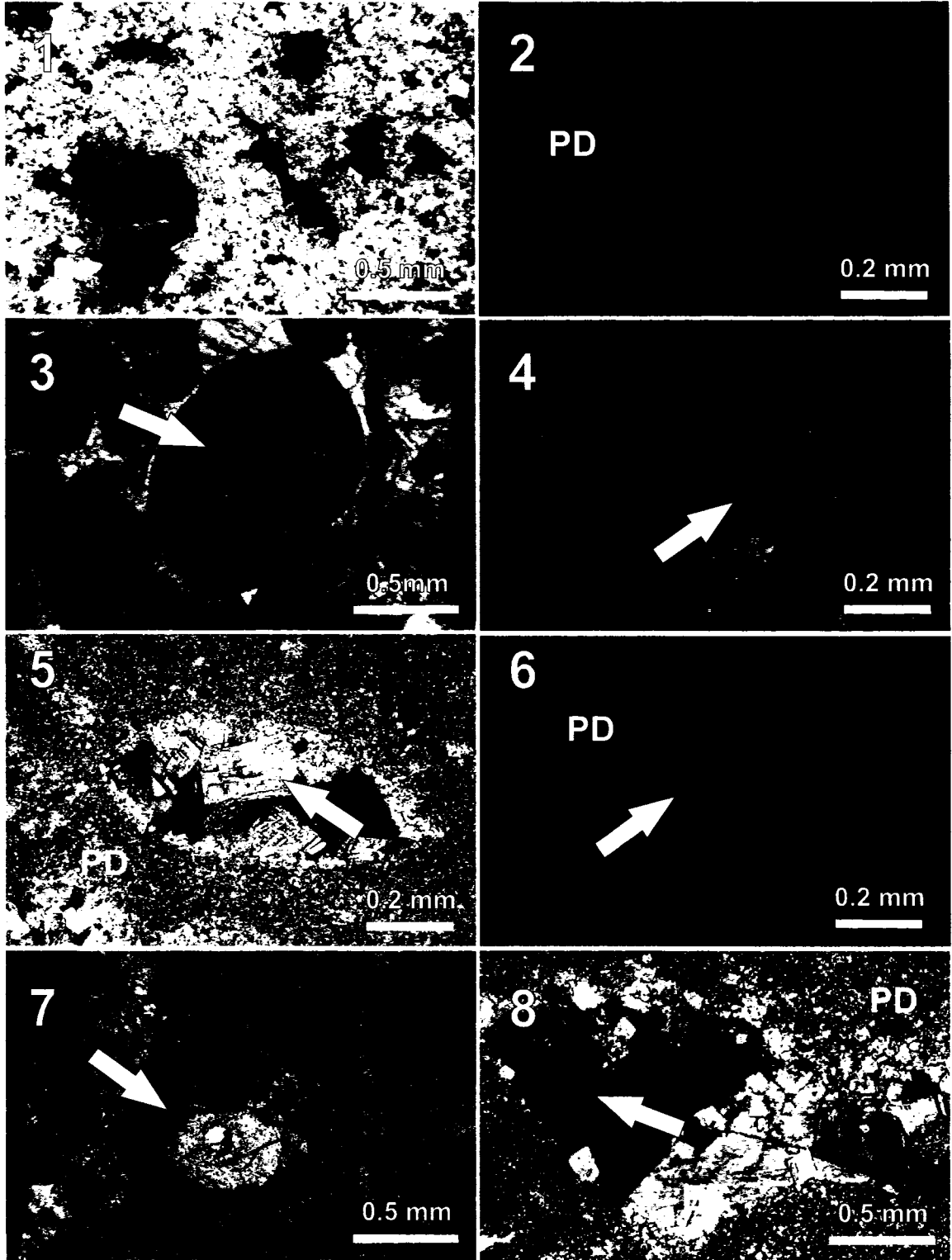
#### **4.6.3 Planar void-filling dolomite**

Planar void-filling dolomite occurs as a mold and vug-filling cement with individual crystal sizes of 40-300  $\mu\text{m}$  and euhedral fabrics. This phase has homogeneous, clear crystals under plane polarized light (Plate D-5 and 8), however reveals bright cores and dull rims with CL (Plate D-6). Since this phase occludes vugs, it is interpreted to have precipitated after dissolution. Void-filling dolomite only occurs within coarser dolostone intervals in wells 1, 7, 8 and 9.

#### **4.6.4 Selective dolomite**

Selective dolomite occurs primarily as matrix replacive (Plate D-4), however it is also found replacing the cores and rims of crinoids in the grainstone facies (Plate D-3). Individual crystals range in size from 10-250  $\mu\text{m}$  and have euhedral to anhedral fabrics. This phase was non-fluorescent and non-luminescent. Fine euhedral crinoid replacive phases formed earlier than coarser anhedral matrix replacive phases. In one instance, selective dolomite has been observed replacing meniscus calcite cement in an intraclast breccia (Plate F-6).

**PLATE D**



#### **4.6.5 Saddle dolomite**

Saddle dolomite is a very minor phase in the diagenetic history of the Pekisko Formation. Dominantly it occurs as cement occluding pore spaces in wells 3 and 4 (Plate D-8). However, sometimes it replaces secondary anhydrite or is associated with late chemical compaction features in wells 3 and 9 (Plate B-7). Individual crystals range in size between 250  $\mu\text{m}$  to 1.5 mm. They have anhedral shapes and typical sweeping extinction.

#### **4.7 Silicification**

Silicification is a relatively minor but important component in the carbonates studied. In the Pekisko Formation it occurs primarily as chert beds or nodules, as authigenic quartz crystals and chalcedony.

The authigenic quartz appears hexagonal in cross section and displays bipyramidal terminations in the mudstone and wackestone facies as scattered 10-25  $\mu\text{m}$  sized crystals. It is often associated with neomorphosed intervals and usually contains inclusions of calcite (Plate E-1). In one instance authigenic quartz crystals have formed layers bounded by stylolites within a dolomitic mudstone (Plate E-2). Crystals observed within dissolution seams are much smaller. Plate E-3 shows a quartz crystal replacing a partially micritized crinoid. Authigenic quartz is seen in wells 1 through 5.

Chert is a rock mainly composed of fine grained quartz crystals and can form in marine and freshwater environments as well as at subaerial exposure surfaces (Knauth 1979, Flügel 2004). It occurs mainly as beds within dolostones and mudstones to wackestones of wells 1, 2 and 5. Some of the chert within bioclastic facies have retained fossil fabrics while others in the dolostones have been replaced by the dolomite and have not retained the precursor fabric (Plate E-6). Only in well 5 does chert form nodules replacing a grainstone facies where textures and fabrics have been preserved (Plate E-5). In this case, the chert is highly selective having replaced crinoids and ooids but not micrite.

Of all silicification types, chalcedony is the least common, observed only in wells 5 and 9. It is associated with neomorphic spar in well 5 (Plate E-4) and secondary anhydrite nodules in well 9.

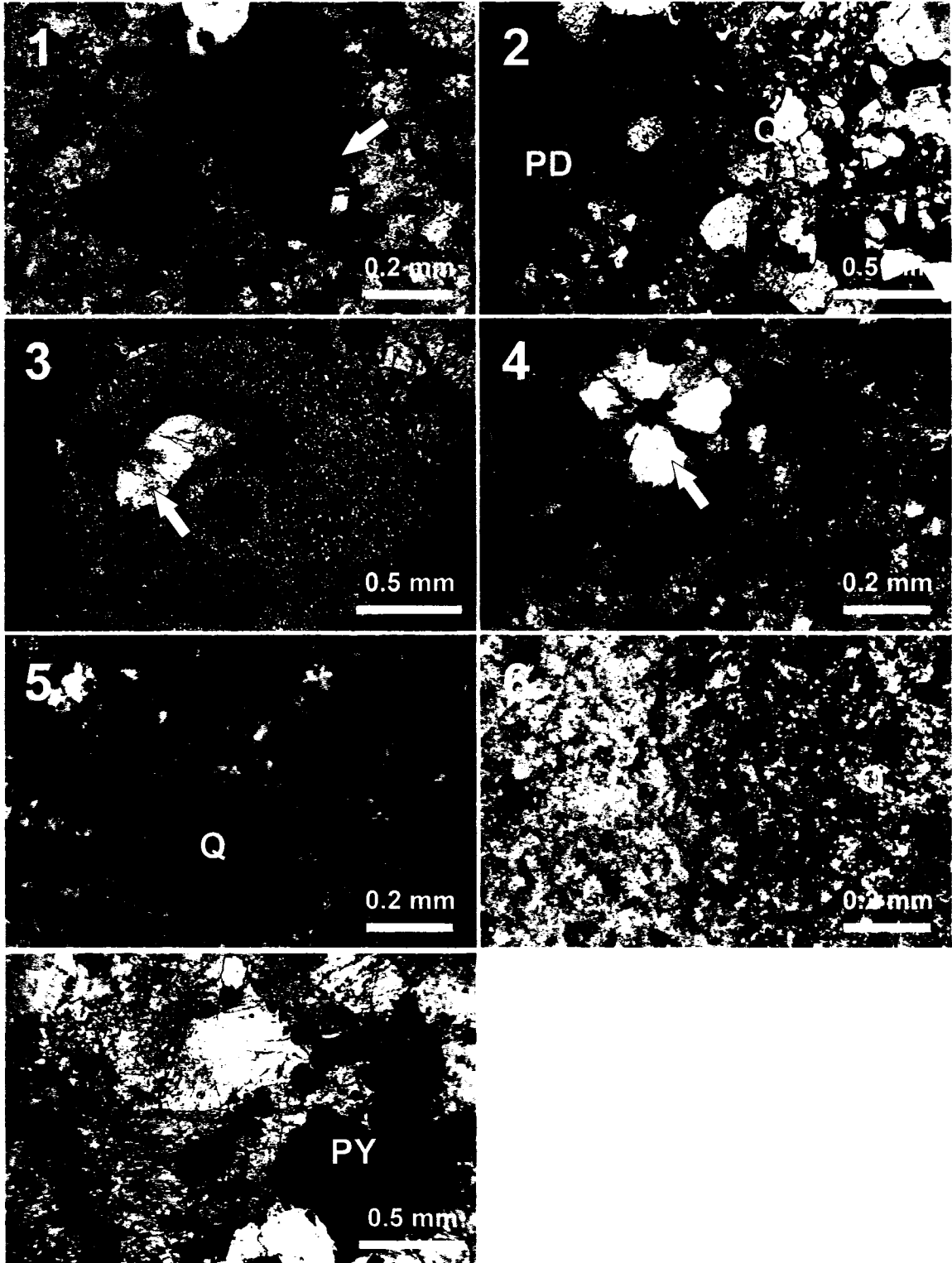
#### **4.8 Sulphide mineralization**

Sulphide mineralization in the Pekisko Formation is a very minor diagenetic phase occurring as pyrite. It usually replaces blocky calcite within intraclast breccias and sometimes in wackestone and dolostone facies in wells 2, 3, 4, 5 and 7. Crystals are generally framboidal (Plate C-1), cubic (Plate E-7) or just bladed and range in size from 5 to 75 $\mu$ m. The pyrite formed early to late in the diagenetic history of the Pekisko carbonates. It replaces all three phases of blocky calcite and neomorphic spar.

#### **4.9 Dissolution**

An important early dissolution process in the Pekisko Formation affects originally aragonitic and high-magnesium calcitic fossils and cement. Due to their instability, they will preferentially be replaced or dissolved out, later to be infilled by a more stable low-magnesium calcite. Micrite envelopes help to preserve the original structures of some of the fossils which include gastropods and ostracods. Although early dissolution is important, later dissolution proves to be much more significant. Large vugs up to 3 cm wide are common within the dolostone lithofacies (Plate D-1, 5, 6 and 8). These are evidence of late dissolution by diagenetic fluids prior to the precipitation of blocky calcite. Since some of the voids are undoubtedly molds of precursor fossils, the vugs may possibly have been molds that were further dissolved by fluids. In the dolostone facies as well, fluorescence and luminescence studies of the dolomite crystals reveal inclusion-rich cores and relatively clear rims with evidence of etching or dissolution prior to the precipitation of the outer rims (Plate I-5 and 6). In some cases dedolomitization has occurred but only in wells that have been partially dolomitized. Petrography shows that the cores of several rhombs have been dissolved out (Plate I-1 and 2).

**PLATE E**



#### **4.10 Pyrobitumen**

Pyrobitumen fills intercrystalline pore spaces and coats some vuggy pores within the dolostone facies of wells 1, 3, 6, 7 and 8. It occurred after pervasive dolomitization and was present when blocky calcite precipitated. The grainstone facies of wells 3 and 6 also have bituminous coatings on many of the grains as well as oil staining along pores. This bitumen may be the product of thermochemical sulphate reduction, a process that changes oil into sour gas (Machel 1987).

#### **4.11 Fracturing**

There are three main fracturing events present in the Pekisko carbonates. The first consists mainly of vertical to subvertical fractures that are hairline to a few millimetres wide filled with calcite cement. In some instances they have been healed by syntaxial cement indicating a very early generation (Plate C-6). The brecciation generation of fracturing occurred during paleoexposure. The resulting erratic fractures are dominantly filled with blocky calcite cement (Plate A-2 and 4). The final generation consists of subvertical to horizontal fractures that are dominantly hairline but one is as wide as 10cm. They crosscut early dissolution seams but are penetrated by later stylolites. Many of these fractures are filled with very coarse blocky calcite cement indicating a later genesis.



## CHAPTER V PALEOEXPOSURE EVIDENCE IN THE PEKISKO FORMATION

### 5.1 Introduction

Paleokarst is the term used to describe an ancient karst usually buried by younger sediments (Flügel, 2004). A humid climate favours karstification during sea level lowstands. Rainwaters on the exposed surface causes dissolution and subsequent formation of caves and sinkholes. Dissolution of the carbonate sequence occurs when waters are undersaturated with respect to  $\text{CaCO}_3$ . Other than a meteoric setting, there are two other environments that may also contribute to karst formation; deep burial, where karst is formed by hydrothermal fluids (sulfuric acid) and mixing zone, where fresh and marine waters mix (Ford, 1988; Wright, 1991 and Williams, 2005). Many factors contribute to the types of karst structures that result and they include: rock type, duration of exposure, climate and vegetation to name a few (Budd et al., 1995; Williams, 2005).

Important criteria for the identification of a paleokarst include; breccias, dikes and fissures, cavity or cave infill sediments, speleothems, carbonate cements and calcretes and silcretes (Flügel, 2004). It has been estimated that reservoirs near subaerial unconformities contain 20-30% of known recoverable hydrocarbons (Hopkins, 1999; Flügel, 2004).

The Pekisko Formation has undergone several exposures since its time of deposition leading to the formation of a subcrop edge. In a recent paper by Williams (2005), the Pekisko Formation has been classified as having undergone polyphase karsting. This type of karsting is essentially a combination of a buried paleokarst, which is karsting that occurred before the burial of the youngest sediments and exhumed paleokarst, whereby previous karsting is re-exposed and karstified again.

Karst features observed in the Pekisko carbonates are outlined below and are only apparent in wells closest to the subcrop edge.

## 5.2 Evidence of paleoexposure

Several features are present within the Pekisko carbonates that can be attributed to the many subaerial exposures that have affected the Pekisko sequence. These include; meniscus and pendant cements, brecciation, sediment filled cavities, speleothem cements, dolomolds and dedolomitization. It is likely that the meteoric fluids which infiltrated these carbonates during teleogenesis were essential in the formation of secondary porosity as well as later dolomite cements. Although no soil surfaces have been observed, they may have existed but were simply not well preserved.

Brecciation typically occurs at the top of Pekisko wells closest to the subcrop edge and are absent in wells farther away. They are clast supported, fitted to non-fitted, angular to subrounded and poorly to moderately sorted (Plate A-2 and 4; Plate F-6). This is the most common karst feature observed in these carbonates. A study by Demiralin (1993) on the Madison limestone shows that the brecciation at the tops of wells may be a good indication that it is karst related.

Cavity infill sediments are relatively uncommon in the Pekisko carbonates, only apparent in wells 4 and 5. They consist of cavities filled with accumulations of debris, in this case quartz and ooids. Often these fills are laminated with alternating dark and light coloured layers. In well 4 cavities are filled with detrital quartz grains. Well 5 displays one cavity that is filled with cherty layers of ooids alternating with chert (Plate F-1). The diagenesis of silica cements is consistent with subaerial exposure and includes; chert, chalcedony and authigenic euhedral crystals. Cherty fossils in a cavity fill suggest early silicification prior to exposure (Mutti, 1995).

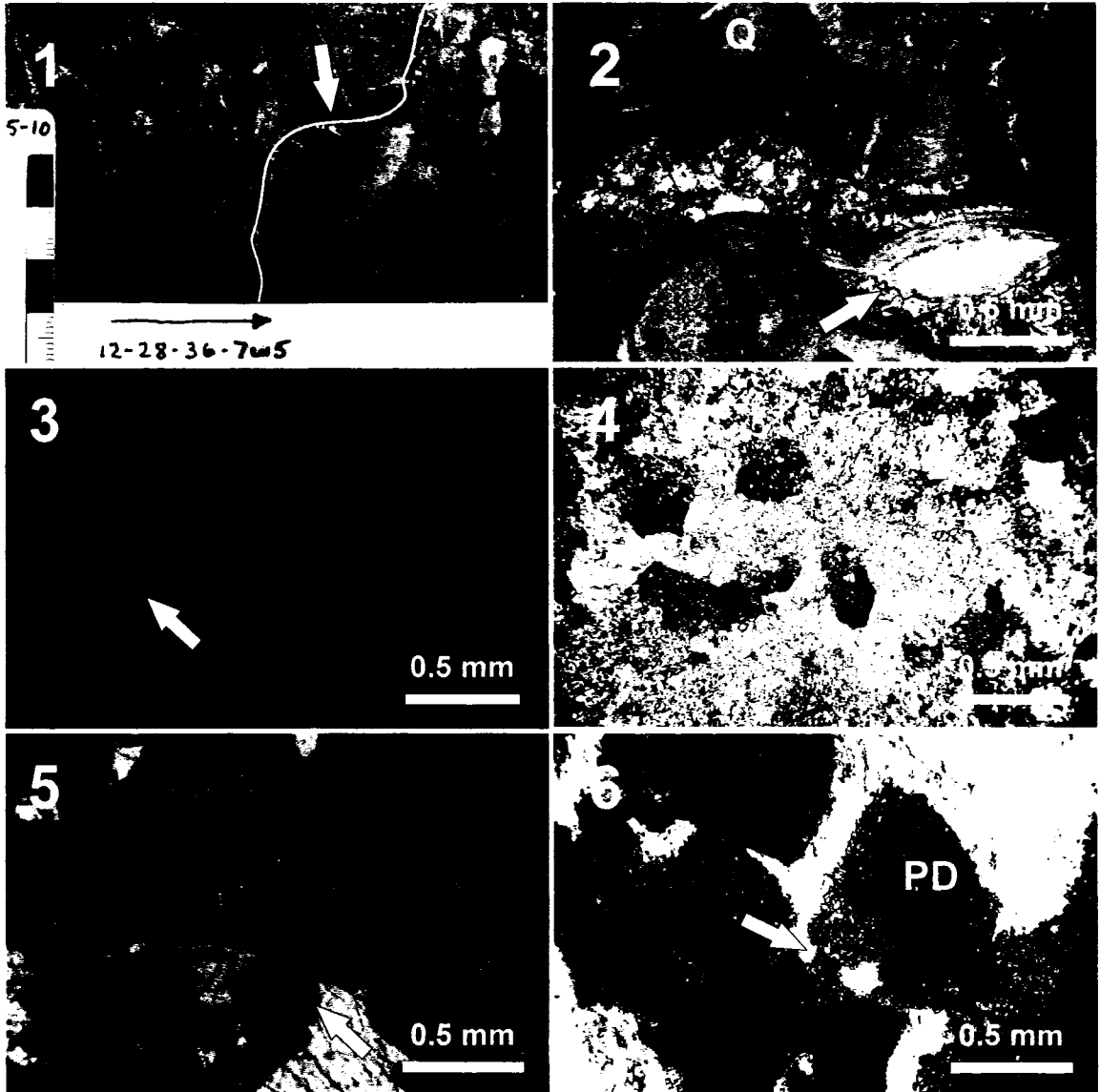
Speleothem carbonates are also rare in the Pekisko carbonates studied. They are radiating fingerlike crusts of calcite cement (colloform calcite cement) that usually line cavities. This type of cement was only observed in one well under cathodoluminescence (Plate F-3). In plane polarized light the calcite cement appears sparry and has no zonations (Plate F-4). It is likely that the fabric was obliterated during neomorphism and that only luminescence studies can detect the relict fabrics.

Open dolomolds observed in well 5, may indicate subaerial exposure and dissolution by karst waters (Braun and Friedman, 1970; Flügel, 2004). These dolomolds occur within the cherty ooid grainstones that fill cavities (Plate F-2).

Dedolomitization or the alteration of dolomite to calcite is observed in dolomite intervals within wells closest to the subcrop edge. According to Kenny (1992), they are common features in near surface vadose zones. Dedolomitization will be discussed in further detail in Chapter 8.

Meniscus and pendant cements have been observed in wells 1 and 3. These typically form in the vadose zone where there is exposure to the atmosphere (Dunham, 1971; Beach, 1995). These appear to have formed prior to any significant compaction since the pendant cement orientations vary according to the orientation of the grains (Plate F-5).

**PLATE F**



## CHAPTER VI

### GEOCHEMISTRY OF THE PEKISKO FORMATION

#### 6.1 Introduction

Several geochemical techniques have been used to analyze carbonates of the Pekisko Formation. Such techniques help to identify the carbonate composition, their relative time of formation and the diagenetic environments in which they have formed. More importantly however, geochemistry allows scientists to discern possible fluid types and sources for each diagenetic phase. The geochemical techniques employed for this study are: (1) carbon and oxygen stable isotopes; (2) radiogenic strontium isotopes; (3) elemental analysis; and, (4) fluid inclusions. The following sections present the concepts and results of these techniques.

#### 6.2 Isotopes

##### 6.2.1 Stable isotope theory

An isotope of an element has the same number of protons but a different number of neutrons (e.g. oxygen has three isotopes;  $^{18}\text{O}$ ,  $^{17}\text{O}$  and  $^{16}\text{O}$ ). When these elements react to form compounds, the resulting molecules will have different masses depending on the isotope it contains. This difference in mass will affect how molecules react to mass dependant physical processes (Faure, 1991). A process called isotope fractionation or isotope exchange reaction is responsible for these observed physical differences in isotope compositions and it occurs during phase transformations, mineral precipitation and diagenetic reactions.

The fractionation factor can be determined at any temperature by this equation:

$$10^3 \ln \alpha_{a-b} = (A \times 10^6)/T^2 + B \quad (1)$$

Where A and B are constants determined for a certain mineral – water or mineral – mineral system and T is the temperature in Kelvin.

The oxygen and carbon isotopic standard used for carbonates is VPDB which stands for the PeeDee Formations *Belemnitella Americana*. The oxygen isotopic composition of water and carbonates can also be reported relative to the VSMOW standard (Standard mean ocean water). The conversion between VSMOW and VPDB is as follows (Coplen et al., 1983 in Veizer, 1983):

$$\delta^{18}\text{O}_{\text{VSMOW}} = 1.03091 \delta^{18}\text{O}_{\text{VPDB}} + 30.91 \quad (2)$$

and

$$\delta^{18}\text{O}_{\text{VPDB}} = 0.97002 \delta^{18}\text{O}_{\text{VSMOW}} - 29.98 \quad (3)$$

All compositions are expressed in per mil (‰) relative to a standard with a known ratio of isotopes.  $\delta^{18}\text{O}$  for a sample is determined as follows:

$$\delta^{18}\text{O} = [(\text{}^{18}\text{O}/\text{}^{16}\text{O})_{\text{sample}} - (\text{}^{18}\text{O}/\text{}^{16}\text{O})_{\text{std}} / (\text{}^{18}\text{O}/\text{}^{16}\text{O}_{\text{std}})] \times 1000 \quad (4)$$

### 6.2.2 Stable isotopes in carbonate diagenesis

Carbon and oxygen stable isotopes are the most commonly used isotopes in the study of carbonate diagenesis. The fluids that precipitate calcite and dolomite can be characterized by their isotopic compositions (Land et al., 1975). The following is a list of controls on the distribution of carbon and oxygen isotopes during diagenesis (Brand and Veizer, 1981; Anderson and Arthur, 1983).

- i) Diagenetic fluid isotopic composition. Meteoric water is typically depleted in  $^{18}\text{O}$  relative to coeval marine water. Since its source is from the evaporation of seawater the lighter isotope preferentially incorporates itself in rainwater when it evaporates. The seawater that does remain after evaporation is then enriched in  $^{18}\text{O}$ .
- ii) Openness of the system (water-rock ratio). In this system there is a constant renewal of isotopes in the fluids. In a closed system isotopes are constantly being recycled between rock and fluids.

- iii) The deviation of fractionation factors from unity determined by the temperature of reaction.
- iv) Salinity of diagenetic fluids (e.g.: interaction with evaporites).
- v) Altitude, latitude and seasonal variations affect the  $\delta^{18}\text{O}$  composition of diagenetic fluids. Generally,  $\delta^{18}\text{O}$  decreases with increasing altitude and latitude.
- vi) Secular variations in seawater isotopic compositions. In general  $\delta^{18}\text{O}$  for carbonate minerals decrease with increasing geologic time (Veizer and Hoefs, 1976).
- vii) Biological fractionation or vital effects. Some organisms, such as crinoids, produce carbonate that is not in isotopic equilibrium with seawater.

### 6.2.3 Carbon and oxygen isotope results

The sections that follow summarize the carbon and oxygen isotopic results for the Pekisko carbonates. A table listing all results may be found in Appendix III.

#### 6.2.3.1 Calcite components

- (1) Micrite (n=10) samples yield  $\delta^{18}\text{O}$  values between -10.02 and -1.79 ‰ VPDB (mean = -7.64 ‰) and  $\delta^{13}\text{C}$  values ranging between 0.96 and 3.07 ‰ VPDB. These values display a departure from original Mississippian marine calcite with a depletion in  $\delta^{18}\text{O}$  and little variation in  $\delta^{13}\text{C}$  (Figure 6.1A).
- (2) Crinoids (n=11) have  $\delta^{18}\text{O}$  values ranging from -9.97 to -3.93 ‰ VPDB (mean = -6.14 ‰) and  $\delta^{13}\text{C}$  values ranging from 0.35 to 2.53 ‰ VPDB. The  $\delta^{18}\text{O}$  values are much depleted with respect to Mississippian marine calcite likely due to the fact that most crinoids have been replaced by syntaxial cements sometime after deposition (Figure 6.1A). On the other hand,  $\delta^{13}\text{C}$  values remain within the Mississippian range or just below.



- (3) Fibrous calcite cements (n=4) are later cements and form within to outside the trend seen in other calcite cements. The  $\delta^{18}\text{O}$  values are from -5.46 to -4.19 ‰ VPDB (mean = -4.99 ‰) and  $\delta^{13}\text{C}$  values from 2.12 to -8.07 ‰ VPDB. This cement shows more of a covariant trend lacking in other calcite cement types (Figure 6.1A).
- (4) Blocky calcite cement (n=33) shows three distinct groups or phases. Phase I has  $\delta^{18}\text{O}$  values that range from -7.36 to -4.08 ‰ VPDB (mean = -5.30 ‰) and  $\delta^{13}\text{C}$  values from -4.74 to 3.61 ‰ VPDB. Phase II  $\delta^{18}\text{O}$  values range from -10.90 to -9.77 ‰ VPDB (mean = -10.55 ‰) and  $\delta^{13}\text{C}$  values of -0.98 to 9.36 ‰ VPDB. Phase III  $\delta^{18}\text{O}$  values range from -16.31 to -13.45 ‰ VPDB (mean = -14.65 ‰) with  $\delta^{13}\text{C}$  values of -9.24 to 1.51 ‰ VPDB. Phases I through to III show progressive depletion in oxygen isotopes relative to postulated Mississippian marine values (Figure 6.1A).
- (5) Drusy mosaic calcite was very difficult to sample due to its small crystal size and amount therefore only one sample could be measured successfully. The  $\delta^{18}\text{O}$  value was -5.56 ‰ VPDB and  $\delta^{13}\text{C}$  value was 1.29 ‰ VPDB. They are both depleted with respect to Mississippian marine calcite (Figure 6.1A).
- (6) Neomorphic calcite spar (n=14) shows slightly more depletion in both isotopes relative to micrite and crinoid values and is associated with Phase II blocky calcite values (Figure 6.1A). The  $\delta^{18}\text{O}$  values range from -13.22 to -8.13 ‰ VPDB (mean = -10.91 ‰) and  $\delta^{13}\text{C}$  values from -3.24 to 5.41 ‰ VPDB.

#### 6.2.3.2 Dolomite

- (1) Pervasive dolomite (n=37) has  $\delta^{18}\text{O}$  values from -10.08 to 0.43 ‰ VPDB (mean = -3.43 ‰) and  $\delta^{13}\text{C}$  values from 1.32 to 4.54 ‰ VPDB for fine (15-50  $\mu\text{m}$ ) pervasive dolomite (n=27). Coarse (50-220  $\mu\text{m}$ ) pervasive dolomite (n=10) has  $\delta^{18}\text{O}$  values from -10.44 to -1.00 ‰ VPDB (mean = -6.20 ‰) and  $\delta^{13}\text{C}$  values from 1.93 to 4.61 ‰ VPDB. Although the stable isotope values are quite scattered the overall trend in results is covariant

whereby some values (for fine samples) are within the postulated Mississippian marine dolomite (Figure 6.1B).

- (2) Selective dolomite (n=5) yield  $\delta^{18}\text{O}$  values from -5.07 to -9.73‰ VPDB (mean = -6.87 ‰) and  $\delta^{13}\text{C}$  values from 0.05 to 2.17 ‰ VPDB. These values also show a covariant trend which is depleted with respect to Mississippian marine dolomite (Figure 6.1B). Some of the  $\delta^{13}\text{C}$  results are more depleted than those of pervasive dolomite.
- (3) Dissolution seam-associated dolomite (n=1) has a  $\delta^{18}\text{O}$  value of -3.97‰ VPDB and a  $\delta^{13}\text{C}$  value of 3.15‰ VPDB (Figure 6.1B). Only one sample could be taken by micro-drilling without contamination, therefore no distinct trends can be determined for this dolomite type.
- (4) Saddle dolomite (n = 1) has a  $\delta^{18}\text{O}$  value of -12.53 ‰ VPDB and a  $\delta^{13}\text{C}$  value of -0.55 ‰ VPDB. This form of dolomite is considered to have formed later due to the extremely depleted carbon and oxygen isotope values (Figure 6.1B) and petrographic evidence.
- (5) Void-filling dolomite (n=5) has  $\delta^{18}\text{O}$  values from -6.26 to -1.53 ‰ VPDB and  $\delta^{13}\text{C}$  values from 1.67 to 2.99 ‰ VPDB. These values highlight once again the covariant trend observed throughout all dolomites (Figure 6.1B).

#### 6.2.4 Strontium isotopes

Strontium is usually observed in carbonates in trace amounts. Its isotope composition is variable due to the decay of naturally occurring radioactive  $^{87}\text{Rb}$  to stable  $^{87}\text{Sr}$  (Faure, 1991). Strontium isotope variations in ancient limestones and dolomites are useful indicators of fluid compositions and diagenetic mechanisms. Unlike oxygen and carbon stable isotopes and trace elements, strontium isotopes are a direct record of the isotopic compositions of the fluid that formed carbonate minerals (Banner, 1995). This is due to the fact that strontium isotopes are not fractionated during the precipitation of carbonates (Faure, 1991). Therefore marine carbonates that have not been subjected to diagenetic fluids should record the strontium isotopic composition of the marine fluids at that time. Based on this premise, several workers such as Burke et al. (1982) and Denison et al. (1994) have constructed  $^{87}\text{Sr}/^{86}\text{Sr}$  curves reflecting the strontium

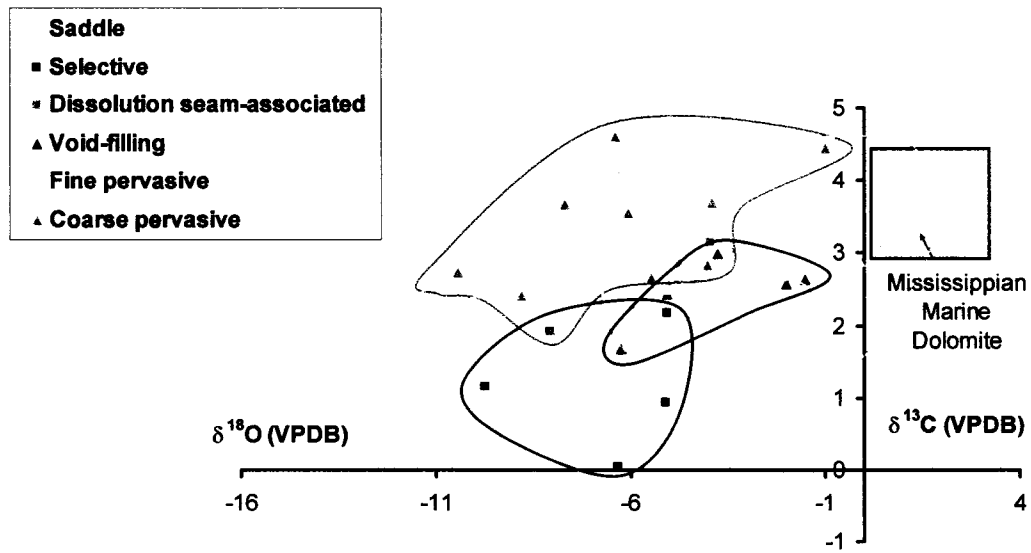
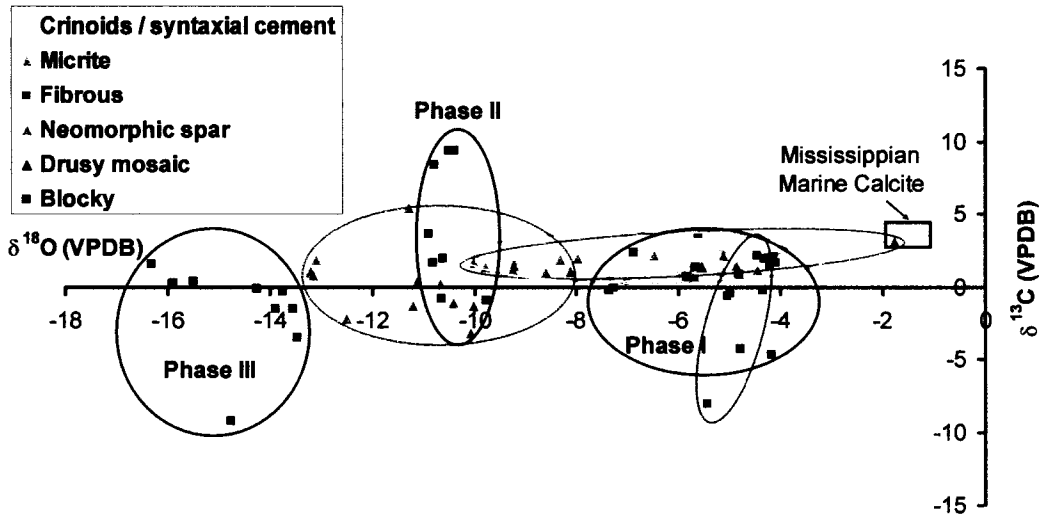


**Figure 6.1 A)** Carbon and oxygen stable isotopic compositions for calcite components. The box represents Mississippian marine calcite (Al-Aasm 2000).  
**B)** Carbon and oxygen stable isotopic compositions for dolomite phases. The box represents Mississippian marine dolomite (Al-Aasm 2000).

isotopic composition through geologic time. An  $^{87}\text{Sr}/^{86}\text{Sr}$  range of 0.7078 – 0.7080 was suggested for the mid-Mississippian (Denison et al., 1994). Carbonate minerals receive their strontium signature from the diagenetic fluids during diagenesis. The composition of these fluids is controlled by prior interaction with rocks and minerals (e.g. clays and feldspars) that are Rb-rich. Therefore a common way of generating fluids with radiogenic strontium isotopic ratios is to have meteoric fluids in contact with sandstones or brines passing through shale sequences. Because of this strontium isotopes are also useful tracers of subsurface fluid movement.

### 6.2.5 Strontium isotope results

Figure 6.2 displays  $^{87}\text{Sr}/^{86}\text{Sr}$  values plotted against  $\delta^{18}\text{O}$  values for certain calcite and dolomite phases within the Pekisko Formation. Calcite cements generally have more enriched strontium isotope values than dolomite phases, with the exception of blocky calcite which records the highest radiogenic strontium value at 0.709957. Fibrous calcite cement has the lowest value of 0.708481. Notice also that with decreasing  $\delta^{18}\text{O}$ , strontium isotope values increase for both calcites and dolomites. All carbonate cements have enriched ratios relative to Mississippian seawater. The dolomites sampled have a broad range of values. Pervasive dolomite (n = 7) has values between 0.708448 and 0.709646, selective dolomite (n = 3) has values from 0.708795 to 0.709499 and void-filling dolomite has a value of 0.708613. Figure 8.4B illustrates  $^{87}\text{Sr}/^{86}\text{Sr}$  values plotted against  $\delta^{18}\text{O}$  values for dolomites and calcites and their associated wells. For well 1, note the pervasive dolomite value compared to the coarse selective dolomite which is post vadose calcite cement. The fine pervasive dolomite is believed to have formed early and the selective dolomite after subaerial exposure. Dolomite recrystallization is believed to have occurred subsequent to meteoric influx at the paleoexposure surface as reflected by more radiogenic values in wells closest to the subcrop edge (wells 2, 5 and 6). This plot also shows that as we pass from well 6 (closest to the subcrop edge) through to well 3 (farthest from the edge) dolomites and calcites become decreasingly radiogenic.

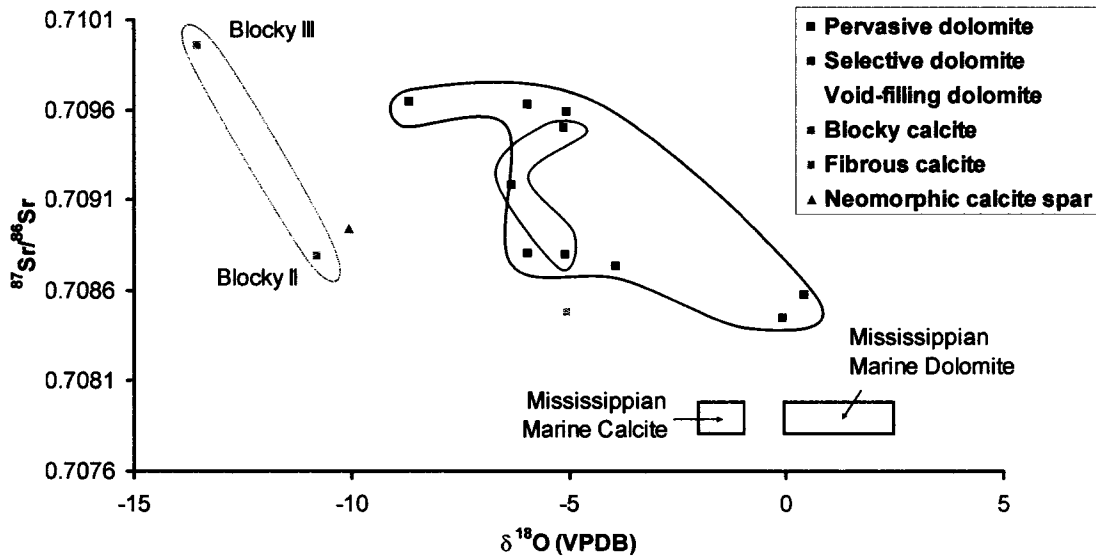


**Figure 6.2**  $^{87}\text{Sr}/^{86}\text{Sr}$  versus oxygen isotope compositions of calcite and dolomite phases. The boxes represent Mississippi marine calcite and dolomite (Burke et al. 1982, Denison et al. 1994).

### 6.3 Elemental analysis

Calcite and dolomite phases in the carbonates of the Pekisko Formation were sampled and analyzed for calcium, magnesium, iron, manganese and strontium using ICP-OES in order to determine stoichiometry, diagenetic pathway models and fluid sources. A table with a complete compilation of all the results can be found in Appendix III.

#### 6.3.1 Elemental theory

Dissolution and re-precipitation processes stabilize carbonates by diagenetic fluids passing through them (Bathurst, 1975). The trace elements within the carbonates are combined with those present in the intervening fluid as a result of these processes. They are subsequently repartitioned during recrystallization, mineral precipitation and stabilization (Veizer, 1983).

Minor and trace elements are incorporated into carbonate minerals in the following ways (McIntire, 1963; Zemmann, 1969 in Brand and Veizer, 1983):

- i) Substitution for  $\text{Ca}^{2+}$  in the  $\text{CaCO}_3$  lattice ( $\text{Ca}^{2+}$  and/or  $\text{Mg}^{2+}$  for dolomites)
- ii) Incorporated interstitially between structural planes
- iii) Substitution at defect sites in the lattice
- iv) Adsorption due to remnant ionic charges

The most common way minor and trace elements are incorporated into the minerals is by substitution, the most important concerning the diagenetic study of carbonates. A common rule is that ions with a larger radii than Ca ( $>1.08 \text{ \AA}$ ) are generally excluded from Mg sites. Ions which have a smaller radii than Mg ( $< 0.80 \text{ \AA}$ ) are almost always excluded from Ca sites (Jacobson and Uzdowski, 1976; Kretz, 1982). The incorporation of trace elements into carbonate minerals is controlled by (Tucker and Wright, 1990):

- (1) the trace element concentration in the fluid;
- (2) the diagenetic system's water/rock ratio; and,
- (3) the trace elements distribution coefficient (D) for a specific mineral-fluid system.

The degree at which D will deviate from unity determines at what magnitude a trace element will be concentrated in the mineral phase or the fluid. If  $D > 1$  the trace element is preferentially incorporated into calcite or dolomite however when  $D < 1$  it is partitioned into the fluid (Veizer, 1983; Tucker and Wright, 1990). In dolomites, Sr, Fe and Mn commonly substitute for  $\text{Ca}^{2+}$ . Since Fe and Mn have smaller radii they fit easily into the lattice and are therefore concentrated in the mineral. However, Sr has a much larger radius and remains behind in the fluid during dolomitization (Allan and Wiggins, 1993). Concentrations of Sr are normally high in formation fluids and seawater and low in fresh water. When values are low, dolomites are often interpreted to have been derived from a mixed meteoric-marine environment. Because Fe and Mn are present in low concentrations in seawater but relatively high in formation fluids, these elements become more important to decipher the dolomitizing environment. With these trends, Fe and Mn are good indicators of burial dolomitization formed from saline formation waters (Land, 1980).

### **6.3.2 Calcium and Magnesium: dolomite stoichiometry**

Calcium and magnesium concentrations were determined for dolomites and calcites in order to establish their stoichiometry. A dolomite which is ideal or stoichiometric contains equal molar proportions of  $\text{CaCO}_3$  and  $\text{MgCO}_3$  and it is in this form that dolomite is least soluble and therefore the most stable (Boggs, 1992). Dolomite crystals that are non-stoichiometric are structurally and compositionally inhomogeneous and therefore unstable and as a result will dissolve or alter more readily. It is for this reason that with time non-stoichiometric dolomite will equilibrate to stoichiometric dolomite and therefore older dolomites are stoichiometric compared to recent dolomites (Lumsden and Chimahusky, 1980). In this study, pervasive dolomite was the only phase that could be sampled without contamination by calcite. These dolomites were found to be non-stoichiometric throughout the study area excluding those in wells 1 and 7 which were nearly stoichiometric. The following describes pervasive dolomite stoichiometries for all of the wells:

- (1) Well 1 pervasive dolomites (n=3) have values ranging from 50.34 to 56.52 mole % CaCO<sub>3</sub> with a mean value of 52.79 mole % CaCO<sub>3</sub>.
- (2) Well 3 (n=2) varies in composition from 55.42 to 58.16 mole % CaCO<sub>3</sub> with a mean of 56.79 mole % CaCO<sub>3</sub>.
- (3) The well 4 (n=1) pervasive dolomite had a composition of 58.45 mole % CaCO<sub>3</sub>.
- (4) Well 5 (n=1) has a value of 61.47 mole % CaCO<sub>3</sub>.
- (5) Well 6 (n=1) has a composition of 53.38 mole % CaCO<sub>3</sub>.
- (6) The pervasive dolomites in well 7 (n=2) have values varying from 51.70 to 55.45 mole % CaCO<sub>3</sub> with a mean composition of 53.58 mole % CaCO<sub>3</sub>.
- (7) Well 8 pervasive dolomites (n=2) have values ranging from 56.23 to 57.06 mole % CaCO<sub>3</sub> with a mean value of 56.65 mole % CaCO<sub>3</sub>.
- (8) Well 9 dolomites (n=2) range in composition from 56.27 to 65.70 mole % CaCO<sub>3</sub>. The mean value is 60.99 mole % CaCO<sub>3</sub>. Values > 60% are dolomitic limestones.

### 6.3.3 Iron and Manganese

Because of their similar behavior in solution and their similar distribution coefficients ( $D > 1$ ) in carbonates, iron and manganese will be described together. The Eh-pH of a fluid will have a great effect on the distribution of these two elements in the fluid and in the carbonate. The Fe<sup>2+</sup> and Mn<sup>2+</sup> that exist within oxidizing fluids with a positive Eh will usually be present in their oxidized forms therefore making them unavailable to be incorporated into the carbonates lattice (Tucker and Wright, 1990). However in a reducing environment both iron and manganese will be incorporated into calcite and dolomite structures. Due to this dependence on Eh-pH conditions, resulting variations in carbonate Fe<sup>2+</sup> and Mn<sup>2+</sup> can be used to determine the diagenetic pathways of carbonates during diagenesis (James and Choquette, 1984; Tucker and Wright, 1990). In the following subsections, results for iron and manganese within both calcite and dolomite components are summarized.



### **6.3.3.1 Calcite**

- (1) Blocky calcite (n=9) concentrations for Fe range from below detection limit (< DL) to 291 ppm with a mean of 53 ppm. Mn values range from 11 to 163 ppm with a mean of 54 ppm.
- (2) Fibrous calcite (n=4) yields values for Fe from < DL to 55 ppm with a mean of 35 ppm. The Mn values range from 14 to 25 ppm with a mean value of 17 ppm.

### **6.3.3.2 Dolomite**

Pervasive dolomite was the only dolomite phase measured for concentrations of Fe and Mn (n=14) and yielded iron concentrations between 39 and 921 ppm with a mean of 338 ppm. Manganese values ranged between 22 and 175 ppm with a mean concentration of 80 ppm.

### **6.3.4 Strontium**

With a distribution coefficient < 1, strontium should be preferentially incorporated into the fluid phase. The following is a summary of results for strontium concentrations in calcite and dolomite.

#### **6.3.4.1 Calcite**

- (1) Blocky calcite (n=9) values for Sr range from 202 to 1382 ppm with a mean of 468 ppm.
- (2) Fibrous calcite (n=4) has concentrations of Sr from 430 to 550 ppm with a mean value of 383 ppm.

### **6.3.4.2 Dolomite**

Pervasive dolomite (n=14) yields a range of Sr values from 59 to 775 ppm with a mean of 176 ppm.

## **6.4 Fluid inclusions**

### **6.4.1 Fluid inclusion theory**

Fluid inclusions are the only direct record of primary diagenetic fluids. They are fluid-filled cavities, usually 1-10 $\mu$ m in diameter, in carbonate minerals (Roedder, 1981). Fluid inclusions form as pore fluid is trapped within lattice defects in actively growing crystals in pores or fractures (Allan and Wiggins, 1993). For this reason cements make better candidates for fluid inclusion studies than replacement dolomites. Primary inclusions are trapped during the crystal growth and contain a sample of the fluid responsible for precipitation of the diagenetic phase (Goldstein and Reynolds, 1994). Secondary inclusions represent the fluid that did not precipitate the dolomite. They are usually trapped along microfractures that cut the surface of the crystal after it has grown. In diagenetic studies there are two common types of fluid inclusions: low temperature (<50°C) single-phase (liquid only) inclusions and higher temperature (>50°C) two-phase liquid-vapor inclusions (Allan and Wiggins, 1993). It is from these two-phase fluid inclusions that the homogenization temperature can be determined. This is the temperature at which two phases become one phase and represents the minimum temperature of crystallization of the host mineral. The salinity of the fluid is determined by freezing an inclusion and then raising its temperature in small increments and recording the temperature at which it fully melts (Allan and Wiggins, 1993). The trapped fluid is composed of any one of the following: an aqueous liquid, an aqueous vapor bubble, a hydrocarbon liquid or a hydrocarbon gas (a halite daughter crystal may exist in aqueous inclusions). For the purpose of this study, fluid inclusions will provide fluid entrapment temperatures to establish the timing of dolomitization and fluid salinity to discriminate between meteoric, marine and hypersaline parent fluids.

#### **6.4.2 Fluid inclusion results**

Due to the extremely small crystal size of the different dolomite phases (with the exception of saddle dolomite) temperature and salinity measurements could not be performed. However upon visual examination of these inclusions it was possible in some cases to decipher whether they were single phase or two phase inclusions. With this information an approximate temperature of formation could be deduced. Within the ten prepared thin sections most inclusions present in pervasive dolomite were single phase inclusions with the exception of some two phase inclusions present in well 5. Since very fine pervasive dolomite is believed to have formed early due to its small crystal size and isotopic trend, it is safe to assume that it formed at relatively low temperatures ( $< 50^{\circ}\text{C}$ ). In contrast to this, void-filling cements (both euhedral and anhedral or saddle) were observed to contain primary two-phase fluid inclusions which were also too minute to measure accurately. This means that they must have precipitated at temperatures  $> 50^{\circ}\text{C}$  and therefore formed later than pervasive dolomite. This is in agreement with petrographic and geochemical interpretations. Primary two-phase fluid inclusions (again too small to measure accurately) were also described within blocky calcite cements throughout the wells. This as stated previously, denotes a later genesis in the presence of hotter fluids ( $>50^{\circ}\text{C}$ ). In several instances, two phase fluid inclusions large enough to measure could not be positively identified as primary and therefore were not measured.

## CHAPTER VII

### POROSITY OF THE PEKISKO FORMATION

#### 7.1 Introduction

An important aspect of petroleum geology is the reservoir potential of carbonate rocks. Since one third of the world's petroleum reserves are within carbonates (Boggs, 1992), it is important for the petroleum geologist to study its reservoir potential using porosity and permeability. It is also important to look at not only the absolute porosity in the rock (defined as the amount of pores in a sedimentary rock) but to measure the effective porosity. This type of porosity takes into consideration the interconnectedness of the pores in a volume of rock which is what will control fluid movement. Not surprisingly, effective porosity will usually be several percent lower in a rock volume than absolute or total porosity.

The modified classification of Choquette and Pray (1970) has been utilized to classify the porosity types in the Pekisko Formation carbonates. Porosity that has formed as a result of sedimentological or depositional processes has been identified as primary porosity, whereas secondary porosity has been used to classify diagenetic types.

For this study qualitative measurements have been made petrographically using a standard microscope and ultraviolet fluorescence. Porosity values for some of the wells were also used, provided by Burlington (Jeff Packard). Quantitative image analysis studies were also attempted but failed mainly due to the fact that thin section epoxies were not impregnated with a blue dye.

Porosity development in the Pekisko Formation has mainly been controlled by dolomitization therefore the origin of dolomite becomes very important. Dolostone sections have porosities that range from very low to 20% and permeabilities from very low up to 20000 mD. Very high permeabilities are mostly associated with fractured intervals.

## **7.2 Primary porosity**

Primary porosity is present in the sediments at the time of their deposition and is usually fabric selective (Moore, 1989). For Pekisko carbonates primary porosity also tends to be facies selective. Observed only in the limestone facies, primary porosity types include: interparticle, intraparticle and fenestral porosities. Most of the pore spaces however have been cemented by different phases of calcite cement.

Interparticle pores are spaces between grains. Where they do occur, very few (<1%) of them have been preserved. Grainstones have the best examples of interparticle porosity (Plate G-1). Peloid and ooid grainstones show relatively little compaction and pores are filled with blocky, syntaxial, bladed and isopachous calcite cements. Other fossiliferous and crinoidal grainstones are often well compacted and have little to no interparticle pores.

Intraparticle porosity is a very minor porosity type within the Pekisko carbonates. It is the pore space within fossils that has been occluded primarily by calcite spar or drusy calcite cements. It has been observed in gastropods, brachiopods, ostracods and calcispheres (Plate G-2).

Fenestral porosity is the open space developed primarily by degassing within algal mudstones (Boggs, 1992). It was observed in only 2 samples where pores were cemented by sparry to blocky calcite (Figure 3.2, second photo from the right).

## **7.3 Secondary porosity**

Secondary porosity originates from diagenetic processes occurring sometime after deposition. Dissolution and dolomitization are the two most important events responsible for the formation of secondary porosity (Moore, 1989). In the Pekisko Formation these processes have created several secondary pore types including: vuggy, moldic, intercrystalline, breccia and fracture. These pore types account for the majority of the porosity in Pekisko carbonates.

Moldic porosity is the partial or complete dissolution of bioclasts and results in molds within an often muddy matrix. This porosity type occurs dominantly in dolostones in association with vuggy porosity (Plate G-4) but also occurs in grainstones whereby fossils have been leached out (Plate G-3 and Plate H-1). This type of porosity is both fabric and facies selective. Molds tend to be large and rounded or arc shaped indicating possible dissolution of ooids, brachiopods or ostracods. Moldic porosity does not tend to be interconnected and therefore contributes very little to the overall permeability of the rock.

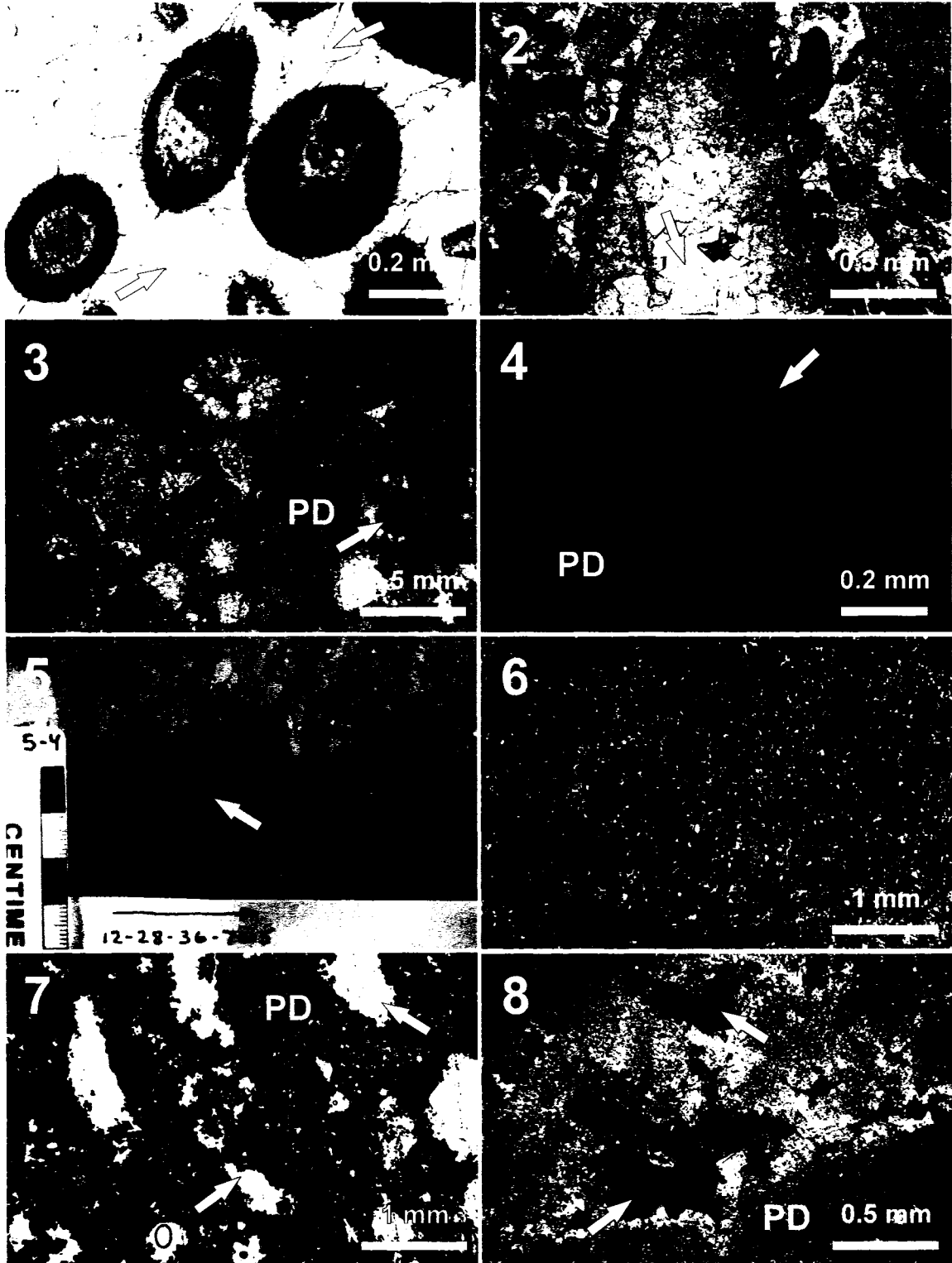
Vuggy porosity is the enlargement of voids by dissolution processes within pervasively dolomitized sections. Vugs usually cross-cut grains and/or cement boundaries indicating that they are not fabric selective however they are facies selective. They are from < 1cm to more than a few centimetres in size and are sometimes lined with bitumen (Plate G-7), filled with blocky calcite and/or lined with void-filling dolomite (Plate G-8 and Plate H-2). Similar to moldic porosity, vugs are poorly connected and contribute little to permeability. Since vugs and molds are associated in some instances it is possible that the vugs are merely molds enlarged by solution.

Intercrystalline porosity is best developed within planar euhedral pervasively dolomitized units between individual crystals (Plate G-6 and Plate H-4). It is both fabric and facies selective in nature. Because of its interconnectedness, it contributes significantly to permeability. However many of these pores have been occluded by pyrobitumen and/or blocky calcite cement leading to a major decrease in porosity and permeability.

Breccia porosity is the result of depositional, solution or karst events. It does not selectively occur in certain fabrics or facies. Although this pore type has the potential to yield very high porosities, breccia pores are always filled with calcite cement and/or dolomite (Plate G-5).

Another important type of porosity not mentioned in previous sections is microporosity. Although not apparent using the highest magnification on a standard microscope, this type of porosity contributes significantly to the overall porosity of carbonates. SEM analysis has shown that micropores are common within and between individual crystals. Plate H-3 shows micro-

**PLATE G**





intercrystalline porosity as well as intracrystalline porosity. Dissolution pits within individual dolomite crystals are more obvious in Plate H-5.

#### **7.4 Relationship between porosity and permeability**

In the Pekisko carbonates, permeability and porosity have been influenced by both sedimentology and diagenesis. Porosity and permeability determine where and how the petroleum will migrate within a reservoir and porosity alone will determine how much of that petroleum will be trapped. Therefore deciphering the origin, evolution and preservation of porosity becomes very important economically as well as academically.

Porosity and permeability play a very important role in the diagenesis of carbonate rocks by regulating the flow of fluids passing through them that result in dissolution and cementation (Boggs, 1992). As a result it becomes very important to quantify the amount of interconnected pore spaces within the rock sequence. In an effort to make these measurements, image analysis studies were performed on all of the prepared thin sections. Unfortunately as time progressed it became clear that this method would not prove effective. Since the thin sections were not impregnated with blue dye, this caused major difficulties in selecting porosity color pixels which were colored similar to that of the rock colour pixels. Attempts that were made to measure very large vugs within the dolostones were unsuccessful as well. Although some pore pixels could be selected successfully, when repeated for the same field of view to determine error, results were off by 5-10% from each other. Error should have been in the order of only a few percent. Whole rock porosity and permeability results were also provided by the Energy and Utilities Board (EUB) core research center and were used for comparison with image analysis results. Core measurement depths were used to get the proper thin section depths for comparison. Again values were off by 10-15%. Another weakness discovered in using image analysis for porosity and permeability measurements is the fact that the thin section is only a representation of two dimensions, whereas measurements made directly on the core is in three dimensions.

The permeability - porosity plot in Figure 7.1A displays a covariant trend for intercrystalline porosity only. This shows that with increasing porosity there is an increase in permeability indicating the effectiveness of intercrystalline porosity in creating interconnectedness. Therefore intercrystalline porosity, if not occluded by cement, will provide an efficient channel system for fluid movement. However for all other porosity types, permeability values associated with porosity values above ~10% remain fairly constant. Therefore permeability is not a function of the amount of porosity and in fact remains fairly constant despite an increase in porosity. This indicates that moldic, vuggy and intracrystalline porosities will be less efficient at providing pathways for fluid circulation.

### **7.5 Diagenetic controls on porosity evolution**

Diagenesis is a process that can both destroy and enhance porosity within carbonate sequences. Porosity distribution within the Pekisko Formation is controlled mainly by dolomitization. Although primary porosity and permeability may have been significant in the Pekisko carbonates initially, diagenesis has contributed to an overall increase in porosity with relatively no change in permeability as discussed previously.

The dolomite percentage - porosity percentage relationship is shown in Figure 7.1B. This plot shows that intergranular porosity is present only in samples with very low amounts of dolomite. It occurs mainly in grainstones at very low percentages and displays a slight increase in porosity with dolomitization. This indicates that partially dolomitized intervals have a higher porosity likely due to the dolomite replacement process. For vuggy and intercrystalline porosity types the percentage of porosity decreases significantly with slightly increasing percentage of dolomite. This indicates that progressive dolomite recrystallization may be responsible for loss of porosity within these wells.

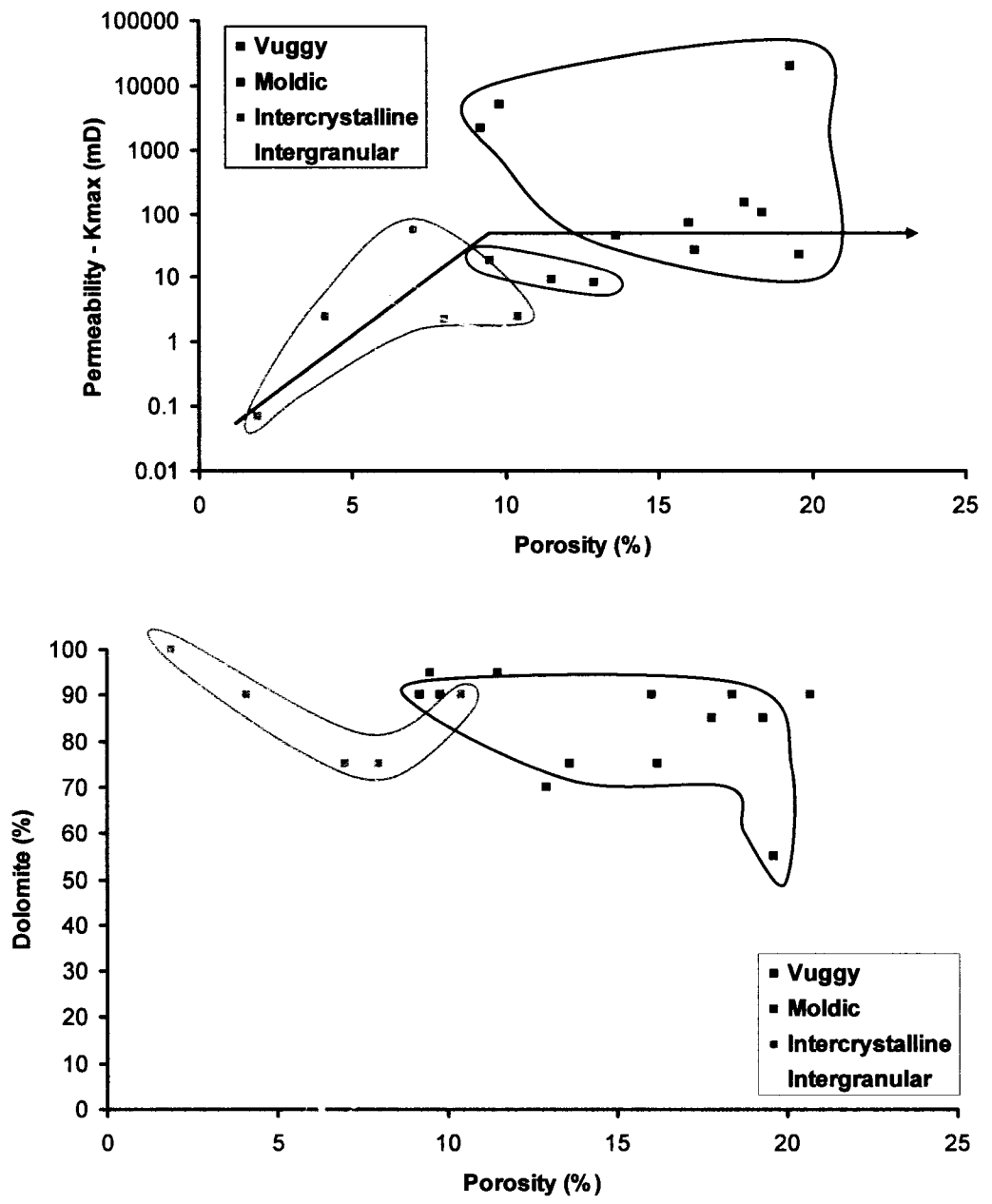
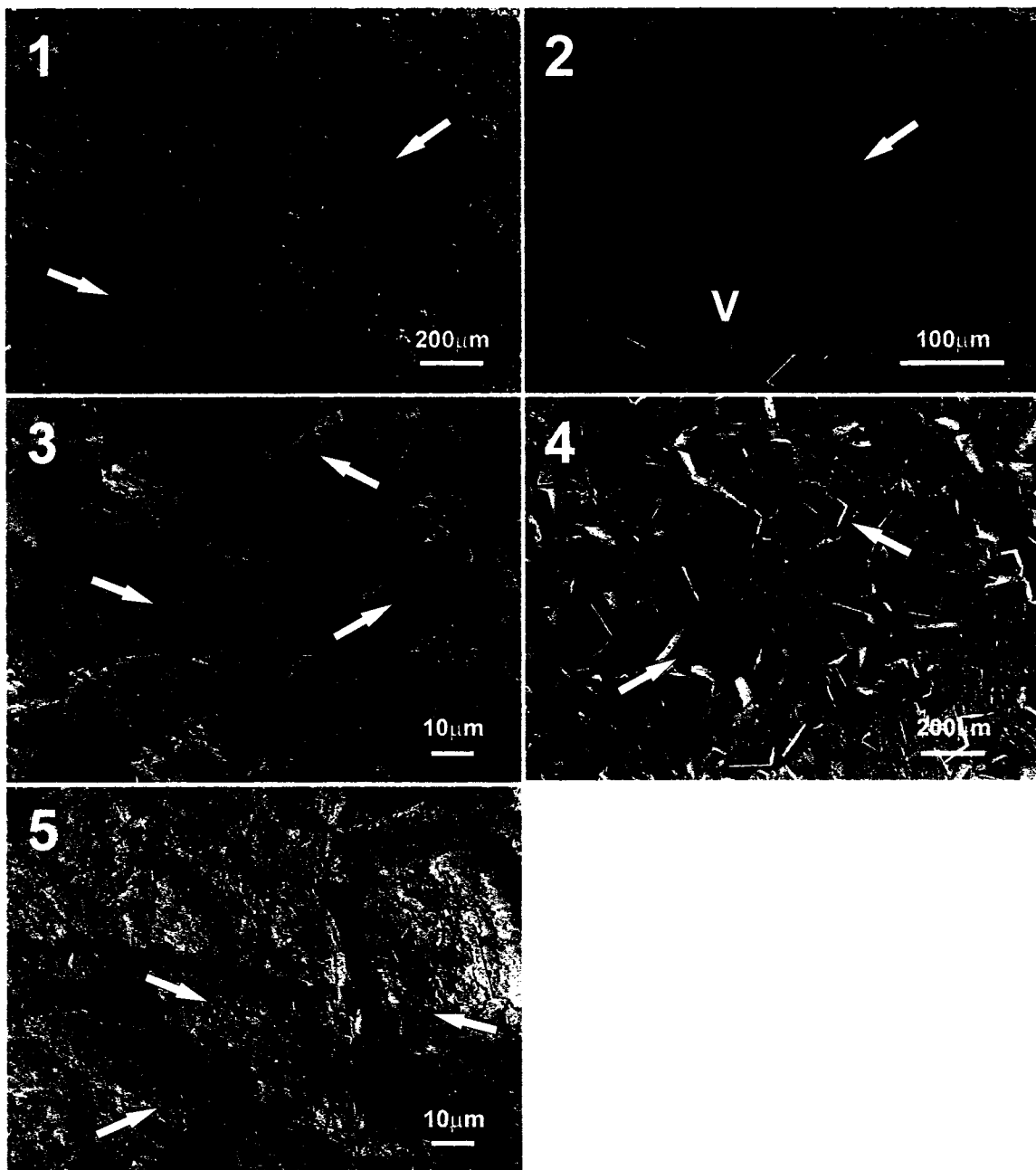


**Figure 7.1 A)** Porosity versus permeability plot for the various porosity types.

**B)** Porosity versus percentage of dolomite for the same porosity types.

**PLATE H**



## **CHAPTER VIII DISCUSSION AND INTERPRETATION OF DIAGENESIS**

### **8.1 Introduction**

The following sections will discuss in detail the diagenesis of the Pekisko Formation carbonates. The interpretations have been made from the combination of stratigraphic, petrographic and geochemical results. These were used to construct a paragenetic sequence of events presented in Figure 8.1. This figure summarizes all diagenetic processes that have affected the carbonates and their relative timing.

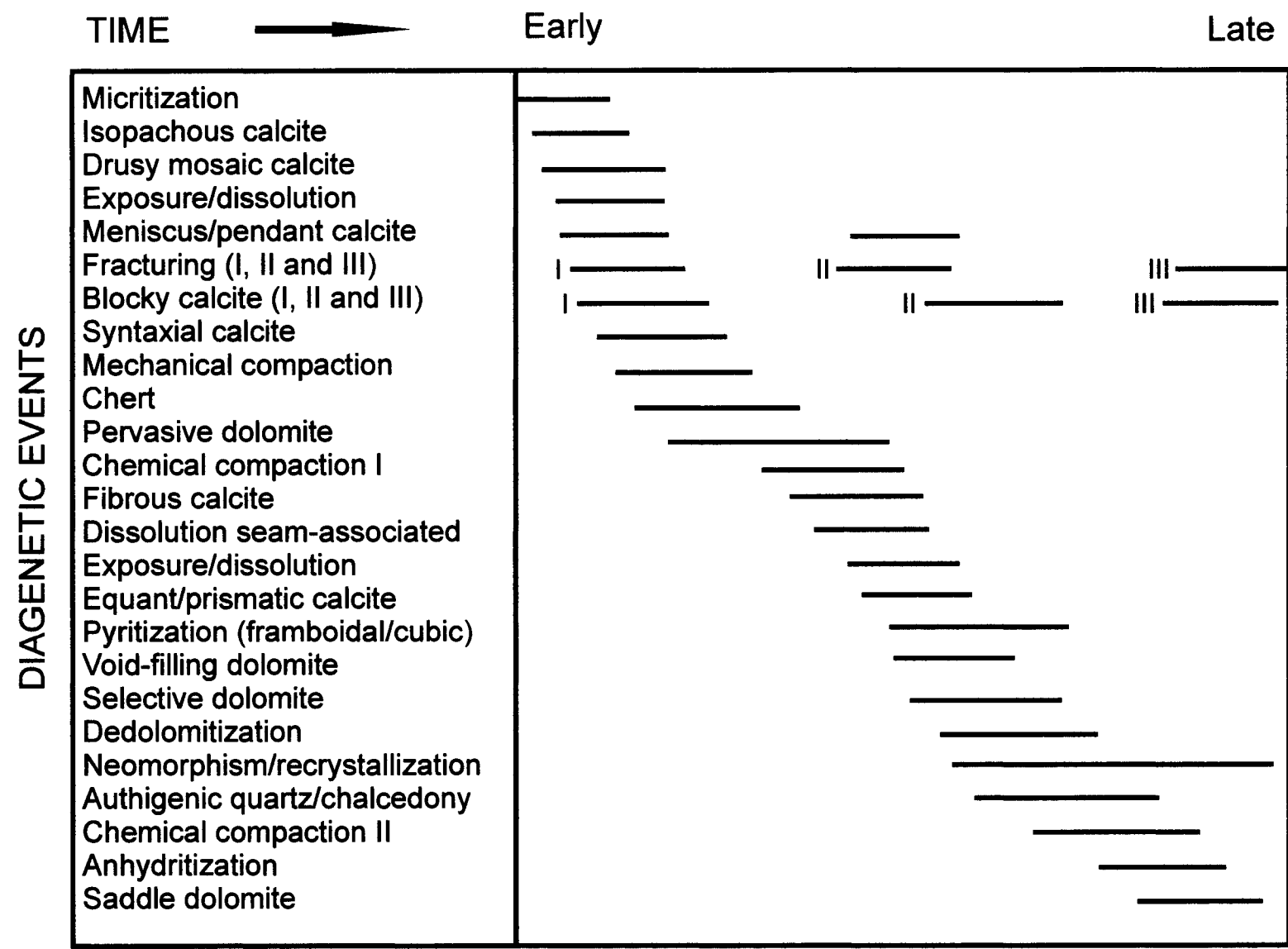
### **8.2 Micritization**

The earliest diagenetic event to occur in the Pekisko Formation is micritization, specifically the formation of micrite rims. Bacteria form these rims by repeatedly boring into the surface of the fossils or allochems leaving behind voids that are subsequently filled with micrite (Bathurst, 1966; Boggs, 1992). In some instances fossils are filled with drusy mosaic calcite cement, but in other instances grain degradation leads to complete micritization of the grain forming a peloid (Tucker, 1981). Since isopachous cements surround grains with micrite envelopes then micritization must have occurred prior to calcite cementation during the initial stages of burial in a marine setting (Plate C-6).

### **8.3 Calcite cementation**

Calcite cementation plays an important role in the diagenetic history of the Pekisko Formation. It began early in the marine environment and continued through to deep burial. As a result much of the potential porosity has been occluded by later calcite cements or never formed due to early lithification.

Figure 8.1 Paragenetic sequence of events for carbonates from the Pekisko Formation.



### 8.3.1 Isopachous rinds

As mentioned previously, isopachous cements are only present as an outer coating of calcite cement on ooids (Plate C-5). The thin elongate crystals that make up these rinds are typically found in environments with a high supply of  $\text{CO}_3^{2-}$  (Given and Wilkinson, 1985). Such then include mixed marine–meteoric environments (Choquette and James, 1987), vadose meteoric environments with rapid fluid flow events (Robertson, 1989) and the sea floor marine environment. Under CL this thin cement is non-luminescent indicating that the incorporation of Mn and Fe did not occur. Generally this is true for cement phases precipitated in an oxidizing marine environment (Steinhauff, 1989). These elements would have been unavailable for incorporation into the calcite lattice (Tucker and Wright, 1990). Petrographic evidence suggests that isopachous cements formed after the formation of micrite rims but prior to early blocky calcite and mechanical compaction. Since sampling for stable isotope and trace element analyses was impossible, conclusions are based exclusively on petrographic evidence. This phase pre-dates compaction and is thought to have formed very early subsequent to deposition by marine fluids.

### 8.3.2 Drusy mosaic calcite

Drusy mosaic calcite can form in meteoric and burial environments (Choquette and James, 1987; Tucker and Wright, 1990). In the Pekisko Formation drusy mosaic calcite cement occurs as crystals within interparticle and intraparticle pores (Plate C-3 and 4). Only one stable isotope measurement was taken resulting in a value of  $-5.56\text{‰}$  for  $\delta^{18}\text{O}$  and a value of  $1.29\text{‰}$  for  $\delta^{13}\text{C}$ . It occurs in the same range of values as micrite (formed early in a marine setting) but also within the range of values for syntaxial cements, formed in a meteoric setting (Figure 6.1A). However drusy mosaic types do not typically form in a marine environment. Further, CL characteristics indicate varying luminescent zones (Plate C-4). The first zone is relatively non-luminescent consistent with a well oxidized environment inhibiting the uptake of  $\text{Fe}^{2+}$  and  $\text{Mn}^{2+}$  (Boggs, 1992). Next there are several thin brightly luminescent zones suggesting more reducing conditions whereby  $\text{Mn}^{2+}$  uptake is favored. The rest of the pore space is filled with dull luminescent cement showing that further burial in association with a reducing environment has



favored  $\text{Fe}^{2+}$  concentrations which quench the luminescence. According to Boggs (1992) this trend in cement stratigraphy is commonly reported and displays a trend from oldest to youngest phases. Based on petrographic and CL observations as well as stable isotopes, this cement seems to have formed throughout meteoric to early burial realms.

### 8.3.3 Blocky calcite

Blocky calcite consists of coarse equant (~ 0.5 mm) crystals with plane sided contacts (Plate C-1 and 2). Petrographically, blocky calcite displays dull to bright CL characteristics indicative of progressive reducing conditions. In some instances it encloses framboidal pyrite (Plate C-1) and pyrobitumen (only Phase II) and fills early to late stage fractures and vuggy pores (Plate D-8). There are three distinct phases of blocky calcite relative to stable oxygen isotopes (Figure 6.1A):

- (1) Phase I is the earliest cement with  $\delta^{18}\text{O}$  values ranging from -7.36 to -4.08‰ and slightly depleted carbon values. Petrographically these calcites fill fractures which are crosscut by early meteoric syntaxial calcite cements within grainstones. However, they precipitated after meniscus and pendant cements (Figure 8.1). The cross-cutting relationships and geochemistry suggests precipitation in a meteoric realm.
- (2) Phase II occurs concurrently with neomorphic spar associated with paleoexposure. Stable oxygen isotope values have a narrow range between -10.90 and -9.77‰ but carbon has a wide range of values, some within Mississippian marine calcite. This phase may have also formed from meteoric fluid infiltration at the subcrop edge mixing with older meteoric or saline formation fluids.
- (3) Phase III is the latest occurring calcite cement phase. Values range from -16.31 to -13.45‰ for  $\delta^{18}\text{O}$  suggesting a very high temperature of formation related to burial or could indicate meteoric infiltration at the subcrop edge since wells closest to the subcrop record the most depleted values.

According to Choquette and James (1990) deep burial cements typically are enriched in Fe and Mn and impoverished in Sr concentrations. Quite the opposite of this, blocky calcites

analyzed for this study have highly depleted Fe (<DL to 291 ppm) and Mn (11 to 163 ppm) to slightly enriched Sr (202 to 1382 ppm) concentrations (Figure 8.3 A and B). The strontium isotope ratios for the blocky calcite are 0.708789 and 0.709957 which are relatively enriched with respect to Mississippian calcite (Figure 6.2). Fluid inclusions were not measured for calcite, however thin section observations show that primary inclusions in Phase II and III cements are dominantly two phase liquid - vapor inclusions formed at temperatures > 50°C (Allan and Wiggins, 1993). Using Figure 8.2 the following compositions of fluids were determined:

- (1) Phase I blocky calcite formed very early prior to syntaxial cement during seafloor diagenesis. According to Machel (2004) seafloor diagenesis occurs within the first 10m. With a geothermal gradient of 25°C/Km the temperatures of formation would be similar to surface temperatures of 20-30°C. This results in fluid  $\delta^{18}\text{O}$  values of -5 to -10 ‰. These are within expected meteoric signatures for the Mississippian at that paleolatitude (Frank and Lohmann, 1995; Veizer et al., 1999).
- (2) According to petrographic and geochemical studies blocky calcite II precipitated later than blocky calcite I, just after selective dolomite but prior to recrystallization during intermediate burial. At this stage of diagenesis Machel (2004) suggests a depth range of 300-1500m. Two phase fluid inclusions within this cement phase also indicate a temperature of formation above 50°C. Using a geothermal gradient of 25°C/Km, temperatures should have been anywhere from 50°C to 62.5°C. As a result fluid  $\delta^{18}\text{O}$  compositions should have been between -3.5 and -7.5 ‰. These values according to Frank and Lohmann (1995) suggest mixed fluids.
- (3) Blocky calcite III contains two-phase fluid inclusions and crosscuts saddle dolomite indicating higher temperatures and deep burial formation. Deep burial cements should form at depths greater than 1500m (Machel, 2004). In the Pekisko carbonates, blocky calcite III was observed as deep as approximately 4800m. At this depth interval, using a geothermal gradient of 25°C/Km, temperatures of formation would have been from 100°C to 145°C. This suggests fluid  $\delta^{18}\text{O}$  values of -3.5 to 4 ‰ which reflect more saline conditions that may be attributed to the influx of deep brines.

Based on petrographic evidence as well as geochemistry and fluid inclusion observations it is suggested that the fluid may have been meteoric in origin (Phase I) and would have become more radiogenic during mixing with formation waters (Phase II). The latest Phase III blocky calcite phase is believed to have formed during deeper burial by basinal fluids as it post-dates saddle dolomite and has the most radiogenic strontium isotope value.

#### **8.3.4 Syntaxial calcite**

Crinoid fragments commonly act as single crystals and as a result are often nucleated by calcite cements (Flügel, 2004). In the Pekisko carbonates most crinoid fragments within the grainstone facies display syntaxial overgrowth cements (Plate C-6). Petrographically these cements are inclusion-rich and cloudy, a good indication of near surface precipitation (Flügel, 2004). However they can also form during burial as much clearer cements (not present here). Marked twinning shows that this cement phase underwent strain by mechanical compaction and therefore probably formed early. Stable oxygen isotope values are depleted with respect to Mississippian calcite by 2 ‰ to as much as 8 ‰ (Figure 6.1A). The carbon isotope values are within or slightly depleted from postulated Mississippian values. This suggests that the origin for carbon was likely from inorganic carbon enriched fluids (i.e. carbonate buffered) infiltrating the rock. Several authors (Frank and Lohmann, 1995; Meyers and Lohmann, 1985) have observed that cements precipitated near paleoexposure surfaces have water dominated compositions whereas those formed in distal parts of the meteoric environment (with increasing water-rock interaction), exhibit rock dominated cement compositions. Accordingly, syntaxial cements sampled from wells closest to the subcrop edge (wells 5 and 6) display more depleted  $\delta^{18}\text{O}$  values than those sampled from wells farther away from the subcrop edge (well 3). In light of these observations, syntaxial calcite cements are interpreted to have precipitated from meteoric waters infiltrating the carbonates at the Pekisko subcrop edge.

### 8.3.5 Fibrous calcite

Fibrous calcite cement is a relatively minor cement phase in carbonates of the Pekisko Formation. Found only in association with stylolites within dolostones and grainstones, it is thought to have precipitated in conjunction with early chemical compaction at approximate depths of 200-300m (Machel, 2004; Plate C-10). According to Bathurst (1971) and later Wanless (1979), the surrounding limestone during chemical compaction usually remains non-responsive; however in some cases pressure dissolved carbonates can reprecipitate as cement adjacent to stylolites or dissolution seams. Both isotope and trace element attributes were determined for fibrous calcite. The  $\delta^{18}\text{O}$  values show depletion by an order of 3 ‰ from the postulated values for the Mississippian marine calcite with a small range in values (Figure 6.1A). This suggests one of three possibilities, a temperature increase during compaction, meteoric influence in cement precipitation or recrystallization (Allan and Wiggins, 1993). Since fibrous calcite cement is thought to have precipitated from compaction-related interstitial fluids, it is much more likely that  $\delta^{18}\text{O}$  values are indicating a temperature increase. The  $\delta^{13}\text{C}$  signatures show significantly more depletion of up to 10 ‰ from postulated Mississippian marine calcite. This implies that the depletion is due to organic contributions. An  $^{87}\text{Sr}/^{86}\text{Sr}$  isotope ratio of 0.708503 was obtained for fibrous calcite present in a pervasively dolomitized unit. This is slightly radiogenic relative to postulated Mississippian seawater values suggesting that the interstitial fluids of formation were not meteoric (Figure 6.2). In support of this, fluid  $\delta^{18}\text{O}$  compositions yielded values between -5 and 0 ‰ (Figure 8.2) indicative of seawater or mixed fluids. The low concentrations of both  $\text{Mn}^{2+}$  (15 to 26 ppm) and  $\text{Fe}^{2+}$  (<DL to 55 ppm) also indicate that there was no meteoric influence. The higher concentrations of Sr (430 to 550 ppm) are also in agreement with this and may show that formation fluids reflect original seawater (Figure 8.3 A and B). Fibrous calcite is therefore interpreted to have formed just after or along with early chemical compaction from reprecipitated carbonate.

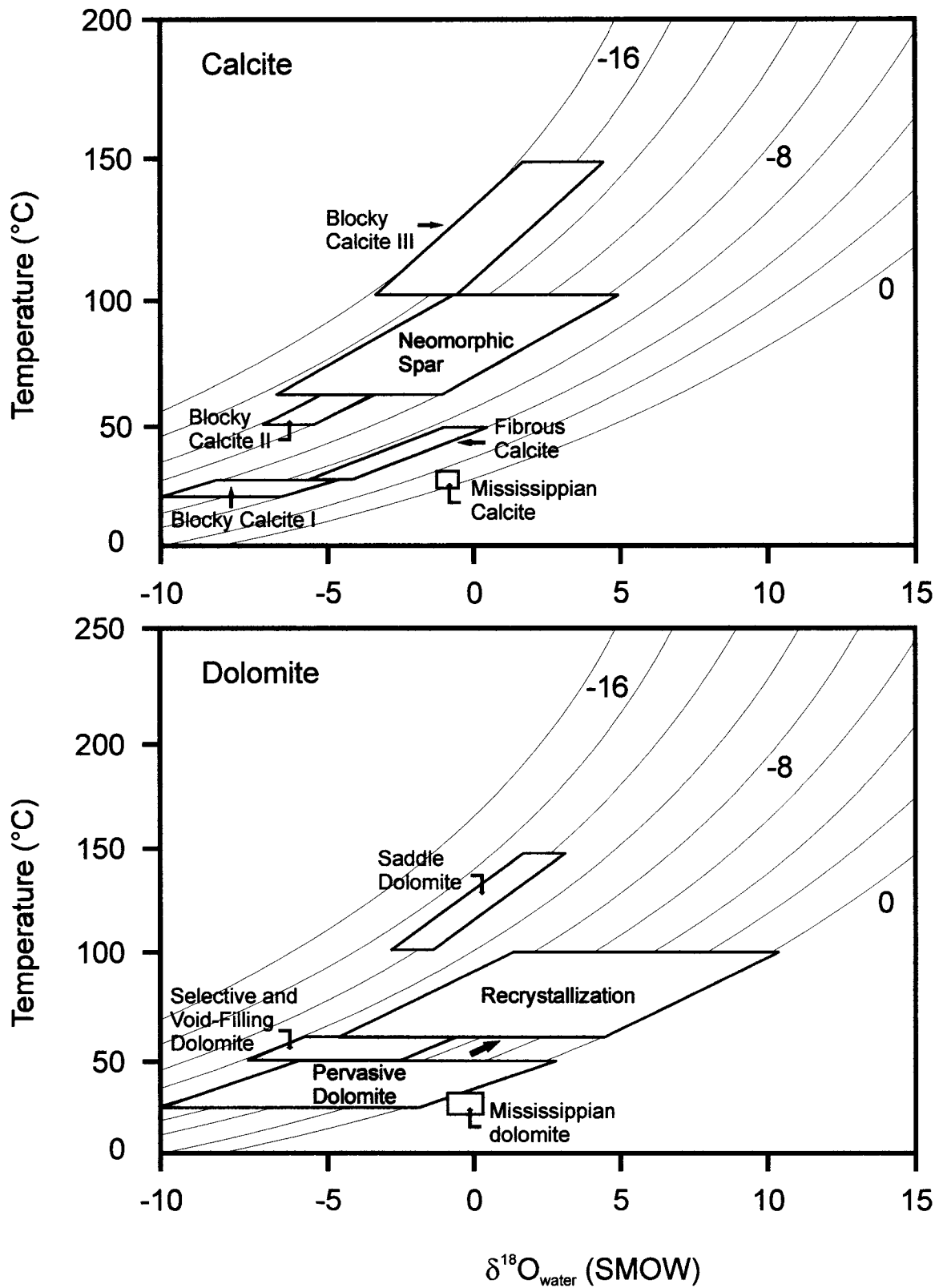


**Figure 8.2** Fluid oxygen isotope composition versus formation temperature for calcite and dolomite phases of different origins. Isochore lines show the oxygen composition of the phases in VPDB. The arrow represents the recrystallization pathway for the pervasive dolomite.

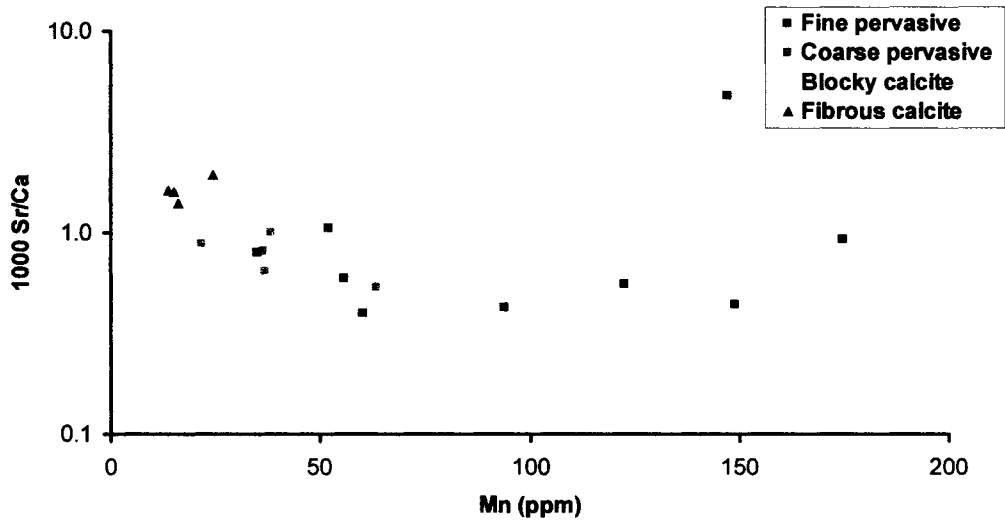
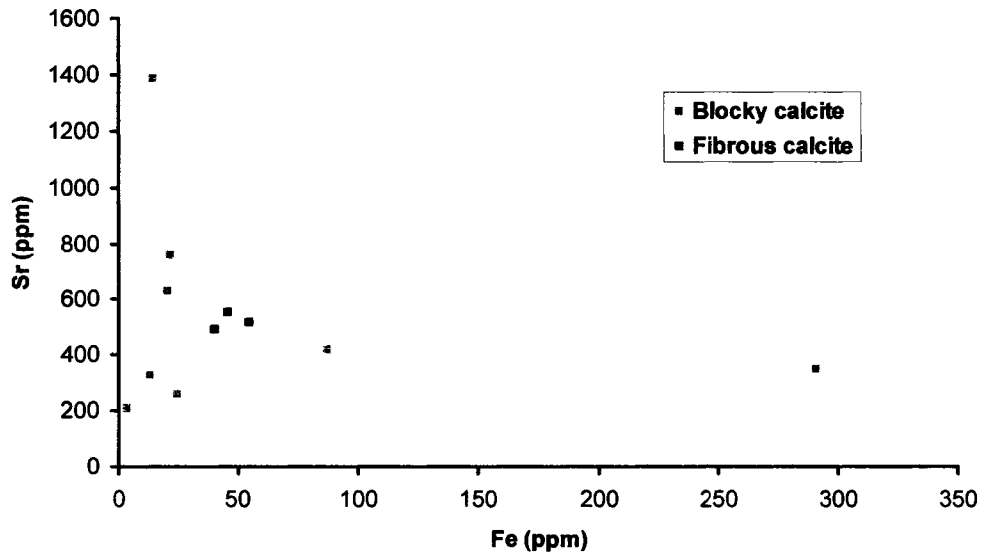


**Fig 8.3 A)** Sr versus Fe concentrations for calcite components.  
**B)** 1000 Sr/Ca versus Mn concentrations for dolomite and calcite phases.

### **8.3.6 Bladed prismatic to equant calcite**

Bladed prismatic to equant calcite cements are found lining the edges of veins and breccia fractures (Plate C-1 and 2). An insufficient amount of powdered sample could be acquired to accomplish stable isotope and trace element measurements, therefore geochemical studies were not performed. However, based on petrographic observations, both under plane polarized light and CL, several inferences about fluid compositions could be made. Cross-cutting relationships reveal that equant cements formed subsequent to stylolitization but prior to blocky calcite precipitation. CL studies show that these cements are dull and lack zonation, possibly conducive to a reducing burial environment. The absence of zonation suggests that fluids precipitating the calcite remained stable with no variations. Such observations are common in deeper burial cements (Choquette and James, 1990). In some cases framboidal pyrite is observed to have formed after equant calcite but prior to blocky calcite. Bladed and equant calcites are therefore interpreted to have formed subsequent to paleoexposure during intermediate burial.

### **8.4 Neomorphism and neomorphic calcite spar**

Based on petrographic and geochemical data, the neomorphism and/or recrystallization of calcite cements were important processes in the Pekisko Formation. Micrites display geochemical trends that suggest neomorphism (aggrading). Evidence that supports this includes depleted  $\delta^{18}\text{O}$  and  $\delta^{13}\text{C}$  values with respect to Mississippian marine calcite (Figure 6.1A).

Neomorphic spar has been observed as replacing the precursor mudstone and peloidal grainstone facies. Dark areas within the spar are relicts of the former grains and/or fossils. Petrographic and geochemical results indicate significant resetting relative to not only pristine values but also to micrite and syntaxial cement values. The  $^{87}\text{Sr}/^{86}\text{Sr}$  ratios also reflect an increase relative to expected early precipitation values. Neomorphosed spars are regarded as evidence for meteoric diagenesis either by low salinity fluids or at subaerial exposure surfaces (Flügel, 2004). They occur exclusively in wells which show evidence of meteoric diagenesis. The range of stable isotope values are similar to those of Phase II blocky calcites interpreted to be of

mixed water origin (Figure 6.1A). Figure 8.2 shows a temperature of formation between 62.5 and 100°C. Calculations were based on a geothermal gradient of 25°C/Km and burial depths of 1500-3000m (Machel, 2004). The resulting fluid compositions have a broad range from -6.5 to 5 ‰. This suggests that many fluids of various compositions may have contributed to neomorphism. Typical neomorphic fabrics include irregular crystals, curved and embayed boundaries and a variety of crystals sizes intermixing (Plate C-7). The neomorphism of calcite is thought to have occurred concurrently with the recrystallization of dolomite by meteoric fluids infiltrating the system at the subcrop edge and subsequently mixing with older meteoric fluids or marine formation fluids.

### **8.5 Silicification**

The sources and timing of silicification are poorly understood. However, in order to form quartz there must be an adequate source of silica. There are three major sources of silica; from siliceous skeletal parts of organisms, from solutions carried by rivers as the result of continental weathering in semi-arid climates and from the hydrothermal solutions supplied by volcanic activity (Laschet, 1984; Flügel, 2004).

Petrographic evidence suggests that chert may have formed early due to its association with early fine pervasive dolomite, the preservation of some skeletal fragments within it (Al-Aasm and Lu, 1994), unconformity associated chert clasts that were chertified prior to redeposition (Hesse, 1990) and indications that chert has been replaced to some extent by pervasive dolomite (Plate E-6). This evidence alone would suggest early formation as was observed for the Turner Valley Formation cherts (Al-Aasm and Lu, 1994) and the Lake Valley Formation cherts (Meyers and James, 1978). Sponge spicules are often referred to in literature as the source for silica; however in this study area no sponge spicules were found. The silica may have come from external fluids flushing through silica-rich sequences. According to Laschet (1984) the input of silica from land sources is very important in ramp and platform settings. Ghosts of fossils within the cherts as well as the preservation of ooids in some cases may indicate early replacement in a marine environment (Plate E-5). According to Knauth (1979) most cherts form early during



diagenesis and can form in marine, freshwater environments or at subaerial exposure surfaces. A possible mechanism for the formation of chert in the Pekisko Formation involves a mixing model proposed by Knauth (1979). The model is applied to shallow water chertification in carbonates and consists of the mixing of marine and meteoric waters. The mixing zone would favor calcite dissolution but silica precipitation would occur if the pH of the system was right. Based on experiments by Lovering and Patten (1961) a solution must be acidic to form silica. It is also possible for chert to form after dolomite and not affect it. This is due to the supersaturated nature of the mixing zone fluid with respect to dolomite.

The presence of authigenic quartz crystals may be attributed to precipitation from saline or hypersaline pore waters and can form early or late diagenetically (Flügel, 2004). As they are here, authigenic quartz crystals are usually restricted to neomorphosed and micritic limestones (Plate E-2). The authigenic quartz crystals have calcite inclusions and straight terminations indicating formation after neomorphism (Plate E-1).

Chalcedony occurs in association with secondary anhydrite. It is crosscut by saddle dolomite and replaces the anhydrite within the dolostone facies in well 9. The other more abundant form of quartz called lutecite (Hesse, 1990) occurs within neomorphosed (Plate E-4) sections (with no evidence of evaporites). Similar to authigenic quartz, lutecite was also observed to contain calcite inclusions.

It is interpreted that silicification occurred throughout the diagenetic history of the Pekisko Formation. First, early chertification occurred due to paleoexposure and replaced limestone intervals prior to pervasive dolomitization. Authigenic quartz crystals and lutecite are both found within neomorphosed micritic units with calcite inclusions indicating formation subsequent to neomorphism during intermediate to late burial. Lastly, chalcedony found in association with secondary anhydrites as well as saddle dolomite was precipitated during deeper burial.

## **8.6 Sulphide mineralization**

The pyrite observed in the Pekisko Formation is of diagenetic origin. Pyrite will usually replace organic material or in proximity to it under reducing conditions. It is relatively uncommon in the Pekisko carbonates, but where present it is framboidal (Plate C-1) or cubic in shape (Plate E-7). It is present in dolostones and neomorphosed mudstones, wackestones and intraclast breccias. Organic matter is the main limiting factor in the formation of pyrite in normal marine sediments (Flügel, 2004). However, Hesse (1990) discounts this statement and argues that no organics are required to form pyrite. He states that framboidal pyrite can form from metastable monosulphides precipitated from sulphides in the sulphate reducing zone. Framboidal pyrite has a distinct spherical shape made up of a cluster of crystals resembling raspberries. It is often observed in shelf carbonates and is formed in one of two ways; either bacterially-controlled (forming petrified sulfur bacteria) or inorganically crystallizing out of iron sulfide gels (Flügel, 2004). The authigenic (cubic and euhedral) pyrite usually forms as overgrowths on framboidal crystals or in reducing conditions replacing organic matter and thus forms later (Hesse, 1990). Hesse (1990) states that this type of pyrite forms in an anoxic sulphidic environment during early diagenesis. They most often occur within micritic limestone but have also been found in shoals susceptible to paleoexposure (Flügel, 2004). Since framboidal pyrite is observed replacing Phase II blocky calcite then it must have formed during intermediate burial subsequent to the paleokarst event. The fluid would have precipitated the cubic pyrite (observed replacing neomorphic spar) under endothermic and reducing conditions.

## **8.7 Dissolution**

Dissolution is a very important process that affected carbonates of the Pekisko Formation. It is essentially the dissolution of metastable carbonate grains as a result of the undersaturation of pore fluids with respect to the carbonate and is controlled by the flux of CO<sub>2</sub> in and out of the water (Flügel, 2004). Dissolution is effective in several different environments which include marine (seafloor), meteoric and deep burial (Tucker, 1981; Steinsund and Hald, 1994). Many examples of dissolution exist and include; dissolution of metastable fossils, the

formation of dissolution seams and stylolites, paleokarst-related dissolution and dissolution in dolomite.

The earliest dissolution process affected metastable fossil grains. It occurred very early likely from the infiltration of meteoric water. The originally aragonitic fossils were dissolved leaving a void that was later filled with calcite cement (Plate G-3). In post-Mississippian time, meteoric infiltration at the subcrop edge led to the dissolution of carbonates and the formation of breccias, later cemented by blocky calcite and selective dolomite (Plate F-6).

As a result of chemical compaction, beds and sequences may be reduced by 20-35% after mechanical compaction (Choquette and James, 1990). The process involves dissolution of grains at contacts between beds or nodules of very different solubilities. These go into solution to be reprecipitated locally or distally. As a result stylolites or dissolution seams may be produced due to the accumulation of insoluble residue. According to Flügel (2004), Mg-poor meteoric pore waters could enhance pressure solution. In the Pekisko Formation these occur within pervasively dolomitized (Plate B-8), crinoidal grainstone and mudstone units (Plate B-4 and 5). Because they crosscut pervasive dolomite they must have formed subsequent to early dolomitization.

The final dissolution event is related to a much later paleoexposure event allowing for the introduction of more meteoric water into the system after dolomitization. The presence of vugs and solution enlarged molds (Plate G-7 and 8), intracrystalline pores and fractures are evidence of dissolution subsequent to dolomitization (Plate H-4). The dissolution of relatively large amounts of dolomite in the subsurface has been observed by many authors for the Mississippian (Meyers, 1988; Dorobek et al., 1993; Hopkins, 1999; Hopkins, 2004 and Williams, 2005). These voids are in some instances unfilled and in others filled with late blocky calcite cement, void-filling dolomite and/or saddle dolomite. Dissolution pits have also been observed on dolomite crystals within dolomitized units (Plate H-3 and 5).

### **8.8 Lithofacies and dolomitization**

All facies in the Pekisko Formation have been dolomitized to varying degrees; however grainstones and mudstones seem to have been preferentially pervasively dolomitized. The finer

pervasive dolostones are thought to have replaced a precursor fine grained mudstone or lithofacies with a muddy matrix. As suggested by Murray and Lucia (1967), muds have greater surface areas than coarser grained rocks therefore have a greater number of nucleation sites for dolomitization to occur. The resulting dolostone then exhibits many small dolomite crystals reflecting the many nucleation sites. Therefore, medium to coarser dolomite crystals then should nucleate from larger or coarser grains or crystals which have fewer nucleation sites. Another possible process responsible for crystal coarsening may be recrystallization. For the Pekisko carbonates a combination of the two processes is thought to have occurred.

## **8.9 Mechanisms of Dolomitization**

### **8.9.1 Pervasive dolomite**

Pervasive dolomite samples were divided into two phases based on petrographic characteristics such as, crystal size, shape and cathodoluminescence. Coarse pervasive dolomite (50-220  $\mu\text{m}$ ) is euhedral whereas fine pervasive dolomite (15-50  $\mu\text{m}$ ) is subhedral to anhedral. The mean  $\delta^{18}\text{O}$  value reported for coarse dolomite is -6.20 ‰ (range: -10.44 to -1.00 ‰, n = 10) and for fine pervasive dolomite it is -3.43 ‰ (range: -10.08 to 0.43 ‰, n = 27). As suggested by Al-Aasm and Packard (2000), coarser dolomite may result from the replacement by dissolution of the earlier finer dolomite and precipitation of coarse crystals or form by replacing limestone not previously altered by dolomite. Due to the subtle solubility differences between the two dolomites it would take extremely supersaturated basinal fluids for dolomite replacement processes. This however is not practical and the replacement of limestone seems much more feasible. The rest must have been reset likely due to recrystallization to coarser pervasive dolomite by later Ca-rich fluids in conditions where stoichiometry was not attained.

Any model used to explain the formation of pervasive dolomite has to account for the regionally extensive distribution of massive dolomite and the relatively early timing of dolomitization. This dolomite phase is by far the most abundant in the Pekisko carbonates. The early fine pervasive dolomite has some  $\delta^{18}\text{O}$  values that are within the postulated Mississippian values indicating that only these have retained initial values. If dolomitization occurred in an

evaporative setting, the negative shift in the rest of the  $\delta^{18}\text{O}$  values could only be explained by recrystallization. Strontium isotope values for pervasive dolomite are radiogenic relative to Mississippian marine dolomites, Sr concentrations are very low and Fe and Mn concentrations are slightly high. Although these geochemical observations are not typical of dolomites formed in a marine setting, original signatures could have been completely obliterated during recrystallization. Secondary evaporites are present only in minor amounts in well 9 and are believed to have formed during deeper burial. Similar to observations made by Durocher and Al-Aasm (1997), the lack of primary evaporite deposits usually associated with hypersaline dolomite implies that marine diagenesis is probably not the model of formation. Diagenesis by marine fluids can also occur after uplift and exposure, however this model cannot account for the regional distribution of pervasive dolomite.

Since early stage chemical compaction in the form of stylolites crosscuts pervasive dolomite units, burial compaction models can also be ruled out. Some studies attribute the Mg source for dolomitization to the dewatering of thick shale sequences during burial compaction (Machel and Anderson, 1989; Durocher and Al-Aasm, 1994). However, sequences rich in clastics adjacent to the Pekisko are missing.

Stable isotope measurements performed on several pervasive dolomite samples exhibit somewhat of a covariant trend (Figure 6.1B). As suggested by Frank and Lohmann (1995) covariant trends are diagnostically attributed to marine-meteoric fluid mixing. The direction of fluid migration as well as the type of fluid involved can be inferred from plots showing regional  $\delta^{18}\text{O}$  distributions (Lewchuk and land, 1989). Studies by Al-Aasm and Lu (1994) on the Turner Valley Formation dolomites show that  $\delta^{18}\text{O}$  values for pervasive dolomite reflect precipitation from shallow circulating groundwater of marine composition diluted by meteoric water during subaerial exposure. If the dolomite is near surface, meteoric waters would have the ability to alter them (Dorobek et al., 1993; Kupecz and land, 1994; Montanez and Read, 1992). This freshwater diagenesis would stabilize metastable skeletal components, promote dissolution and precipitate meteoric cements, which have been identified within some of the Pekisko lithofacies. A later study by Al-Aasm (2000) also attributes meteoric diagenesis to the formation of mesodolomite. The

dolomite in the study was interpreted to have been altered during the post-Mississippian exposure. The presence of breccias and dedolomitization in the Pekisko Formation is evidence of this unconformity event. The post-Mississippian subaerial exposure event is also documented by Hopkins (1997) for the Pekisko Formation. In a third study on dolomites in the Debolt Formation (Durocher and Al-Aasm, 1997) the timing of dolomite formation has been established as concurrent with vuggy and moldic porosity formation but before stylolite formation. Porosity formed as a result of meteoric influx at the unconformity surface during uplift. Similar to this, petrographic analyses performed on dolostones for the Pekisko carbonates indicate that early compaction post-dates dolomitization and that dissolution may have occurred after or concurrent with dolomitization.

As mentioned in chapter 5 several karst features are present as a result of post-Mississippian exposures. If the unconformity surface made any meteoric contributions then the  $\delta^{18}\text{O}$  values should show depletion away from the edge. Figure 8.4A shows pervasive dolomite values within the studied wells. Wells 6 through to 3 are located progressively away from the subcrop, however  $\delta^{18}\text{O}$  results are not reflecting the depletion trend expected.  $\delta^{13}\text{C}$  isotopes reveal little to no depletion relative to Mississippian marine dolomite. It may be that carbon isotopes were buffered by previous carbonates and therefore retained the original signature or close to it. The slight depletion in  $\delta^{13}\text{C}$  may indicate a contribution of oxidized organic carbon (Lewchuk et al., 1998; Al-Aasm and Packard et al., 2000). The depleted carbon values observed in pervasive dolomites of well 2 are believed to be associated with the decomposition of algal organic matter during sulfate reduction (Durocher and Al-Aasm, 1997). Although  $\delta^{18}\text{O}$  values are not revealing trends away from the subcrop it has been suggested by several authors (Banner, 1995; Faure and Powell, 1972; Buschkuehle and Machel, 2002) that radiogenic Sr isotopes can be used to reconstruct paleomigration pathways of diagenetic fluids in conjunction with porewater evolution (Carpenter and Lohmann, 1989). The highest ratios are restricted to certain areas marking the fluid entrance into the system or the fluid source. In Figure 8.4B, Sr isotopes were plotted against oxygen isotopes for several phases with associated wells. Results show that Sr ratios are highest at the subcrop edge and progressively decrease away from it with increasing

oxygen values. This would indicate that the paleoexposure surface was the entrance for external fluids rich in radiogenic strontium. As fluids flowed through the strata, they contributed less and less Sr to dolomite being formed. In order to have radiogenic Sr isotopes there had to have been contributions of Rb through shales or Rb rich clastics. Since no such facies exist adjacent to the Pekisko Formation the fluid source must have been external. If the fluids were of deep burial origin we would expect much more radiogenic Sr ratios (Al-Aasm and Lu, 1994). Therefore, these ratios most likely reflect meteoric waters passing through clastics prior to entering the Pekisko system. These variations in Sr isotope values may also indicate modifications in pore fluids during recrystallization. Assuming a surface temperature of 25°C, that pervasive dolomite formed early in a relatively shallow burial environment at a temperature below 50°C (single phase fluid inclusions) and a geothermal gradient of 25°C/km then Figure 8.2 suggests that the fluids of dolomite formation were between -10 and 1 ‰ (SMOW). Estimated meteoric water  $\delta^{18}\text{O}$  values of -10 to -5 ‰ (Veizer et al., 1999) and -5.1 +/- 3.1 ‰ (Frank and Lohmann, 1995) have been suggested for the Mississippian for paleolatitudes between 15°N and 15°S. This shows that pervasive dolomite most likely formed initially from marine fluids and was later reset by meteoric fluids mixing with other formation fluids during recrystallization.

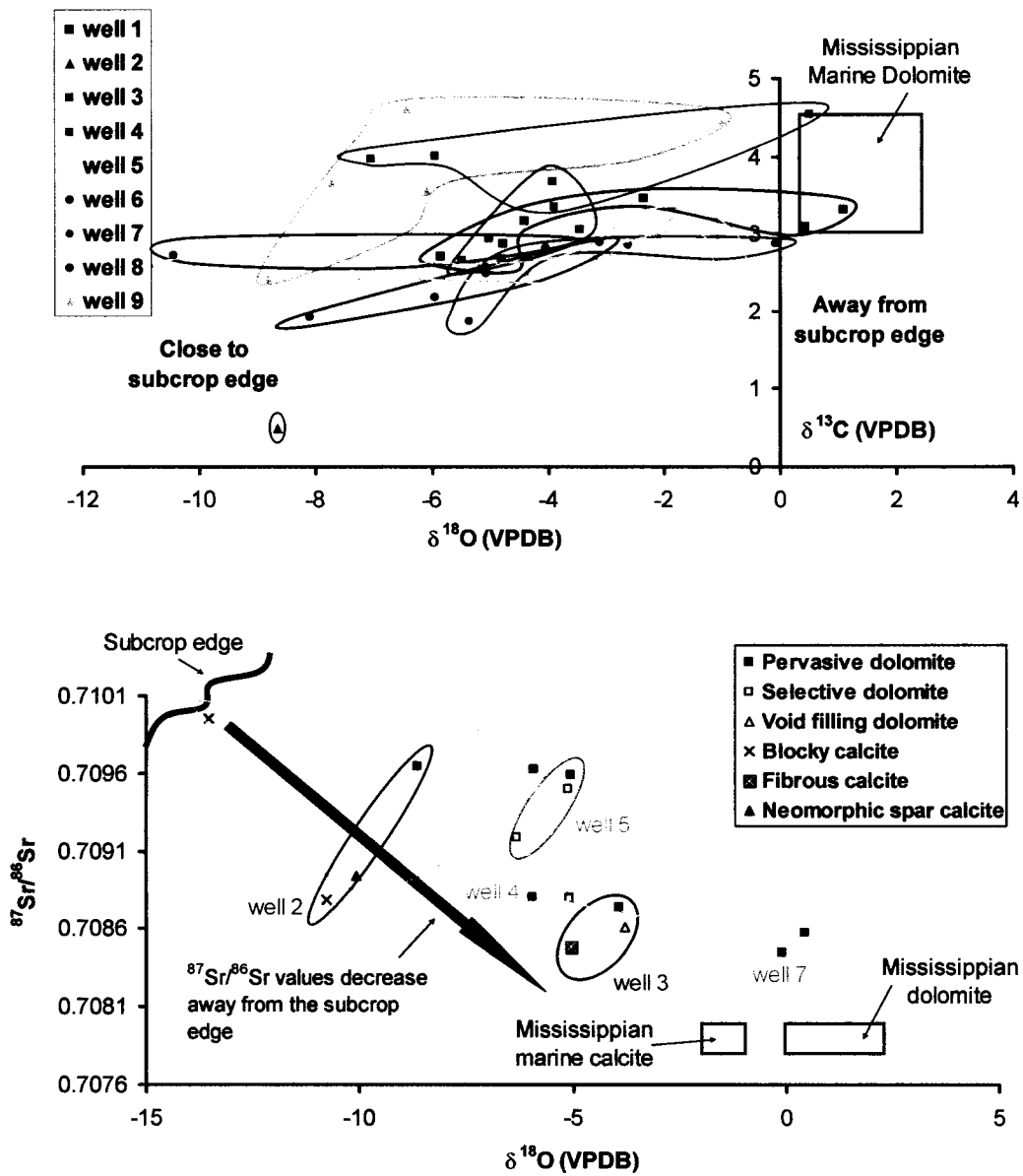
For recrystallized dolomites we would expect stoichiometric achievement. In the case of Pekisko dolomites (Appendix III) only three fine pervasive dolomite samples seem to have reached stoichiometry. According to petrographic evidence, it is apparent that coarser pervasive dolomites are overall less stoichiometric. One possible explanation for such a trend is that these stoichiometries reflect the mean average of the cores and rims of the coarser crystals (Plate D-2). Separate measurements were not performed on cores and rims of this dolomite and they may have shown very substantial stoichiometric differences. Sibley's (1990) model predicts that dolomite crystals should have Ca-rich cores and stoichiometric rims because as recrystallization proceeds non-stoichiometric precursors become increasingly stoichiometric. Despite this stoichiometry has not been achieved in the Pekisko pervasive dolomites. This phenomena has been observed in many other carbonates of the WCSB (Al-Aasm and Lu, 1994; White and Al-Aasm, 1997). In an experimental study by Malone et al. (1996) dolomites were subjected to

temperatures of 50°C – 200°C. This resulted in dolomite recrystallization and stoichiometry that proceeded quickly at first but slowed as reactions progressed. Despite complete recrystallization at 200°C, dolomite stoichiometry was not achieved. Another explanation could be that the coarser planar dolomite simply has not been recrystallized as extensively as fine non-planar dolomite. Gregg and Sibley (1984) and Wright et al. (2003) suggest that planar dolomite forms at temperatures < 50°C whereas non planar dolomite forms at higher temperatures (> 70°C). They argue that recrystallization will destroy zonations resulting in homogeneous CL.

The mesodolomite observed in Sylvan Lake (Al-Aasm, 2000), comparable to the coarse pervasive dolomite of this study, has been described as nonstoichiometric, euhedral, with homogeneous CL, depleted oxygen isotopes and extremely low concentrations of Mn, Fe and Sr. It was interpreted to have formed during paleoexposure post-Mississippian time. These observations have also been made in this study and therefore the same process of formation can be applied. In Figure 8.5, increases in Mn and Fe and low Sr concentrations are observed with decreasing crystal size (also Figure 8.3B). According to Al-Aasm and Lu (1994) low Sr concentrations may be attributed to flushing by lower Sr content fluids, such as meteoric waters. Frank and Lohmann (1995) also noted an increase in Mn and Fe with decreasing  $\delta^{18}\text{O}$  and  $\delta^{13}\text{C}$  result from progressive mixing of marine (Mn and Fe poor) and meteoric (Mn and Fe rich) waters. This is consistent with the geochemical results for the Pekisko carbonates discussed above.

It is interpreted, based on all of the above information, that pervasive dolomite formed early by marine fluids subsequent to the first paleoexposure event. After the second paleoexposure, recrystallization altered the pervasive dolomite by meteoric water mixing with marine formation fluids.





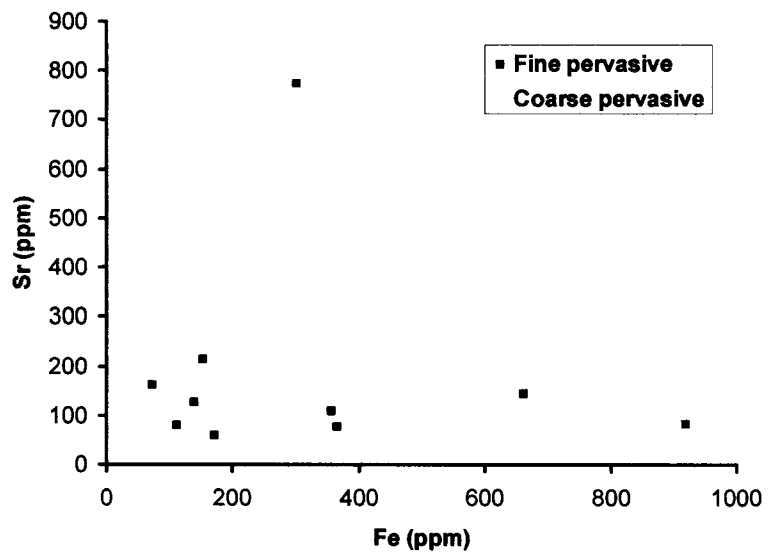
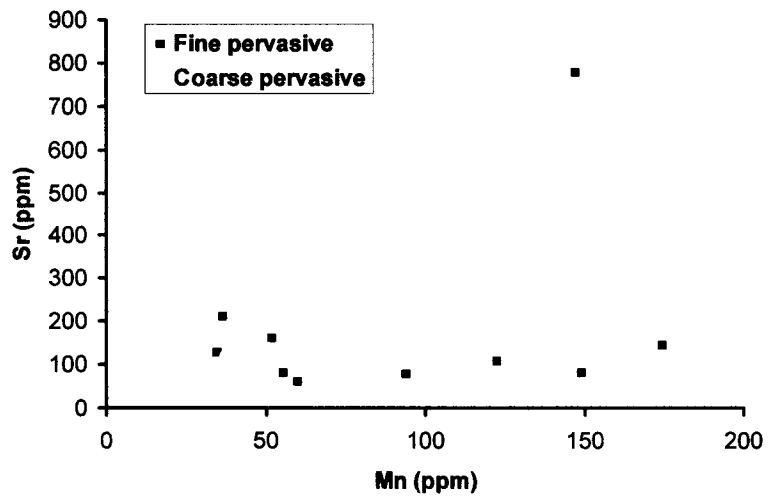


**Figure 8.5 A)** Sr versus Mn concentrations for fine and coarse pervasive dolomites.  
**B)** Sr versus Fe concentrations for fine and coarse pervasive dolomites.

### **8.9.2 Dissolution seam-associated dolomite**

Dissolution seam-associated dolomite occurs as fine euhedral crystals concentrated along dissolution seams within grainstone facies (well 3) in zones that are relatively undolomitized pervasively. (Plate D-7). Geochemistry suggests that this phase occurred relatively early likely in association with early chemical compaction (Figure 6.1B). Al-Aasm and Lu (1994) describe a patchy dolomite that has formed in association with dissolution seams. It is thought to have formed early during or right after early chemical compaction. Fluids are believed to be of marine origin at temperatures of approximately 35°C based on a geothermal gradient of 25°C/Km and a shallow burial depth of ~400m (Machel, 2004). Due to the small volume of this type of dolomite within these carbonates less Mg was needed initially for their formation. The fluids of marine or connate water origin would have flowed through the compaction fabrics that act as channels for diagenetic fluid transport. Another possible source for the dissolution seam-associated dolomite is fluids involved in the stabilization of magnesium calcite which would release Mg (Al-Aasm and Lu, 1994).

### **8.9.3 Void-filling dolomite**

Void-filling dolomite is a very minor phase of dolomite observed only in pervasively dolomitized units in wells 1, 3 and 7 (Plate D-5, 6 and 8). Since this cement occludes vugs and molds it is safe to assume that it precipitated subsequent to dissolution caused by meteoric waters from the paleoexposure event. Petrographic observations reveal that it precipitated prior to saddle dolomite and blocky calcite III. However, it is difficult to determine its timing relative to other phases due to a lack of more cross-cutting relationships. Despite this, a look at stable isotope geochemistry reveals that values are depleted relative to pristine dolomite but lie within the results for pervasive dolomite (Figure 6.1B). Further, they are enriched relative to selective dolomite and show the same recrystallization trend as other phases. The strontium isotope measurement is radiogenic relative to Mississippian dolomite, however is less radiogenic than selective dolomite values (Figure 6.2; Figure 8.4B). This means that void-filling dolomite must have precipitated some time after paleoexposure and prior to selective dolomitization and

recrystallization. Fluid inclusions analyses reveal that this cement contains two-phase fluid inclusions therefore formed at a temperature greater than 50°C. With this information and approximate intermediate burial depths of 300 to 1500m (Machel, 2004) and a geothermal gradient of 25°C/km, fluid compositions have been determined to be from -7.5 to -1 ‰ (Figure 8.2). This along with isotope trends suggests that it was precipitated from mixed fluids.

#### **8.9.4 Selective dolomite**

This dolomite occurs as matrix, grain and cement selective types depending on the location within the Pekisko Formation (Plate D-4). All are described here as one dolomite type due to their similar geochemical signatures. Both  $\delta^{18}\text{O}$  and  $\delta^{13}\text{C}$  values are depleted with respect to pristine values and exhibit a distinct recrystallization trend (Figure 6.1B). The value most enriched in both isotopes belongs to a dolomite in well 1 that is replacing meniscus cements within a brecciated dolomudstone. Strontium isotope values are radiogenic compared to the postulated Mississippian dolomite interval (Figure 6.2; Figure 8.4B). Replacement occurred subsequent to pervasive dolomitization and brecciation (paleoexposure) but prior to blocky calcite cementation within the breccia fractures. In some units selective dolomite is being replaced by neomorphic spar crystals indicating that it pre-dates recrystallization. It is possible that the fluids of formation were supplied during exposure as meteoric water mixing with saline formation fluids. To confirm this, the composition of the fluids of formation was assumed to be between -7.5 and -1 ‰ (Figure 8.2). The same fluid composition was observed for void-filling dolomite which was determined to have formed from mixed fluids. Some grainstones much deeper in the section that have seemingly not been affected by paleoexposure contain crinoids whose cores are being selectively dolomitized by micro crystalline dolomite (Plate D-3). It is difficult to ascertain the fluid source for its formation due to a lack of cross-cutting relationships.

#### **8.9.5 Saddle dolomite**

Saddle dolomite is a very minor component in the carbonates of the Pekisko Formation. It has only been identified within three wells (3, 4 and 9) occluding vuggy pore spaces (Plate D-8).

Petrographically, it cross-cuts void-filling dolomite cement, secondary anhydrite and bitumen, and is cross-cut by blocky calcite (Phase III). Crystals have sweeping extinction and curved surfaces and are very coarse. Since saddle dolomite does not fluoresce, there was no organic contribution to the lattice during the crystal growth. Saddle dolomite has dull luminescence, an indication of precipitation in a deeper burial reducing environment where Fe was available for incorporation (Boggs, 1992). Another indication of deeper burial or a higher temperature of formation is the presence of two-phase fluid inclusions. According to Machel (2004) deep burial begins at depths greater than 1500m. With a geothermal gradient of 25°C/Km, temperatures of formation would be anywhere from 100°C-145°C. From Figure 8.2, these temperatures yield fluid compositions between -3 and 3 ‰, a range suggesting saline formation fluids. Geochemically, saddle dolomite exhibits very depleted  $\delta^{18}\text{O}$  and  $\delta^{13}\text{C}$  values relative to original marine values as well as all other phases except the latest burial blocky calcite (Figure 6.1B). A study of saddle dolomite (or megadolomite) in the Mississippian Turner Valley by Al-Aasm and Lu (1994) reveals that it is a late diagenetic product forming at higher temperatures during deep burial. Since there is such a small volume of this phase within these carbonates only a minor amount of Mg is needed. The Mg may have been derived from relicts of partially dissolved pervasive dolomite. Its close association with stylolites in some instances may indicate that these stylolites acted as conduits for dolomite forming fluids.

#### **8.10 Dolomite recrystallization in the Pekisko Formation**

The recrystallization of pervasive dolomite in the Pekisko Formation has been suggested, based on petrographic and geochemical analyses.

For dolomite recrystallization, Machel (1997) suggested that the term significant recrystallization be applied to dolomites which have undergone one of the following:

- (1) Change in texture (e.g.: coarsening crystal size or increase in non-planar boundaries)
- (2) Change in structure (progressive ordering and strain)
- (3) Change in composition (this includes isotopes, trace elements, stoichiometry, fluid inclusions, zonations) and

#### (4) Change in paleomagnetic properties

For example, if  $\delta^{18}\text{O}$  measurements for dolomite are outside that of the suggested pristine values (within all analytical errors) than this sample is said to be significantly recrystallized with respect to stable isotopes but insignificantly recrystallized for all other properties (Machel, 1997).

Recrystallization of earlier formed dolomite is a common process within Mississippian platform carbonates (Land, 1985; Hardie, 1987; Smith and Dorobek, 1993; Kupecz and Land, 1997; Durocher and Al-Aasm, 1997). In fact, several previous studies on dolomites from Mississippian successions suggest the occurrence of dolomite recrystallization by comparing reset samples to pristine samples in order to properly identify the recrystallization event (Packard, 1992; Machel, 1997; Durocher and Al-Aasm, 1997).

In the Pekisko Formation, recrystallization of pervasive dolomite occurred later during deeper burial and may have involved meteoric, mixed meteoric-marine or saline fluids (possibly from the second or third karstification event). Petrographic evidence for recrystallization includes the presence of excessive intracrystalline dissolution in the form of pits or completely dissolved cores as seen with SEM (Sibley, 1990; Plate J-1), the dissolved or etched contacts between cores and rims as seen with CL (Plate I-5 and 6), an increase in crystal size (Plate I-2; Plate J-3) and the presence of non-planar crystal boundaries (Plate I-4; Plate J-5).

Intracrystalline dissolution and dedolomitization are common within brecciated intervals especially in well 5 of the Pekisko Formation. These consist of pitted surfaces or completely dissolved or replaced crystal cores. Several authors interpret this to indicate that cores were less stable than the surrounding higher stability rims and so were preferentially dissolved by late-stage fluids. The magnitude of dissolution in the core may be determined by the degree of recrystallization (Sibley, 1990; Al-Aasm, 2000). Irregular contacts between bright rims and dull cores are also abundant in zoned dolomites (Plate I-5 and 6). These suggest dissolution prior to the precipitation of the rim, recrystallization or possibly a little of both (Durocher and Al-Aasm, 1997). When examined under SEM, cores appear to be dissolved out or have pitted surfaces.

In the Pekisko dolomites, coarsening crystal textures have been observed in many wells (Plate I-2; Plate J-3). Micro-crystals change progressively to coarser zoned and sometimes

dedolomitized crystals. The increase in crystal size during recrystallization is thought to be attributed to the Ostwald ripening theory (Morse and Mackenzie, 1990). Dissolution, transfer and growth are the three kinetic steps involved in the process that consists of coarser crystals growing at the expense of finer crystals driven by surface energy.

Non-planar crystal boundaries are relatively uncommon in the Pekisko carbonates; however they do provide proof of recrystallization (Plate I-4; Plate J-5). Several authors (Sibley and Gregg, 1987; Kupecz et al., 1993) have observed patches of non-planar dolomite within more planar dolomite as well as an increase in the number of non-planar crystal interfaces and attribute them to recrystallization.

Several geochemical lines of evidence support recrystallization: (1) depletion in  $\delta^{18}\text{O}$  and to some extent  $\delta^{13}\text{C}$  values with respect to Mississippian dolomite, (2) enrichment in radiogenic  $^{87}\text{Sr}/^{86}\text{Sr}$  ratios, and (3) Mn and Fe enrichment and depletion in Sr concentrations (Kupecz et al., 1993).

Stable oxygen isotopes are probably the most widely used geochemical tools in carbonate studies. However, they are the most fluid buffered since most oxygen resides in pore waters rather than in dolomite. Therefore where recrystallization occurs, stable oxygen isotope signatures are the first to be affected (Land, 1985; Banner, 1986; Kupecz et al., 1993). The recrystallization of fine pervasive dolomite to coarser pervasive dolomite and/or the recrystallization of coarse dolomite exhibits depletion in  $\delta^{18}\text{O}$  with a slight depletion in  $\delta^{13}\text{C}$  (Figure 6.1B). The covariant trend is similar to observations in mesodolomite from Sylvan Lake of the Pekisko Formation (Al-Aasm, 2000). It was postulated in the study that possible pathways for  $\delta^{18}\text{O}$  evolution may reflect a change in temperature from increased burial, a change in fluid chemistry due to fluid rock interactions or a combination of the two. Results of the Al-Aasm (2000) study were interpreted to reflect recrystallization and or mixing during exposure to meteoric fluids. In Figure 6.2,  $\delta^{18}\text{O}$  isotope signatures show that dolomite is reset relative to pristine samples and Sr isotopes become increasingly radiogenic. The decrease in  $\delta^{18}\text{O}$  and  $\delta^{13}\text{C}$ , and the increase in radiogenic Sr have been used by several researchers (Kupecz et al., 1993; Al-Aasm and Lu, 1994; Al-Aasm, 2000) as criteria for dolomite recrystallization. However, these same observations

are inconsistent with mixing-zone trends (Durocher and Al-Aasm, 1997). The presence of two-phase fluid inclusions in some coarser pervasive dolomite crystal rims, suggesting higher a temperature of formation ( $>50^{\circ}\text{C}$ ), are also inconsistent with mixing-zone formation. Therefore since the model of formation for pervasive dolomite has already been evaluated as being marine, evolved to mixed marine-meteoric waters, fluid inclusions must record recrystallization temperatures. As suggested, recrystallization proceeded during deeper burial at a depth greater than 1500m (Machel, 2004). With a geothermal gradient of  $25^{\circ}\text{C}/\text{Km}$ , recrystallization occurred at temperatures between  $62.5^{\circ}\text{C}$  and  $100^{\circ}\text{C}$ . This corresponds to fluid compositions of -5 to 10 ‰ (Figure 8.2). Such a broad fluid composition range indicates that various fluids and/or water-rock interactions contributed to the recrystallization process. These fluids may have been mixed in the beginning and evolved to brines as diagenesis progressed.

Figure 8.5 shows concentrations of Sr versus Mn and Fe and reflect a decrease in Sr concentration with increasing Fe and Mn concentrations. These may be evidence of diagenetic modification of a precursor dolomite by recrystallization (Kupecz et al., 1993). In a study by Al-Aasm (2000) on Pekisko dolomites of the Sylvan Lake field, low Sr concentrations are attributed to recrystallization by mixed meteoric waters. Mn concentrations were also observed to be higher in fine pervasive dolomite than in coarser ones. It is possible that during recrystallization pore fluids were simply enriched in Mn (Montanez and Read, 1992; Al-Aasm, 2000).

Petrographic and geochemical results outlined above provide evidence of dolomite recrystallization. In terms of timing, recrystallization began after the paleoexposure event and proceeded to late deep burial diagenesis. Fluids responsible for early recrystallization were likely mixed meteoric-marine. The meteoric end-member was derived from the exposure surface. As recrystallization progressed into the deeper burial realm, the fluids responsible for the alteration became increasingly saline.

### **8.11 Diagenetic Model**

The Pekisko carbonates have undergone a complex diagenetic history. Environments of diagenesis range from early marine to deep burial. In the following section, seven stages of



diagenesis have been outlined to explain the diagenetic phases present in the Pekisko Formation.

**Stage 1:** The Pekisko Formation was deposited during the Tournaisian (Early Mississippian) on a marine carbonate ramp. This produced mudstone, wackestone, packstone and grainstone lithofacies. At the time of deposition, both micritization of grains and precipitation of isopachous calcite cement occurred. This is followed by the shallow burial precipitation of drusy mosaic calcite in inter- and intraparticle pores.

**Stage 2:** A fall in sea level exposed these sediments to meteoric waters leading to the dissolution of fossils (leaving molds). Grains stable enough to escape dissolution act as precipitation surfaces for meniscus and pendant cements. Dissolution processes also lead to fracturing and veining later occluded by blocky calcite (phase I). Crinoids are replaced by syntaxial calcite generated from meteoric water influx.

**Stage 3:** An increase in sea level and burial depth leads to mechanical compaction evidenced by twinning, strain and broken fabrics in fossils and cements. Chert forms as beds and nodules from mixed fluids. Marine fluids also produce pervasive dolomitization within most porous mudstone and grainstone intervals and replace some chert. Molds are left unfilled, while the original limestone is partially to completely dolomitized. Early chemical compaction begins at intermediate burial affecting all lithofacies. Sutured contacts and fitted fabrics become apparent within grainstones. Local dissolution processes form dissolution seams. Minerals dissolved are re-precipitated along seams as euhedral dissolution seam-associated dolomite (only in grainstones) and fibrous calcite associated with stylolites (in both grainstones and dolostones). Add this time a second stage of fracturing begins.

**PLATE I**

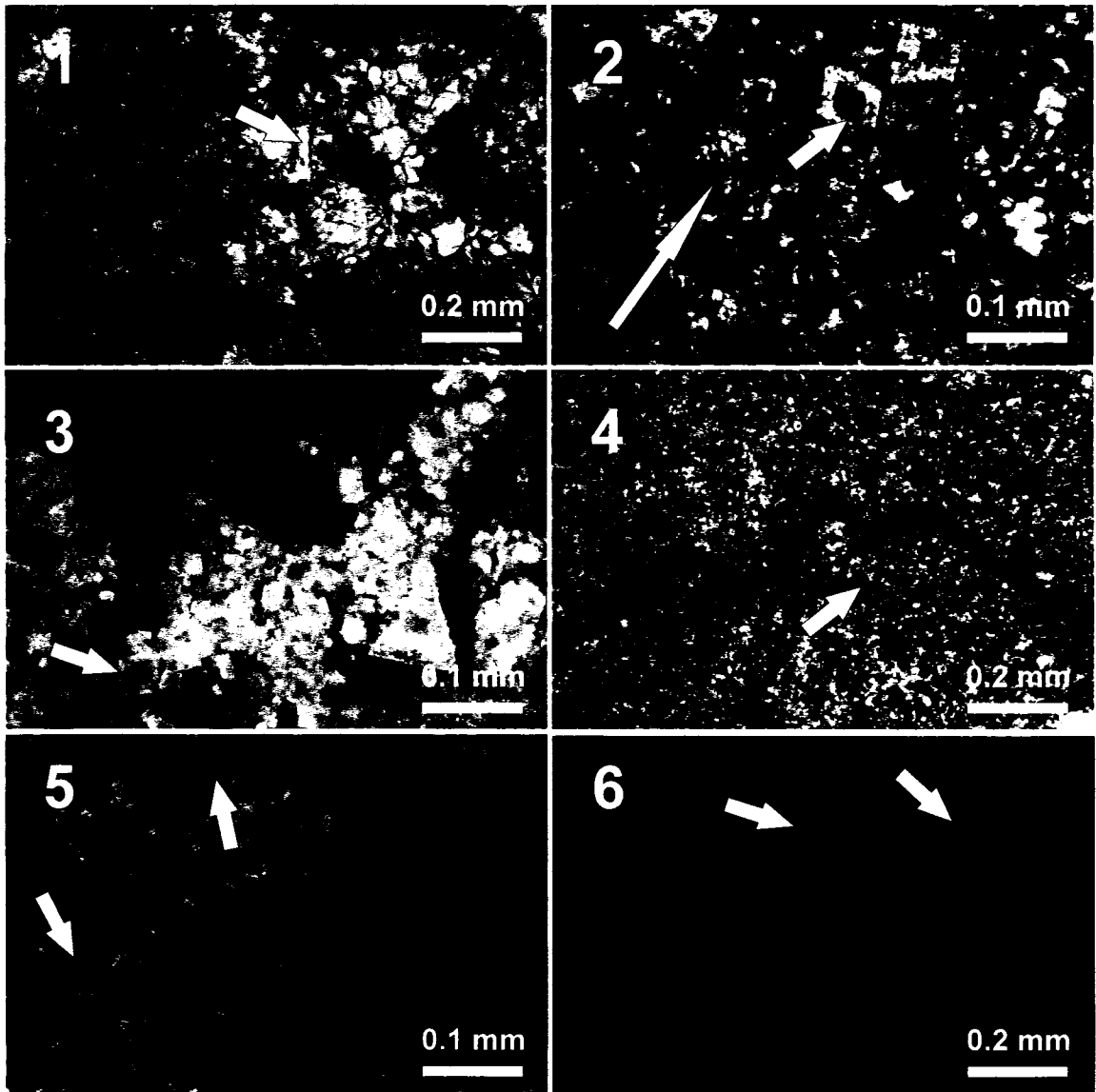
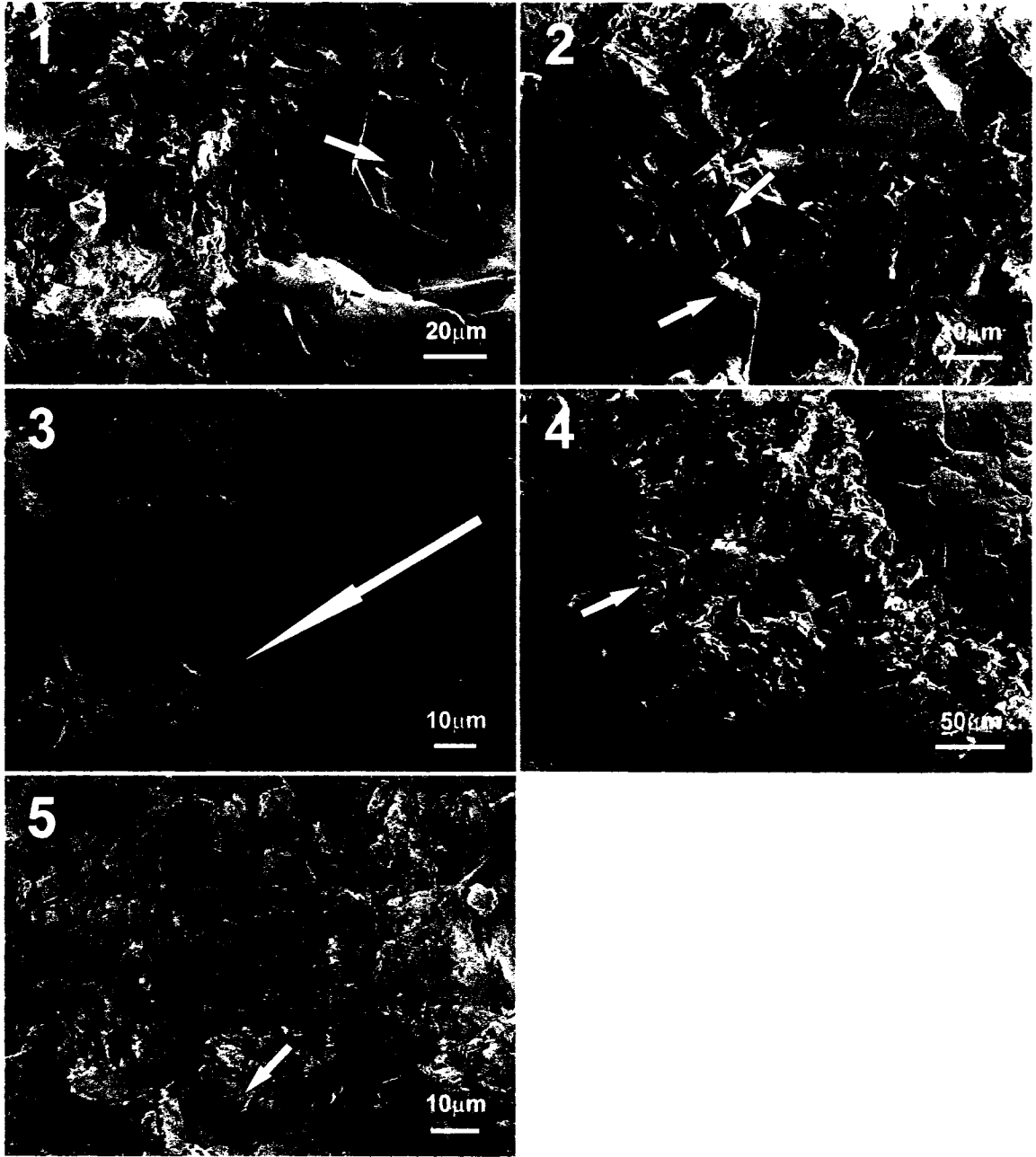


**PLATE J**



**Stage 4:** At this stage post Mississippian exposure leads to the formation of a subcrop edge and subsequent karstification by meteoric fluids. Dissolution and brecciation are important processes. Brecciation occurs at the top of the sequence only and affects mainly mudstones, wackestone, peloidal grainstones and dolostones. Dolostones are also partially dissolved resulting in vugs (often solution enlarge molds). Rocks are exposed to meteoric and mixed fluids that precipitate meniscus cement between clasts and equant and prismatic cements along surfaces of clasts.

**Stage 5:** Void filling dolomite cements precipitate in vugs of dolostones by mixed fluids. Slightly more depleted fluids (in terms of stable isotopes) encourage selective replacement of meniscus cement and the matrix of some grainstones. Subsequently, blocky calcite (phase II) is precipitated into the remaining breccia pores and some molds. Framboidal pyrite forms concurrent with or just before blocky calcite II.

**Stage 6:** With progressive burial, dedolomitization, neomorphism and recrystallization begin to affect the carbonates by mixed fluids. Cross-cutting relationships show authigenic quartz and chalcedony replacing neomorphic sparry calcite.

**Stage 7:** Deeper burial processes include late chemical compaction in association with secondary anhydrite and saddle dolomite. Both of these phases are only present at the base of the deepest wells within dolostones. Fluids for precipitation likely originated from dissolution along stylolites (enough to form the minor amount seen). Later deep basinal fluids precipitated blocky calcite (phase III) into remaining pores. Late fracturing crosscuts all of these phases. Hydrocarbons may have formed and migrated at this time.

## CHAPTER IV CONCLUSIONS

Core examinations, petrographic studies and geochemical analyses of carbonate samples collected from the Pekisko Formation in west central Alberta are the basis for the following conclusions:

1. Carbonates of the Pekisko Formation were deposited in a restricted to protected marine carbonate ramp environment. Lithofacies observed include crinoidal grainstones, oolitic/bioclastic grainstones, peloidal grainstones, wackestones/packstones, mudstones, intraclast breccia mudstones and dolostones.
2. Calcite phases are abundant in the Pekisko carbonates and include micrite, isopachous cement, drusy mosaic cement, meniscus and pendant cements, blocky cement (phases I, II and III), syntaxial cement, fibrous cement, equant and bladed prismatic cements and neomorphic spar. These formed in early marine to deep burial environments.
3. Mechanical compaction began subsequent to early calcite cementation but prior to pervasive dolomitization. Chemical compaction processes were evident throughout the diagenetic history of the Pekisko carbonates and resulted in the formation of dissolution seams and rings, stylolites and fitted fabrics. These processes aided in the formation of dissolution seam-associated dolomite, fibrous calcite and saddle dolomite.
4. Dolomitization is the most important process in the Pekisko Formation. All lithofacies have been affected partially to completely. There are five types of dolomite present: pervasive dolomite, dissolution seam-associated dolomite, void-filling dolomite, selective dolomite and saddle dolomite.
5. Pervasive dolomite is the most abundant and earliest phase affecting mudstone and grainstone facies. Petrographic and geochemical evidence suggests that it formed after paleoexposure during shallow burial by marine fluids and was later recrystallized by mixed meteoric-marine fluids after a later paleoexposure event.
6. Dissolution seam-associated dolomite (DSAD) formed during early chemical compaction. It is a relatively minor phase occurring only within crinoidal grainstone facies. Fluids of

formation may have come from the dissolution of metastable grains flowing along seams and re-precipitating as euhedral DSAD crystals.

7. Void-filling dolomite occurs as cement occluding vugs and molds within dolostone intervals only. It formed during intermediate burial before or concurrent with selective dolomite formation. Geochemical attributes are similar to those of pervasive dolomite indicating that void-filling dolomite likely formed from mixed fluids.
8. Selective dolomite occurs as grain, matrix and cement replacement phases. Crosscutting relationships and geochemical analyses reveal that this phase formed during intermediate burial by meteoric waters mixed with more saline formation fluids.
9. Saddle dolomite is a very minor constituent of Pekisko carbonates. It occurs only within the deepest dolomitized sections in the deepest wells. It occludes vugs or molds and is associated with late chemical compaction. Petrographic observations along with stable isotope measurements indicate that it formed late during deep burial possibly by fluids released during chemical compaction.
10. Recrystallization and neomorphism are very important processes affecting all phases in the Pekisko Formation. Aggrading neomorphism is common in brecciated mudstone intervals related to paleoexposure. It is believed to be the cause of dedolomitization, present only in brecciated zones. Petrographic and geochemical analyses show that it occurred at the same time as the recrystallization of dolomites by meteoric fluids entering the system and mixing with older meteoric or marine fluids. Several lines of evidence for recrystallization have been observed such as: increasing crystal size, zonations, etched surfaces between cores and rims of crystals (dissolution pits), dedolomitization, increased anhedral crystal contacts, a depletion in both carbon and oxygen stable isotopes and an increase in radiogenic strontium ratios.
11. Porosity evolution in the Pekisko carbonates has been very complex. Early calcite cements, mechanical compaction and chemical compaction destroyed most of the primary intraparticle, interparticle and fenestral porosity. Post Mississippian exposure events contributed significantly to the generation of secondary porosity, the principle



reservoir porosity. Several porosity types exist and include: moldic porosity formed from the dissolution of metastable grains by meteoric waters during paleoexposure, fracture porosity occurring throughout the burial history of the Pekisko Formation, breccia porosity formed as a result of dissolution from exposure, vuggy porosity within dolostone intervals that are likely solution enlarged molds, and intercrystalline porosity associated with pervasive dolomitization of the precursor limestone. The precipitation of equant/prismatic calcite cement, blocky calcite cement, saddle dolomite cement and void-filling dolomite cement has significantly reduced all porosity types.

## REFERENCES

- Al-Aasm, I.S. 2000. Chemical and Isotopic Constraints for Recrystallization of Sedimentary Dolomites from the Western Canada Sedimentary Basin. *Aquatic Geochemistry*, **6**, 227-248.
- Al-Aasm, I.S. and Lu, F. 1994. Multistage dolomitization of the Mississippian Turner Valley Formation, Quirk Creek Field, Alberta: chemical and petrologic evidence. *Canadian Society of Petroleum Geologists, Memoir 17*, 657-675.
- Al-Aasm, I.S. and Packard, J.J. 2000. Stabilization of early-formed dolomite: a tale of divergence from two Mississippian dolomites. *Sedimentary Geology*, **131**, 97-108.
- Al-Aasm, I.S., Taylor, B.E., and South, B. 1990. Stable isotope analysis of multiple carbonate samples using selective acid extraction. *Chemical Geology (Isotope Geoscience Section)*, **80**: 119-125.
- Allan, J.R. and Wiggins, W.D. 1993. Dolomite Reservoirs: Geochemical Techniques for Evaluating Origin and Distribution. *AAPG Continuing Education Course Note Series #36*.
- Anderson, T.F. and Arthur M. A. 1983. Stable isotopes of oxygen and carbon and their application to sedimentologic and paleoenvironmental problems. *In: Stable isotopes in sedimentary geology*. Society of Economic Paleontologist and Mineralogist, Short Course No. 10, p. 1-1 to 1-151.
- Bamber, E.W., Macqueen, R.W. and Ollerenshaw, N.C. 1981. Mississippian stratigraphy and sedimentology, Canyon Creek (Moose Mountain), Alberta, *In: Thompson, R.I. and Cook, D.G., eds., Field Guides to Geology and Mineral Deposits: Calgary, Geological Association of Canada, Mineralogical Association of Canada, Canadian Geophysical Union*, p. 175-195.
- Banner, J.L., Hanson, G.N. and Meyers, W.J. 1988. Water-rock interaction history of regionally extensive dolomites of the Burlington-Keokuk Formation (Mississippian): isotopic evidence. *In: Sedimentology and geochemistry of dolostones* (eds. V. Shukla and P. Baker). Society of Economic Paleontologists and Minerologists Special Publication 43, p. 97-113.
- Banner, J.L., and Hanson, G.N. 1990. Calculation of simultaneous isotopic and trace element variations during water – rock interaction with applications to carbonate diagenesis. *Geochimica et Cosmochimica Acta*, **54**: 3123-3137.
- Banner, J.L. 1995. Application of the trace element and isotope geochemistry of strontium to studies of carbonate diagenesis. *Sedimentology*, **42**: 805-824.
- Bathurst, R.G.C. 1966. Boring algae, micrite envelopes and lithification of molluscan biosparites: *Geological Journal*, **5**, 15-32.
- Bathurst, R.G.C. 1971. Carbonate sediments and their diagenesis. *In: Developments in Sedimentology 12*, Elsevier, 620p.
- Bathurst, R.C.G. 1975. Carbonate sediments and their diagenesis. Elsevier, Amsterdam, 658p.
- Beauchamp, B., Richards, B.C., Bamber, E.W. and Mamet, B.L. 1986. Lower Carboniferous lithostratigraphy and carbonate facies, upper Banff Formation and Rundle Group, east-central British Columbia. *In: Current Research, Part A, Geological Survey of Canada, Paper 86-1A*, p. 627-644.
- Bodnar, R.J. 1993. Revised equation and table for determining the freezing point depression of H<sub>2</sub>O-NaCl solutions. *Geochimica et Cosmochimica Acta*, **57**: 683-684.

- Boggs, S. 1992. Petrology of sedimentary rocks. Macmillan Publishing Company, New York, 707p.
- Brand, U. and Veizer, J. 1980. Chemical diagenesis of a multicomponent carbonate system – 1. Trace elements. *Journal of Sedimentary Petrology*, **50**, 1219-1236.
- Brand, U. and Veizer, J. 1981. Chemical diagenesis of a multicomponent carbonate system – 2: Stable isotopes. *Journal of Sedimentary Petrology*, **51**, 987-997.
- Brand, U. and Veizer, J. 1983. Origin of Coated Grains: Trace Element Constraints. *In: Coated Grains*. Peryt, T.M. (ed.). p. 9-26.
- Budd, D.A. and Perkins, R.D. 1980. Bathymetric zonation and paleoecological significance of microborings in Puerto Rican shelf and slope sediments. *Journal of Sedimentary Petrology*, **50**: 881-890.
- Burke, W. H., Denison, R.E., Hetherington, E.A., Koepnick, R.B., Nelson, H.F. and Otto, J.B. 1982. Variations of seawater  $^{87}\text{Sr}/^{86}\text{Sr}$  throughout Phanerozoic time. *Geology*, **10**, 516-519.
- Buschkuehle, B.E. and Machel, H.G. 2002. Diagenesis and paleofluid flow in the Devonian Soutesk-Cairn carbonate complex in Alberta, Canada. *Marine and Petroleum Geology*, **9**, 219-227.
- Buxton, T.M., and Sibley, D.F. 1981. Pressure solution features in shallow buried limestones: *Journal of Sedimentary Petrology*, **51**, 19-26.
- Carpenter, S.J. and Lohmann, K.C. 1989.  $\delta^{18}\text{O}$  and  $\delta^{13}\text{C}$  variations in Late Devonian marine cements from the Golden Spike and Nevis reefs. Alberta Canada. *Journal of Sedimentary Petrology*, **59**, 792.
- Choquette, P.W., and James, N.P. 1987. Diagenesis 12. Diagenesis in limestones – 3. The deep burial environment. *Geoscience Canada*, **14**, 3-35.
- Choquette, P.W., and James, N.P. 1990. Limestones – the burial diagenetic environment. *In: Diagenesis*. Edited by I.A. McIlreath and D.W. Morrow. *Geoscience Canada Series 4*, p. 75-112.
- Choquette, P.W., and Pray, L.C. 1970. Geological nomenclature and classification of porosity in sedimentary carbonates. *American Association of Petroleum Geologists Bulletin*, **54**, 207-250.
- Denison, R.E., Koepnick, R.B., Burke, W.H., Hetherington, E.A. and Fletcher, A. 1994. Construction fringing-reef complex: Leduc Formation, Peace River Arch area, Alberta, *Canadian Journal of Sedimentary Petrology*, **63**, 628-640.
- Dickson, J.A. 1965. Carbonate identification and genesis as revealed by staining. *Journal of Sedimentary Petrology*, **63**, 107-118.
- Dorobek, S.L., Smith, T.M. and Whitsit, P.M. 1993. Microfabrics and Geochemistry of Meteorically Altered Dolomite in Devonian and Mississippian Carbonates, Montana and Idaho, *In: Carbonate Microfabrics*, R. Rezak and D.L. Lavoie, (eds.), Ch. 16, p. 205-224.
- Douglas, R.J.W. 1953. Carboniferous stratigraphy in the southern foothills of Alberta, *Alberta Society of petroleum Geologists, Guide Book, Third Annual Field Conference*, p. 68-88.
- Dravis, J. J., and Yurewicz, D. A. 1985. Enhanced carbonate petrography using fluorescence microscopy. *Journal of Sedimentary Petrology*, **55**, 795-804.

- Dunham, R.J. 1962. Classification of carbonate rocks. *In: Classification of carbonate rocks, a symposium. Edited by W.E. Ham. American Association of Petroleum Geologists, Memoir 1, pp. 108-121.*
- Dunnington, H.V. 1967. Aspects of diagenesis and shape change in stylolitic limestone reservoirs. *Proceedings of the 7<sup>th</sup> World Petroleum Congress, Mexico, 2, 337-352.*
- Durocher, S. and Al-Aasm, I.S. 1997. Dolomitization and Neomorphism of Mississippian (Visean) Upper Debolt Formation, Blueberry Field, Northeastern British Columbia: Geologic, Petrologic, and Chemical Evidence. *AAPG Bulletin, 81, No. 6, 954-977.*
- Embry, A.F. and Klovan, J.E. 1972. Absolute water depth limits of late Devonian paleoecological zones. *Geol. Rundschau, 61, 672-686.*
- Fattahi, S. 2001. Sedimentology and Paragenetic Evolution of the Mississippian Pekisko Formation, Minnehik-Buck lake Field and Adjacent Area, Alberta, Canada. Unpublished MSc. Thesis. University of Calgary. 252pp.
- Faure, G. 1991. Principles and Applications of Inorganic Geochemistry, Prentice Hall (eds.), 626 p.
- Faure, G. and Powell, J.L. 1972. Strontium isotope geology. Springer, Berlin, 188p.
- Feazel, C.T., and Schatzinger, R.A. 1985. Prevention of carbonate cementation in petroleum reservoirs. *Edited by N. Schneidermann, and P.M. Harris. Carbonate cements: Society of Economic Paleontologists and Sedimentologists Special Publication 36. 97-106.*
- Flügel, E. 2004. Microfacies of carbonate rocks: analysis, interpretation and application. Springer, 976p.
- Folk, R.L. 1965. Some aspects of recrystallization in ancient limestones. *In: Dolomitization and limestone diagenesis. Edited by L.C. Pray and R.C. Murray. Society of Economic Paleontologists and Mineralogists, Special Publication No. 13, pp. 14-48.*
- Folk, R.L. 1987. Detection of organic matter in thin sections of carbonate rocks using a white card. *Sedimentary Geology, 54, 193-200.*
- Ford, D. 1988. Characteristics of dissolutional cave systems in carbonate rocks. *In: Paleokarst. Edited by N.P. James and P.W. Choquette. Springer-Verlag, p. 25-57.*
- Frank, T.D. and Lohmann, K.C. 1995. Early cementation during marine-meteoric fluid-mixing: Mississippian lake valley Formation, New Mexico. *Journal of Sedimentary Research, A65, No. 2, 263-273.*
- Given, R.K., and Wilkinson, B.H. 1985. Kinetic control of morphology, composition and mineralogy of abiogenic sedimentary carbonates. *Journal of Sedimentary Petrology, 55, 109-119.*
- Goldstein, R.H. and Reynolds, T.J. 1994. Systematics of Fluid Inclusions in Diagenetic Minerals. *SEPM Short Course 31, p.199.*
- Gregg, J.M., and Sibley, D.F. 1984. Epigenetic dolomitization and the origin of xenotopic dolomite texture. *Journal of Sedimentary Petrology, 54, 908-931.*

- Hardie, L.A. 1987. Perspectives-dolomitization: a critical view of some current views. *Journal of Sedimentary Petrology*, **57**, 166-183.
- Hesse, R. 1990. Silica diagenesis: Origin of inorganic and replacement cherts. *In: Diagenesis. Edited by I.A. McIlreath and D.W. Morrow. Geoscience Canada Series 4*, pp. 253-275.
- Hoefs, J. 1997. Variations of stable isotope ratios in nature. *In: Stable Isotope Geochemistry. Springer, (eds.), Ch. 3*, p.65-167.
- Hopkins, J.C. 1997. Reservoir heterogeneity in the Pekisko Formation, Medicine River Field, Alberta, Canada. *CSPG Joint Convention*. p. 159-168.
- Hopkins, J.C. 1999. Characterization of Reservoir Lithologies Within Subunconformity Pools: Pekisko Formation, Medicine River Field, Alberta, Canada. *AAPG Bulletin*, **83**, No. 11, 1855-1870.
- Hopkins, J. 2004. Porosity distribution in a mudstone reservoir: Medicine River Pekisko E pool. *CSPG Seminar and Core Conference, Dolomites*. pp18.
- Hrabi, K.D. and Lawton D.C. 2001. Seismic Modelling of Pekisko Porosity. p.323-341. Web reference.
- Illing, L.V. 1959. Deposition and diagenesis of some upper Paleozoic carbonate sediments in western Canada. *Fifth World Petroleum Congress, New York, Proceedings Section 1*, p. 23-52.
- Jacobson, R.L., and Usdowski, H.E. 1976. Partitioning of strontium between calcite, dolomite and liquids. *Contributions to Mineralogy and Petrology*, **59**, 171-185.
- James, N.P. and Choquette, P.W. 1984. Diagenesis 9. Limestones-the meteoric diagenetic environment. *Geoscience Canada*, **11**, 161-194.
- Jones, B. 2005. Dolomite crystal architecture: genetic implications for the origin of the Tertiary dolostones of the Cayman Islands. *Journal of Sedimentary Research*, **75**, No. 2, 177-189.
- Kirkby, K.C. 1994. Growth and reservoir development in Waulsortian mounds: Pekisko Formation, west central, Alberta and Lake Valley Formation, New Mexico. Unpublished Ph.D. Thesis. University of Wisconsin. 371pp.
- Knauth, L.P. 1979. A model for the origin of chert in limestone. *Geology*. **7**, 274-277.
- Kosa, E., Hunt, D., Fitchen, W.M., Bockel-Rebelle, M. and Roberts, G. 2003. The heterogeneity of paleocavern systems developed along syndepositional fault zones: the Upper Permian Capitan Platform, Guadalupe Mountains, U.S.A. *In: Permo-Carboniferous Carbonate Platforms and Reefs, SEPM Special Publication No. 78 and AAPG Memoir 83*, p. 291-322.
- Kreitner, M.A. 1999. Facies, diagenesis, and depositional environments of the Mississippian Pekisko Formation, west-central Alberta. BSc Thesis, The University of Western Ontario. pp60.
- Kretz, R. 1982. A model for the distribution of trace elements between calcite and dolomite. *Geochimica et Cosmochimica Acta*, **46**, 191-195.
- Kupez, J.A., and Land, L.S. 1991. Late-stage dolomitization of the lower Ordovician Ellenburger Group, west Texas. *Journal of Sedimentary Petrology*, **61**, 551-574.
- Kupez, J.A., Montanez, I.P. and Gao, G. 1993. Recrystallization of Dolomite with time. *In: Carbonate microfabrics. Edited by R. Rezak and D.L. Ivoie. Elsevier*. 187-194pp.

- Kupecz, J.A., and Land, L.S. 1994. Progressive recrystallization and stabilization of early-stage dolomite: Lower Ordovician Ellenburger Group, West Texas. *In: Dolomites, a volume in honor of Dolomieu. Edited by B. Purser, M. Tucker and D. Zenger. International Association of Sedimentology Special Publication 21. p. 255-279.*
- Land, L.S. 1975. Paleohydrology of ancient dolomites; geochemical evidence: *AAPG Bulletin*. **59**, 1602-1625.
- Land, L.S. 1980. The isotopic and trace element geochemistry of dolomite, the state of the art. *In: Concepts and models of dolomitization. Edited by D.H. Zenger, J.B. Dunham, and R.L. Etherington. Society of Economic Paleontologists and Mineralogists, Special Publication No. 28, pp. 87-110.*
- Land, L.S. 1985. The origin of massive dolomite. *Journal of Geologic Education*, **33**, 112-125.
- Lewchuk, M.T., Al-Aasm, I.S., Symons, D.T.A. and Gillen, K.P. 1998. Dolomitization of Mississippian carbonates in the Shell Waterton gas field, southwestern Alberta: insights from the paleomagnetism, petrology and geochemistry. *Bulletin of Canadian petroleum Geology*. **46**, No. 3, 387-410.
- Lewis, D.W. and McConchie, D. 1994. Analytical Sedimentology. Chapman and Hall (eds.) 197pp.
- Lovering, T.G., and Patten, L.E. 1962. The effect of CO<sub>2</sub> at low temperature and pressure on solutions supersaturated with silica in the presence of limestone and dolomite. *Geochimica et Cosmochimica Acta*, **26**, 253-284.
- Lucia, F.J. 1983. Petrophysical Parameters Estimated From Visual Descriptions of Carbonate Rocks: A Field Classification of Carbonate Pore Space. *Journal of Petroleum Technology*, **35**, 629-637.
- Lumsden, D.N., and Chimahusky, J.S. 1980. Relationship between dolomite nonstoichiometry and carbonate facies parameters. *In: Concepts and models of dolomitization. Edited by D.H. Zenger, J.B. Dunham, and R.L. Etherington. Society of Economic Paleontologists and Mineralogists, Special Publication No. 28, pp. 123-137.*
- Machel, H. G. 1987. Saddle dolomite as a by-product of chemical compaction and thermochemical sulphate reduction. *Geology*, **15**, 936-940.
- Machel, H.G. and Anderson, J.H. 1989. Pervasive subsurface dolomitization of the Nisku Formation in central Alberta. *Journal of Sedimentary Petrology*. **59**, 891-911.
- Machel, H.G. 1997. Recrystallization versus neomorphism, and the concept of "significant recrystallization" in dolomite research. *Sedimentary Geology*. **113**, 161-168.
- Machel, H.G. 2004. Concepts and models of dolomitization: a critical reappraisal. *In: The Geometry and Petrogenesis of Dolomite Hydrocarbon Reservoirs. Geological Society, London, Special Publications 235, p. 7-63.*
- Macqueen, R.W. and Bamber, E.W. 1967. Stratigraphy of Banff Formation and lower Rundle Group (Mississippian), southwestern Alberta, Geological Survey of Canada, Paper 67-47.
- Malone, M.J., Baker, P.A. and Burns, S.J. 1996. Recrystallization of dolomite: an experimental study from 50-200°C. *Geochimica et Cosmochimica Acta*, **60**, 2189-2207.
- Martindale, W. and Boreen, T.D. 1997. Temperature-stratified Mississippian carbonates as hydrocarbon reservoirs – examples from the foothills of the Canadian Rockies. *In: Cool-water*

Carbonates. *Edited by* N.P. James and J.A.D. Clarke. Society of Economic Paleontologists and Mineralogists, Special Publications, **56**, 391-409.

McIntire, W.L. 1963. Trace element partition coefficients – a review of theory and application to geology. *Geochimica et Cosmochimica Acta*, **27**, 1209-1264.

McMechan, M. E. and Thompson, R. I. 1989. Structural style and history of the Rocky Mountain Fold and Thrust Belt. *In: Western Canada Sedimentary Basin: A Case History. Edited by* B. D. Ricketts. *Canad. Soc. Petrol. Geol.*, 47-71.

Meyers, W.J., and James, A.T. 1978. Stable isotopes of cherts and carbonate cements in the Lake Valley Formation (Mississippian), Sacramento Mountains, New Mexico. *Sedimentology*, **25**, 105-124.

Meyers, W.J. 1988. Paleokarstic features in Mississippian limestones, New Mexico. *In: Paleokarst. Edited by* N.P. James and P.W. Choquette. Springer-Verlag, p. 306-328.

Meyers, W.J., and Lohmann, K.C. 1985. Isotope geochemistry of regionally extensive calcite cement zones and marine components in Mississippian limestones, New Mexico. *In: Carbonate cements. Edited by* N. Schneidermann and P.M. Harris. Society of Economic Paleontologists and Mineralogists, Special Publication No. 36, pp. 223-239.

Middleton, G.V. 1963. Facies variation in Mississippian of Elbow Valley area, Alberta, Canada. *Bulletin of American Association of Petroleum Geologists*, **47**, 1813-1827.

Montanez, I.P., and Read, J.F. 1992. Fluid-rock interaction during stabilization of early dolomite, Upper Knox Group (Lower Ordovician), U.S. Appalachians. *Journal of Sedimentary Petrology*. **62**, 753-778.

Moore, C.H. 1989. Carbonate diagenesis and porosity. *Developments in sedimentology* 46. Elsevier, Amsterdam, 338p.

Morrow, D.W. 1982. Descriptive field classification of sedimentary and diagenetic breccia fabrics in carbonate rocks. *Bulletin of Canadian Petroleum Geology*, **30**, 227-229.

Morse, J.W. and Mackenzie, F.T. 1990. *Geochemistry of Sedimentary Carbonates*. Elsevier, New York, 707p.

Murray, R.C. and Lucia, F.J. 1967. Cause and control of dolomite distribution by rock selectivity. *Geological Society of America Bulletin*, **78**, 21-35.

O'Connell, S.C. 1990. The development of the Lower Carboniferous Peace River Embayment as determined from Banff and Pekisko formations depositional patterns. *Bulletin of Canadian Petroleum Geology*, **389A**, 93-114.

Osadetz, K.G. 1989. Basin analysis applied to petroleum geology in Western Canada. *In: Western Canada Sedimentary Basin: A Core History. Chapter 12 CSPG, Edited by* B.D. Ricketts, p.287-303.

Packard, J.J. 1992. Early formed reservoir dolomites of the Mississippian Upper Debolt Formation: Dunvegan gas field: A highly stratified reservoir hosting 1.2 TCF of sweet gas in Mississippian sabkha and contiguous subtidal sediments, NW, Alberta, CA. *In: Canadian Society of Petroleum Geologists and Faculty of Extension of the University of Alberta*, 11p.

- Podruski, J.A., Barclay, J.E., Hamblin, A.P., Lee, P.J., Osadetz, K.G., Procter, R.M., and Taylor, G.C. 1988. Conventional oil resources of western Canada, part 1: Resource Endowment: Geological Survey of Canada Paper 87-26, p. 7-125.
- Procter, R.M. and Macauley, G. 1968. Mississippian of Western Canada and Williston Basin. *AAPG Bulletin*, **52**, 1956-1968.
- Reading, H.G., Allen, P.A., Baldwin, T.C., Collinson, J.D., Edwards, M.B., Elliott, T., Jenkyns, H.C., Johnson, H.D., Mitchell, A.H.G., Schreiber, B.C., Sellwood, B.W. and Stow, D.A.V. 1986. *Sedimentary Environments and Facies*, second edition. *Edited by* H.G. Reading. 615pp.
- Reid, S.J. 1998. Anatomy of a Paleokarst Reservoir: Sedimentation and Diagenesis of the Pekisko Formation in Twining Oil Field, Alberta, Canada. Unpublished MSc. Thesis. University of Calgary. 279pp.
- Richards, B.C., Barclay, J.E., Bryan, D., Hartling, A., Henderson, C.M. and Hinds, R.C. 1994. Carboniferous strata. *In: Geological Atlas of the Western Canada Sedimentary Basin*, G.D. Mossop and I. Shetson (comp.), Canadian Society of Petroleum Geologists and Alberta Research Council, Calgary, Alberta,  
URL<[http://www.ags.gov.ab.ca/publications/ATLAS\\_WWW/ATLAS.shtml](http://www.ags.gov.ab.ca/publications/ATLAS_WWW/ATLAS.shtml)>, [February 13<sup>th</sup>, 2004].
- Robertson, K.E. 1989. Meteoric cements. *In: The fabric of cements in Paleozoic limestones. Edited by* K.R. Walker. Geological Society of America, Short Course #20, 54-65.
- Roedder, E. 1981. Origin of fluid inclusions and changes that occur after trapping. *In: Short Course in Fluid Inclusions: Applications to petrology. Edited by* L.S. Hollister and M.L. Crawford. Mineralogical Assoc. Canada, p. 101-137.
- Rollinson, H. 1993. Using stable isotope data. *In: Using geochemical data: evaluation, presentation, interpretation. Longman Singapore Publishers Ltd. (eds.), Ch. 7, p.266-315.*
- Saller, A.H., Budd, D.A. and Harris, P.M. 1994. Unconformities and porosity Development in Carbonate Strata: Ideas from a Hedberg Conference. *AAPG Bulletin*, **78**, No. 6, 857-872.
- Shinn, E.A., and Robbin, D.M. 1983. Mechanical and chemical compaction in fine-grained shallow water limestones. *Journal of Sedimentary Petrology*, **53**, 595-618.
- Sibley, D.F. and Gregg, J.M. 1987. Classification of Dolomite Rock Textures. *Journal of Sedimentary Petrology*, **57**, No. 6, 967-975.
- Sibley, D.F. 1990. Unstable to stable transformations during dolomitization. *Journal of Geology*. **98**, 967-975.
- Smith, T.M., and Dorobek, S.L. 1993. Alteration of early formed dolomite during shallow to deep burial: Mississippian Mission Canyon Formation, central to southwestern Montana. *Geological Society of America Bulletin*. **105**, 1389-1399.
- Speranza, A. 1985. Sedimentation and Diagenesis of the Pekisko Formation (Mississippian), Canyon Creek, Alberta. Unpublished MSc. Thesis. University of Calgary. 275pp.
- Steinhauff, D.M. 1989. Marine cements. *In: The fabric of cements in Paleozoic limestones. Edited by* K.R. Walker. Geological Society of America, Short Course #20, 37-53.
- Swinchatt, J.P. 1969. Algal boring: a possible depth indicator in carbonate rock sediments. *Geological Society of America Bulletin*, **80**, 1391-1396.



- Taylor, G.C., Macqueen, R.W. and Thompson, R.I. 1975. Facies changes, breccias and mineralization in Devonian rocks of Rocky Mountains, northeastern British Columbia (94B,G,K,N). *In: Current Research, Part A, Geological Survey of Canada, Paper 75-1A*, p. 577-585.
- Tucker, M.E. 1981. *Sedimentary petrology, an introduction*. Blackwell Scientific Publications, Oxford, 252p.
- Tucker, M.E., and Wright, V.P. 1990. *Carbonate sedimentology*. Blackwell Scientific Publications, Oxford, 482p.
- Veizer J. and Hoefs J. 1976. The nature of  $^{18}\text{O}/^{16}\text{O}$  and  $^{13}\text{C}/^{12}\text{C}$  secular trends in sedimentary carbonate rocks. *Geochimica et Cosmochimica Acta*. **40**, 1387-1395.
- Veizer, J. 1983. Trace elements and isotopes in sedimentary carbonates. *In: Carbonates: mineralogy and chemistry. Edited by R.J. Reeder*. Mineralogical Society of America. Reviews in Mineralogy Volume 11, pp. 265-300.
- Veizer, J., Ala, D., Azmy, K., Bruckschen, P., Buhl, D., Bruhn, F., Carden, G.A.F., Diener, A., Ebner, S., Godderis, Y., Jasper, T., Korte, C., Pawellek, F., Podlaha, O.G. and Strauss, H. 1999.  $^{87}\text{Sr}/^{86}\text{Sr}$ ,  $\delta^{13}\text{C}$  and  $\delta^{18}\text{O}$  evolution of Phanerozoic seawater. *Chemical Geology*, **161**, 59-88.
- Wang, B. and Al-Aasm, I.S. 2002. Karst-controlled diagenesis and reservoir development: Example from the Ordovician main-reservoir carbonate rocks on the eastern margin of the Ordos basin, China. *AAPG Bulletin*. **86**, No. 9, 1639-1658.
- Wanless, H.R. 1979. Limestone response to stress: pressure solution and dolomitization. *The Society of Economic Paleontologists and Mineralogists*. **79**.
- White, T. and Al-Aasm, I.S. 1997. Hydrothermal dolomitization of the Mississippian Upper Debolt Formation, Sikanni gas field, northeastern British Columbia, Canada. *Bulletin of Canadian Petroleum Geology*. **45**, No. 3, 297-316.
- Williams, S.H. 2005. Paleokarst in the Pekisko, west-central Alberta: its origin, recognition from horizontal and vertical well loss and impact on reservoir development. *Reservoir*, **32**, 27-34.
- Wright, V.P. 1991. Paleokarst: types, recognition, controls and associations. *In: Paleokarsts and paleokarstic reservoirs. Edited by V.P. Wright, M. Esteban and P.I. Smart*. Postgraduate Research Institute for Sedimentology, University of Reading Contribution 152, p. 56-88.
- Wright, W.R., Somerville, I.D., Gregg, J.M., Johnson, A.W. and Shelton, K.L. 2003. Dolomitization and neomorphism of Irish Lower Carboniferous (early Mississippian) limestones: evidence from petrographic and isotopic data. *Permo-Carboniferous Carbonate platforms and Reefs, SEPM Special Publication No. 78 and AAPG Memoir 83*, p. 395-408.
- Zemann, J. 1969. Crystal chemistry. *In: Handbook of geochemistry, v.1. Edited by K.H. Wedepohl*. Springer-Verlag, Berlin, pp.12-36.

## **APPENDIX I WELL LOCATIONS**

**Well 1:** 03-28-59-15w5 PETROCAN ET AL WINDFALL  
**Well 2:** 10-23-59-15w5 FINA AMOCO HB WIND  
**Well 3:** 12-11-37-14w5 SHELL 2 RAM  
**Well 4:** 08-27-39-11w5 P.S. ANCONA #1  
**Well 5:** 12-28-36-07w5 IMP HB RICINUS  
**Well 6:** 16-27-41-05w5 JETCO ET AL WILLGR  
**Well 7:** 10-04-56-13w5 MOBIL CHEVRON SHINING  
**Well 8:** 09-29-43-10w5 PCR PCP ET AL FERRIER  
**Well 9:** 16-18-48-13w5 HB WEST PEMBINA

### **SAMPLE NUMBERS**

E.g.: sample # **1-2-3-4**

**1** – Well number  
**2** – Core number  
**3** – Assigned unit number  
**4** – Assigned sample number

### **ABBREVIATIONS**

Mst – mudstone  
Wst – wackestone  
Pst – packstone  
Gst – grainstone  
Eu – euhedral  
Sub – subhedral  
An - anhedral  
PD – pervasive dolomite  
SCD – selective dolomite  
VFD - void filling dolomite  
SD – saddle dolomite  
DSAD – dissolution seam associated dolomite  
NSC – neomorphic sparry calcite  
BC – blocky calcite  
MC – micrite  
DMC – drusy mosaic calcite  
FC – fibrous calcite  
CRC – crinoid  
< DL – below detection limit

## APPENDIX II THIN SECTION DESCRIPTIONS

### Well 1

**TS #:** 1-2-3-1

**Name:** intraclast breccia dolostone

**Dolomite:** pervasive – 50-60%, <5 $\mu$ m, too small to see shape, replaced original mst selective – 25-30%, 20-50 $\mu$ m, eu-an, replacing breccia pores

**Porosity:** breccia – 40-50%, filled with calcite and selective dolomite

**Calcite:** blocky/poikilolotopic – 10-15% fills breccia fractures, fractured

**Fluorescence:** little to no UV

**General description:** Clasts are angular to subrounded and <1mm to 1.5cm in size. Many are still fitted and are polymodal. Intraclast matrix is fine dolomite replacing blocky to poikilolotopic calcite. Rock is almost completely dolomitized by microdolomite can't tell what the original fabric was. <1% quartz crystals scattered throughout.

**Paragenesis:** deposition, pervasive dolomitization (cannot tell precursor fabric), brecciation, blocky calcite, selective dolomite, quartz.

---

**TS #:** 1-2-5-1

**Name:** dolostone

**Dolomite:** pervasive – 95%, 20-40 $\mu$ m, eu-an

void filling – very little 1-2%, 10-90 $\mu$ m, eu, lining pores

**Porosity:** vuggy/moldic – 5-8%, filled and unfilled, some lined with dolomite

**Calcite:** blocky/poikilolotopic – fills vugs, fractured, few inclusions

**Fluorescence:** little to no UV, <2% organics

**General description:** completely dolomitized and porous. Under white card faint circular shapes are seen, could be crinoids or ooids also see brachiopods. 10-15% of the porosity is not filled. Rest is filled with blocky calcite or lined with void filling dolomite. See laminations, very faint, many vugs follow seams that crosscut laminations. Calcite cement is the same through out except for one vug where it is twinned. Void filling occurred before the blocky calcite.

**Paragenesis:** deposition, pervasive dolomitization (cannot tell precursor fabric), dissolution (vugs), void lining, blocky calcite.

---

**TS #:** 1-2-5-2

**Name:** dolostone

**Dolomite:** pervasive – 98-100%, <5 $\mu$ m, too small can't tell shape

void filling – very little <1%, 30-100 $\mu$ m, eu, lining pores

**Porosity:** vuggy – 5%, some lined with dolomite

**Calcite:** none

**Fluorescence:** none

**General description:** completely dolomitized, under white card see faint laminations that are slightly wavy. Vugs are sometimes lined with void filling dolomite. One stylolite apparent.

**Paragenesis:** deposition, pervasive dolomitization (cannot tell precursor fabric), dissolution (vugs), void lining, stylolite.

---

**TS #:** 1-3-6-1

**Name:** dolostone

**Dolomite:** pervasive – 75-80%, 20-50 $\mu$ m, sub-an

**Porosity:** vuggy – 2-5%, not filled

intercrystalline – 15-20%, filled with bitumen

**Calcite:** none

**Fluorescence:** some rhombs show some fluorescence

**General description:** shows sharp contact between two facies; dolostone and chert. Pores are filled with bitumen, evenly distributed. See faint cross laminations in chert, may point to transgressive – regressive sequence. Oil stained – bitumen. Under white card can see circular and crescent shapes therefore it was likely fossiliferous.

**Paragenesis:** deposition, pervasive dolomitization, left with intercrystalline pores, bitumen, and silicification.

---

**TS #:** 1-3-6-2

**Name:** dolostone

**Dolomite:** pervasive – 75%, 30-50 $\mu$ m, sub-an, coarse, cloudy and dirty

**Porosity:** vuggy – 2-5%, not filled, lined with bitumen

intercrystalline – 10-15%, filled with bitumen

**Calcite:** none

**Fluorescence:** some rhombs show some fluorescence

**General description:** shows sharp contact between two facies; dolostone and chert separated by a low amplitude stylolite. As you move away from the contact into the chert get progressively more dolomite until back to very porous dolomite facies. The original fabric is completely obliterated

**Paragenesis:** deposition, pervasive dolomitization, dissolution (vugs), silicification (or chert then dolomite, not sure which), stylolite.

---

**TS #:** 1-3-11-1

**Name:** dolostone

**Dolomite:** pervasive – 90-95%, 10-40 $\mu$ m, sub-an

void filling – very little 5-10%, 50-150 $\mu$ m, eu, lining pores

**Porosity:** vuggy/moldic – 35%, most unfilled, some lined with dolomite or bitumen

**Calcite:** none

**Fluorescence:** little to no uv

**General description:** completely dolomitized and very porous and slightly less coarse than 1-2-5-1. Under white card faint circular dark spots are seen, could be crinoids, peloids or ooids also see brachiopods. Vugs lined with void filling dolomite and/or bitumen. Looks as though most of porosity is moldic, fossils leached out.

**Paragenesis:** deposition, pervasive dolomitization (cannot tell precursor fabric), dissolution (vugs and molds), void lining, bitumen.

---

**TS #:** 1-3-13-1

**Name:** dolostone

**Dolomite:** pervasive – 95%, 30-60 $\mu$ m, eu-an

void filling – very little 5-7%, 60-160 $\mu$ m, eu, lining pores

saddle – one large crystal in a vug

**Porosity:** vuggy/moldic – 25% some lined with dolomite or bitumen

**Calcite:** none

**Fluorescence:** little to no uv

**General description:** completely dolomitized and very porous and coarser than 1-3-11-1. Under white card pseudomorphic dolomite of crinoids and very little saddle with sweeping extinction.

Coarser grained than previous in porous coarse zones and finer grained in less porous zones.

<1% quartz crystals associated with dissolution seams. Vugs lined with void filling dolomite and/or bitumen. Looks as though some of porosity is moldic, fossils leached out. Stylolite postdates pervasive dolomite and saddle dolomite postdates the stylolite.

**Paragenesis:** deposition, pervasive dolomitization (cannot tell precursor fabric), dissolution (vugs and molds), void lining, bitumen, saddle.

---

**TS #:** 1-3-14-1

**Name:** dolostone

**Dolomite:** pervasive – 95%, 30-70 $\mu$ m, eu-an

void filling – very little 5-7%, 50-130µm, eu, lining pores  
**Porosity:** vuggy/moldic – 35% some lined with dolomite  
**Calcite:** none

**Fluorescence:** little to no uv

**General description:** completely dolomitized and very porous. Highly fractured and dirty as per well 1 so far. Coarse as per last slide. Under white card see circular areas of dissolved (?) out fossils filled with slightly lighter and coarser dolomite than matrix also see crescent shaped pores.

**Paragenesis:** deposition, pervasive dolomitization (cannot tell precursor fabric), dissolution (vugs and molds), void lining.

---

## Well 2

**TS #:** 2-2-3-1

**Name:** wst

**Dolomite:** <1% scattered

**Porosity:** fracture – 5-8%, hairline and calcite filled  
intraparticle – 3-5%, calcite filled

**Calcite:** bladed equant – along brachiopods, line veins  
blocky – vein, fractured

micrite – micritized throughout, 1-2µm

**General description:** beginning of breccia – lots of veining, finely laminated wackestone, non-ferroan, very bioturbated and highly micritized. Most veins are vertical and 1-3 mm wide. The matrix is mostly micrite with few fossils distinguishable, some brachiopods, ostracods, and calcispheres. Stylolite cuts very large vertical vein and was the last event. Veins are lined with stubby equant calcite and filled with blocky calcite that is fractured. Veins crosscut hairline fractures. Bitumen is associated with veins along their edges and occurs before blocky and after equant. Calcite shows twinning indicating compaction. Broken shell fragments are aligned fairly well. White shows many flattened and aligned ostracods

**Paragenesis:** deposition, micritization, sparry calcite, leached calcispheres filled with drusy, veining, equant calcite, bitumen, blocky calcite, subvertical fracturing, stylolite, scattered microdolomite.

---

**TS #:** 2-2-4-1

**Name:** breccia

**Dolomite:** <1% scattered

**Porosity:** breccia – 55-60%, filled with bladed equant, fibrous and blocky  
interparticle – 2-3%, sparry calcite filled

**Calcite:** bladed equant – line breccia pores  
blocky – breccia, large, fractured, inclusion rich  
micrite – clasts

fibrous – line pores after equant

sparry – breccia, small, fractured

**Fluorescence:** Organics associated with micrite in allochems are very bright, overgrowths/zones fluoresces slightly in blocky calcite.

**General description:** The breccia has angular to subangular clasts, 1mm to 1.5 cm. Clasts are micritic and fossiliferous with brachiopods, ostracods where they are sometimes filled with drusy mosaic calcite and micrite. Also some peloids. Clasts are surrounded by calcite spar in smaller spaces and blocky in larger spaces. Some peloids have darker cores and cement rims, earlier calcite cement. Several grains have sweeping extinction. Faint laminations on some clasts.

**Paragenesis:** deposition, micritization, sparry calcite, brecciation, bladed equant calcite, radial fibrous, blocky calcite, scattered microdolomite.

---

**TS #:** 2-2-5-1

**Name:** breccia

**Dolomite:** <1% scattered, 30-100 $\mu$ m, anhedral, in clasts

**Porosity:** breccia – 55-60%, filled with bladed equant and blocky

interparticle – 2-5% filled with coarse sparry

intraparticle – 2-5% filled with coarse sparry

**Calcite:** bladed equant – line breccia pores

blocky – breccia, large, fractured, inclusion rich, twinned

micrite – clasts

fibrous – line pores after equant

sparry – breccia, small, fractured

**Fluorescence:** In large crystals see zones of yellow overgrowths with green cores.

**General description:** The breccia has angular to subangular clasts; 1mm to 1.5 cm. Clasts are micritic and peloidal with some ostracods. Also some peloids clasts are surrounded by calcite spar in smaller spaces and blocky in larger spaces. Some clasts look shattered with several small fragments all over surrounded by dissolution seams. Some blocky calcite (2%) being altered to anhydrite, shows that it's slightly stained but has cleavage of anhydrite and colour. Sweeping extinctions on several blocky crystals. Allochems include peloids, brachiopods, ostracods and calcispheres. Breccia filled with drusy fabric. Dissolution rings deflect around tiny fossils and cross cut veins and fractures. Large blocky is associated with bitumen.

**Paragenesis:** deposition, micritization, sparry calcite, brecciation, bladed equant calcite, fibrous, blocky calcite, chemical compaction, anhydritization, scattered microdolomite.

---

**TS #:** 2-2-5-2

**Name:** breccia

**Dolomite:** none

**Porosity:** breccia – 10-15%, filled with bladed equant and blocky

interparticle – 20-25% filled with coarse sparry

intraparticle – 2-3% brachiopods and ostracods filled with coarse sparry

**Calcite:** bladed equant – line breccia pores

blocky – breccia, large, fractured, twinned

micrite – clasts

sparry – breccia, small

**Fluorescence:** In large crystals see zones of yellow overgrowths with green and cores.

**General description:** Beginning of brecciation with blocky calcite filling veins, twinned. Precursor was a peloidal pst to gst, allochems include peloids, grapestones, brachiopods, ooids (?) dissolved out. Fractures lined with bladed equant and filled with blocky calcite.

**Paragenesis:** deposition, micritization, sparry calcite, brecciation, bladed equant calcite, blocky calcite, chemical compaction.

---

**TS #:** 2-2-6-1

**Name:** peloidal grainstone

**Dolomite:** <1% scattered

**Porosity:** fracture – 5%, hairline and calcite filled

interparticle – 35-40%, sparry calcite filled

**Calcite:** sparry – in interparticle pores

blocky – vein, fractured, twinned

micrite – peloids and in ostracods

**General description:** Peloids are well sorted made up of non ferroan micrite, 70-200  $\mu$ m.

Interparticle spaces are filled with spar. Several broken and unbroken brachiopods and ostracods, some filled with micrite and spar. Several horizontal hairline fractures crosscut vertical veins but not the one large one. Large one is filled with blocky calcite that is fractured and twinned. Bitumen seams associated with fractures. Microstylolites affecting some peloids. Most peloids have dark brown centers and lighter rims. This may be micrite rims that formed later.

Sparry calcite in pores came after mechanical breakup of peloids. Large vein same time and fluids as sparry in pores. One stylolite later.

**Paragenesis:** deposition, micritization, mechanical compaction, veining, sparry and blocky calcite, fracturing, bitumen, stylolites, scattered microdolomite.

---

**TS #:** 2-2-7-1

**Name:** brecciated mst to wst

**Dolomite:** selective – 30%, 5-15 $\mu$ m, euhedral, replacing clasts

**Porosity:** breccia – 15-20%, calcite filled

**Calcite:** bladed equant – lines veins

blocky – fills vein, fractured, twinned, inclusion rich

fibrous – follows equant, before blocky in vein

**General description:** A brecciated mst to wst made up of micrite and dolomite. Several vertical and subvertical dissolution seams 1-2mm wide, some finer ones are horizontal. Quartz crystals scattered throughout, 2-5%, 50 $\mu$ m associated with bitumen seams. Some pyrite also associated with seams. Brecciation followed by dissolution seam formation crosscuts vein. Veins filled with blocky calcite

**Paragenesis:** deposition, micritization, mechanical compaction, veining, bladed equant, fibrous, blocky calcite, fracturing, bitumen, dissolution seams, quartz, selective microdolomite.

---

**TS #:** 2-2-9-1

**Name:** brecciated wst to pst

**Dolomite:** scattered – 2-5%, 5-15 $\mu$ m, euhedral, clasts and cement

**Porosity:** breccia – 60%, calcite filled

**Calcite:** sparry – fills breccia pores

micrite – clasts

**Fluorescence:** Some zoning in calcite cement, bright overgrowths on some of large calcite crystals. Center seems dirty, these may have been allochems recrystallized.

**General description:** A brecciated wst to pst that may have been peloidal before. Clasts are micritized and pores are filled with sparry calcite. There are 2-5% quartz crystals scattered throughout cement with calcite and fluid inclusions within. Clasts are 500 $\mu$ m – 7mm.

Microdolomitized throughout. Possibly aggrading neomorphism from micrite to sparry calcite.

**Paragenesis:** deposition, micritization, brecciation, sparry calcite, neomorphism, microdolomite, quartz.

---

**TS #:** 2-2-10-1

**Name:** wackestone

**Dolomite:** scattered – 2-3%, 10-40 $\mu$ m, euhedral to anhedral

**Porosity:** moldic – 20-25%

**Calcite:** sparry – all over, inclusion rich, slightly fractured

micrite – all over

**Fluorescence:** none

**General description:** Non ferroan sparry wst, mostly micritized with interstices filled with coarser sparry calcite. 2% bitumen occurs as scattered specs. Very few vertical to subvertical hairline fractures cross cut all. There is more micrite in this thin section than in the previous. Scattered quartz throughout spar and micrite, 25 $\mu$ m.

**Paragenesis:** deposition, micritization, brecciation (?), sparry calcite, neomorphism, microdolomite, quartz.

---

**TS #:** 2-2-12-1

**Name:** chert

**Dolomite:** none

**Porosity:** moldic/vuggy – 5-7%, several vugs and dissolved fossils filled with calcite, most empty

**Calcite:** sparry – in molds

**Fluorescence:** organics fluoresces brightly in mud

---

**General description:** White card studies show ostracod remnants and possible rhomb shapes, dolomite altered by chert (?). Chert that is finely laminated and slightly bioturbated, possibly laminated bioclastic wst – pst originally. Chert intermixed with clays. Tiny leached fossils filled with calcite spar. Brachiopod fragments are aligned to laminations may show slight compaction.  
**Paragenesis:** deposition, dissolution, sparry calcite, silicification.

---

**TS #:** 2-2-14-1

**Name:** peloidal to fossiliferous grainstone

**Dolomite:** none

**Porosity:** interparticle – 70%, secondary

**Calcite:** sparry – all over, inclusion rich, slightly fractured

micrite – all over

**Fluorescence:** tiny bright inclusions or organics within messy micrite

**General description:** This thin section is very messy. There are several horizontal to sub-horizontal hairline fractures. Fossils include ostracods and brachiopods with a matrix that is hard to distinguish from allochems. Matrix is coarse spar with fossil outlines, peloids are well sorted and rounded to elongate and fossils are well aligned. This facies is laminated. There are calcite overgrowths on many grains. Increasing chemical compaction as proceed down the slide with seams and stylolites. The spar is very dirty and full of inclusions, neomorphism seams to be gradually obliterating peloids, and now is a sparstone.

**Paragenesis:** deposition, micritization, sparry calcite, neomorphism, chemical compaction.

---

**TS #:** 2-2-15-1

**Name:** chert

**Dolomite:** none

**Porosity:** interparticle – 30-40%, between clasts more chert

**Calcite:** sparry – in nodules or molds?

**Fluorescence:** slight fluorescent in fine matrix

**General description:** This is almost completely chert with some possible clay minerals, this may have been peloidal before(?). Large rounded clasts are coarser than the matrix made up of non ferroan calcite. This is a messy nodular facies. White card shows circles and arc shapes that may have been, ooids or brachiopods or ostracods, this may have been gst facies.

**Paragenesis:** deposition, silicification, sparry calcite.

---

### Well 3

**TS #:** 3-1-1-1

**Name:** Crinoidal wst-pst

**Dolomite:** dsa – 3%, 20-50 $\mu$ m, eu-an

scattered – 3-5%, 30 $\mu$ m, sub-eu, inclusion rich

**Porosity:** fracture – 20%, veins

interparticle – 10%

**Calcite:** isopachous – around brachiopods

syntaxial – crinoids

blocky – vein, associated with bitumen, fractured, inclusion rich, 20-100 $\mu$ m

micrite – micritized throughout, 1-2 $\mu$ m

**General description:** highly micritized crinoidal wst-pst with scattered dolomite rhombs, silica and anhydrite are present in small amounts mainly associated with the large vein (1cm) filled with blocky calcite. Fossils present include: crinoids, brachiopods and mollusks. Micritization occurred before the veining. Isopachous cement occurred before syntaxial cement. Anhydrite in vein is replacing calcite. Dissolution rings are also present. Bitumen is along the edges of and within the large vein. Most fossils are not touching.

**Paragenesis:** deposition, isopachous cement, syntaxial cement crinoids, micritization, blocky vein, bitumen, dsa dolomite, scattered dolomite.



---

**TS #: 3-1-2-1A****Name:** dolostone**Dolomite:** pervasive – 100%, 10-60 $\mu$ m, eu-sub, very dirty mostly eu, inclusion rich saddle – very little <1%**Porosity:** fracture – associated with stylolite, 2%, hairline up to 3mm wide, branching off from larger calcite filled fracturevuggy – 5%, ~ 50 $\mu$ m**Calcite:** fibrous – associated with stylolite, late stage blocky – fills fractures**Fluorescence:** dolomite rhombs fluoresce, with grass green cores and gradually brightens towards edges, 15-20% of dolomite does this, most have a thin bright green zone along the edge.**General description:** completely dolomitized, some fractures branching off of larger calcite filled fractures, cross cut stylolite and associated fibrous calcite. Sample 3-1-2-1B shows fine laminations with alternating finer and coarser dolomite.**Paragenesis:** deposition, pervasive dolomitization (cannot tell precursor fabric), fracturing before and after late stage stylolitization with associated fibrous calcite.

---

**TS #: 3-1-2-2****Name:** dolostone and crinoidal gst**Dolomite:** pervasive – 75-80%, 50-70 $\mu$ m, eu-subsaddle – 2-5%, 40-150 $\mu$ m, an, selectively replacing vein of calcitedsa – 15%, 10-50 $\mu$ m, eu, along seams**Porosity:** intercrystalline – 15-20%, filled with bitumen and calcite

vuggy – 5%, filled with calcite

**Calcite:** fibrous – associated with stylolite

blocky – fills intercrystalline pores

micrite

**Fluorescence:** organics fluoresce in micrite mud.**General description:** contact sample between dolostone and crinoidal gst facies. Gst is at the top and the dolostone is below. Contact is messy with high amount of high amplitude stylolites. Gst is highly micritized and partially dolomitized and includes peloids and crinoids and other bioclasts. Veining (vertical, 1mm wide) event crosscuts stylolite at contact and is filled with calcite prior to dolomitization. Dolomite is highly associated with stylolite at contact. Crinoids are inclusion rich, twinned, calcified, and dirty and fractures. Fine seams run throughout this facies horizontally. Dolostone facies is 100% dolomitized, this may have been a laminated or disturbed bed facies, some pyrite. Scattered oval shapes throughout with unit extinction may be flattened crinoids.**Paragenesis:** as per previous

---

**TS #: 3-1-7-1****Name:** crinoidal- peloidal gst**Dolomite:** selective microdolomite – <1%, 2-10 $\mu$ m, eu-sub, replacing interiors of crinoids**Porosity:** fracture – <1% hairline

interparticle – 10%, primary

intraparticle – 2-5%, primary

**Calcite:** micrite – envelopes on all grains

blocky – fills interparticle pores, fractured and inclusion rich

syntaxial – crinoids, filling interparticle pores

pendant – on some grains

**Fluorescence:** < 5% organics, very bright**General description:** very condensed gst, with some ooids and brachiopods, many microstylolites at grain contacts, fractures are post depositional crosscutting bioclasts and peloids, pre-dates blocky calcite in interparticle pores. Crinoids are micritized and inclusion rich.

Well compacted with point, concave and sutured contacts, grains are fairly aligned, few broken fossils. Early cementation is absent.

**Paragenesis:** micrite envelopes on all grains (early compaction feature), pendant cements, syntaxial overgrowths on crinoids and blocky calcite in pores, fractures filled with blocky calcite, selective dolomitization of crinoid cores.

---

**TS #:** 3-2-8-1

**Name:** crinoidal- peloidal pst-gst

**Dolomite:** scattered – 1-2%, 5-20 $\mu$ m, sub-an, not significant

dsa – 5%, 25-50 $\mu$ m, eu, associated with stylolite

**Porosity:** interparticle – 5%, primary, mosaic calcite filled  
intraparticle – 2-3%, primary, mosaic calcite filled

**Calcite:** fibrous – associated with stylolites

micrite – highly micritized all over

drusy mosaic – brachiopods: equant, fibrous and blocky

syntaxial – crinoids

**Fluorescence:** organics associated with allochems very bright.

**General description:** vertically oriented stylolites throughout, fibrous calcite associated with these. This calcite has been dissolved from adjacent areas and recrystallized here. Shows strained fabric. Allochems include, crinoids, peloids, ooids and brachiopods, some coated grains. Crinoids are twinned, contacts between grains are concave and sutured, and some allochems are broken. Micritization of calcite spar in pores and in centers of grains. Brachiopods are filled with drusy mosaic calcite – equant, fibrous and blocky. Syntaxial calcite cement overgrowths on crinoids also micritized.

**Paragenesis:** compaction, micritization, stylolitization and fibrous calcite

---

**TS #:** 3-2-9-1

**Name:** dolostone

**Dolomite:** pervasive – 100% (matrix), 15-30 $\mu$ m, eu-an, fine matrix

saddle – 2-5%, 1.5mm, an, cement in vugs, associated with stylolite

void filling – planar, 40-50 $\mu$ m, eu, lining vugs

pseudomorphic – replacing crinoids, <1%

**Porosity:** fracture – 1-2% hairline

vuggy to moldic – 15%, secondary

**Calcite:** blocky – fills vuggy pores and fractures, fractured and inclusion rich

**Fluorescence:** ~25% of dolomite rhombs fluoresce, all the same brightness and no zones.

**General description:** completely dolomitized, saddle dolomite is associated with a large stylolite, replaces blocky calcite within a vug, pore lining dolomite also within these vugs prior to calcite, followed by saddle. Vertical fractures filled with blocky calcite crosscut by horizontal fractures. Stylolite is later than both fracture events. White card shows possible brachiopod (ostracod?) pores filled with lighter dolomite, some crinoid ghosts.

**Paragenesis:** dolomitization, horizontal fractures filled with calcite, vertical fractures filled with calcite, stylolitization with associated calcite, void filling dolomite, saddle dolomite.

---

**TS #:** 3-2-10-1

**Name:** crinoidal gst

**Dolomite:** scattered – 1-2%, 20-250 $\mu$ m, eu-an, not significant

dsa – 2-4%, 20-170 $\mu$ m, eu, associated with seam

**Porosity:** interparticle – 10-15%, primary, syntaxial calcite filled

intraparticle – 2-3%, primary, mosaic calcite filled

**Calcite:** micrite – highly micritized all over

syntaxial – crinoids, twinned

**Fluorescence:** organics associated with micrite very bright.

**General description:** crinoidal gst with very large allochems up to 1-2 mm, highly micritized, 90% of thin section pores are filled with syntaxial cement, shows strain, therefore before

compaction. Allochems include crinoids, brachiopods, bryozoans, peloids, ostracods (filled with mosaic and lined with microspar). Messy stylolites going every which way. 10-15% silicification by chert. Contacts are sutured and fossils are broken. Highly microfractured and tight. Erratic dissolution seams with dissolution rings nearby.

**Paragenesis:** deposition, calcite cements, micritization, mechanical and chemical compaction, stylolite, dolomitization and silicification.

---

#### **Well 4**

**TS #:** 4-19-2-1

**Name:** dolomitic mudstone

**Dolomite:** pervasive – 40-45%, 5-15 $\mu$ m, eu-an

**Porosity:** vugs/molds – < 5%, calcite filled and follow laminations

**Calcite:** micrite – highly micritized all over with dolomite and clay or chert  
blocky – cement within quartz layers

**Fluorescence:** pervasive dolomite exhibits orange fluorescence, other larger rhombs are grass green, no zoning

**General description:** Half of slide is fine laminated mudstone with equal amounts of calcite, dolomite and chert or clays. Laminated facies separated from brecciated or quartz layered facies by a stylolite where stylolites crosscut quartz crystals. Quartz crystals are subrounded to subangular and form as aggregates with straight contacts, 40-90 $\mu$ m is size and inclusion rich. These are possibly original detrital quartz grains, highly fractured. Could just be megachert layers. Quartz may have nucleated from tiny crystals in the matrix.

**Paragenesis:** deposition, chert layers, blocky calcite, chemical compaction

---

**TS #:** 4-19-4-1

**Name:** mudstone

**Dolomite:** scattered - < 1%, 10-20 $\mu$ m, eu-an

**Porosity:** fenestral – 25%, sparry filled

interparticle – 6-8%

intraparticle – 6-8%

fracture – 5%, may be from coring

**Calcite:** micrite – highly micritized all over

sparry – coarse in nodules/pores, 250 $\mu$ m, twinned

**Fluorescence:** < 2% organics brightly fluoresces

**General description:** Non ferroan micritized mudstone with several nodules/fenestral pores of coarse sparry calcite cements. Several horizontal hairline fractures crosscut calcite cement. Very few vertical fractures. Calcispheres are also present filled with sparry calcite.

**Paragenesis:** deposition, fenestral pores, sparry calcite, fracturing

---

**TS #:** 4-19-5-1

**Name:** breccia

**Dolomite:** pervasive - 30%, 5-50 $\mu$ m, eu-sub, in clasts, pre-breccia

**Porosity:** breccia – 60%, filled with calcite, dolomite and bitumen

**Calcite:** bladed – line pores

blocky – fill pores, twinned, sweeping extinction

**Fluorescence:** bright orange fluorescence, organics associated with messy micrite, dolomite is bright yellow with bright rims, calcite is green

**General description:** Brecciated dolomudstone with clast sizes from <1mm – 8mm, angular to subangular. Breccia pores filled with drusy mosaic; bladed and blocky. Later chemical compaction in the form of stylolites and dissolution seams with associated dolomite (<1%). Bitumen fills some pores instead of blocky calcite. Poorly made thin section.

**Paragenesis:** deposition, dolomitization, brecciation, bladed calcite, blocky calcite, chemical compaction

---

**TS #: 4-19-7-1**

**Name:** dolostone

**Dolomite:** pervasive - 90%, 15-50 $\mu$ m, eu-an  
selective - 5%, 60-240 $\mu$ m, eu-sub

saddle - 1-2%, 100-250 $\mu$ m, an, fills vugs

**Porosity:** vuggy/moldic - 10%, filled with calcite and dolomite

**Calcite:** blocky - clear, some fractures

**Fluorescence:** large dolomite rhombs fluoresce slightly, no zones

**General description:** Dolomitized, stylolite is low amplitude and 1mm thick and separates two facies. Facies 1: Completely dolomitized, inclusion rich and organic stained. There is also coarser selective dolomite replacing calcite, this is also inclusion rich and fractured but mainly euhedral. There are some microfractures crosscutting the coarser dolomite and the calcite cement. Many dolomite rhombs show signs of etchings along their edges. Within dolomite areas 10% bitumen blobs are scattered. Facies 2: Mudstone, completely dolomitized, many pale brown dissolution seams, crosscut by a few stylolites. Some molds (?) of fossils partially filled with dolomite.

**Paragenesis:** deposition, dolomitization, dissolution seams, blocky calcite, selective dolomite, chemical compaction (stylolite), saddle dolomite

---

**TS #: 4-19-12-1**

**Name:** crinoidal grainstone

**Dolomite:** scattered - 2-3%, 10-40 $\mu$ m, eu-sub

dsa - 1-2%, 10-20 $\mu$ m, eu

**Porosity:** intraparticle - 5-8%, filled with blocky calcite

interparticle - 20%, filled with blocky calcite

**Calcite:** coarse sparry - clear, striated and strained

syntaxial - on crinoids

**Fluorescence:** organic inclusions within allochems fluoresces

**General description:** Allochems are largely in contact with many sutured and concave contacts. Grains have been slightly flattened, broken and deformed indicating mechanical compaction. Pores are filled with syntaxial or blocky calcite cement. Thin section was poorly made.

**Paragenesis:** deposition, syntaxial, sparry, mechanical compaction, chemical compaction, dissolution seam associated dolomite

**Well 5**

---

**TS #: 5-5-1-1**

**Name:** breccia

**Dolomite:** pervasive - 50%, 5-25 $\mu$ m, eu-an, clasts only, pre-breccia

**Porosity:** breccia - 40-45%, filled with blocky calcite

**Calcite:** coarse sparry - in matrix

blocky - strained fabric, sweeping extinction

**Fluorescence:** bright green dolomite rhombs with yellow rims

**General description:** Highly bioturbated and deformed breccias. Was a dirty limestone, matrix is sparry calcite. 5% silicification, quartz crystals are actually chalcedony with a radial texture.

Authigenic quartz throughout as well. Dirty mudstone layer likely made up of clays. Original quartz or siliceous organisms in matrix acted as nucleation sites for chalcedony. Many quartz crystals have carbonate inclusions. Authigenic quartz is post stylolitization or contemporaneous with stylolite. Pyrite and bitumen are very fine and after dolomite.

**Paragenesis:** deposition, dolomitization, brecciation, sparry calcite, blocky calcite, quartz/chalcedony, euhedral dolomite rhombs, pyrite and bitumen.

---

**TS #: 5-5-2-1**

**Name:** brecciated?dolostone

**Dolomite:** pervasive - 95%, 5-20 $\mu$ m, eu-sub, inclusion rich

**Porosity:** vuggy - 10-15%, filled with blocky calcite and some eu dolomite

---

**Calcite:** blocky – strained fabric, sweeping extinction  
**Fluorescence:** orange to yellow fluorescence of dolomite  
**General description:** Faintly laminated microcrystalline dolomite with several wispy dark brown organic rich layers. Mechanically compacted, can see flattened burrows along laminations. Microfracture perpendicular to laminations and crosscut burrows, dolomite and pyrite nodules.  
**Paragenesis:** deposition, dolomitization, dissolution, blocky calcite, replaced by euhedral rhombs of dolomite (void filling?), pyrite, fracturing

---

**TS #:** 5-5-3-1

**Name:** breccia

**Dolomite:** pervasive – 65-70%, 5-10 $\mu$ m, clasts only, pre-breccia  
selective – 60% of breccia cement, replaces calcite in pores, 10-75 $\mu$ m, eu, cloudy

**Porosity:** breccia – 30-35%, filled with blocky calcite and eu dolomite

**Calcite:** blocky – twinned, fractured

**Fluorescence:** Fine matrix dolomite fluoresces orange to yellow with no zoning, larger dolomite fluoresces green, zoned yellow – green – yellow.

**General description:** A brecciated dolomite with some clays angular clasts 100 $\mu$ m – 4mm, very messy. Pores filled with selective dolomite. Bitumen and pyrite are non selective and scattered throughout. Quartz crystals highly fractured and inclusion rich (dolomite and fluids), irregular shapes 100 $\mu$ m. Some blocky calcite cement between some grains some being replaced by quartz. Quartz grain contacts are sutured and grains have sweeping extinction. A stylolite surrounds some quartz grains, won't dissolve. Large amount of dedolomitization in pores.

**Paragenesis:** deposition, dolomitization, brecciation, blocky calcite, quartz/chalcedony, euhedral dolomite rhombs, pyrite and bitumen.

---

**TS #:** 5-5-3-2

**Name:** breccia

**Dolomite:** pervasive – 75-80%, 5-50 $\mu$ m, eu-an  
scattered – 10-15%, 20-100 $\mu$ m, eu-sub.

**Porosity:** intercrystalline – 10%, filled with bitumen  
vuggy – 5%, unfilled

**Calcite:** blocky – in nodules

**Fluorescence:** Fine matrix dolomite fluoresces orange, larger rhombs have cloudy brown cores followed by an orange zone rimmed by bright green.

**General description:** Highly brecciated nodular dolomitic mudstone with horizontal and subhorizontal stylolites. 5% quartz crystals that are inclusion rich (fluids, calcite) and fractured, 50 $\mu$ m – 3mm. Several horizontal dissolution seams with associated quartz. Large nodules are completely dolomitized, may have seen a brachiopod. Silica and calcite occur along some of the seams. Nodules are more calcitic. Dissolution seams are later crosscut by a stylolite. Dedolomitization present as well. Several horizontal and vertical fractures some filled with calcite, occurred before pervasive dolomite and crosscut by a stylolite.

**Paragenesis:** deposition, pervasive dolomitization, brecciation, blocky calcite, quartz/chalcedony, euhedral dolomite rhombs, pyrite and bitumen.

---

**TS #:** 5-6-4-1

**Name:** breccia

**Dolomite:** pervasive – 30-35%, <2-8 $\mu$ m, replacing clasts  
selective – 35-40%, 10-340 $\mu$ m, eu-sub, replacing matrix.

**Porosity:** interparticle/breccia – 65-70%, filled with selective dolomite and calcite

**Calcite:** coarse spar – in breccia pores

**Fluorescence:** dolomite rhombs are zoned with brown cores and orange rims. Can see a nodular fabric or breccia, micritic mud is associated with organics.

**General description:** Breccia with clast sizes of 50 $\mu$ m to 2mm and angular to subangular.

Silicification occurs as hexagonal crystals that are inclusion rich (calcite, fluid, quartz), 400  $\mu$ m. Clasts are dolomitic mudstone and some larger ones have fine laminations. Scattered specs of

bitumen (5%) occur throughout. A coarse calcite spar is also in the matrix. There are several dissolution seams associated with clasts, mudstone ones mainly. These occur after dolomitization. Several dedolomitized rhombs, cores are etched out. These occur in breccia fill. The rock was not dolomitized prior to brecciation. Quartz is dolomitized as well.

**Paragenesis:** deposition, brecciation, coarse calcite spar, authigenic quartz, dolomitization of clasts, dolomitization of matrix, dedolomitization and stylolitization.

---

**TS #:** 5-6-5-1

**Name:** mudstone/chert

**Dolomite:** pervasive – 35-45%, <5-50 $\mu$ m, an, scattered throughout calcite

**Porosity:** vugs/moldic – 10% of chert layers, filled with calcite, many shaped like brachiopods.

**Calcite:** blocky – in molds and in calcite beds

**Fluorescence:** no zoning, slight fluorescence

**General description:** Interbedded mudstone with beds that are 3mm-1cm thick comprised of alternating calcite and chert beds. Calcite beds are 35-40% dolomitized by very microcrystalline dolomite, shape is variable and hard to distinguish. It is in a calcite cement matrix. Chert beds have several dissolved molds of ooids (?) rounded molds, and brachiopods (crescent shaped molds) filled in with calcite. There is an abrupt change between beds, looks like sudden clay or chert enrichment. Some fractures occur along bed contacts filled with equant calcite crosscut by another fracture filled with dolomite or clay parallel to the above fracture. Bitumen is associated with the largest vein.

**Paragenesis:** deposition, dissolution, chert, veining, blocky calcite, bitumen.

---

**TS #:** 5-6-6-1

**Name:** dolomitic mudstone with chert nodules

**Dolomite:** pervasive – 40-50%, <5-100 $\mu$ m, an-sub, scattered throughout the matrix

**Porosity:** interparticle – 2-5%, blocky calcite fills in nodules

**Calcite:** coarse spar – mudstone matrix

blocky – in molds, nodules

**Fluorescence:** none

**General description:** Several horizontal hairline fractures crosscut a vertical vein. Within the oolitic grainstone in chert nodules, dedolomitization is occurring with 45-50% dolomite left rest is a calcite spar, some larger dolomite rhombs have been completely calcified. A coarse sparry calcite in molds of fossils, round and arc shaped. %% quartz crystals throughout the matrix 80-90  $\mu$ m. A large horizontal stylolite associated with nodules or cavity fills. The largest nodule is 2 cm and irregularly shaped, others are as small as 2mm, the average is 1cm. Nodules are silicified ooid crinoidal grainstones. Calcite cement with dolomite shape encroaching on chert allochems, this may have been dolomite, dedolomitized. Grains are replaced by chert and megaquartz. Rims of allochems are fibrous quartz, inside is chert and centers are megaquartz. Contacts are concave and point.

**Paragenesis:** deposition, micritization, neomorphism to spar, dolomitization and silicification. Nodules – oolitic grainstone, chert, dolomitized, dedolomitization, blocky calcite, stylolitization.

---

**TS #:** 5-6-6-2

**Name:** mudstone /chert

**Dolomite:** pervasive – 85%, <5-60 $\mu$ m, eu-an, mostly fine and scattered throughout the matrix

**Porosity:** fracture – 5-10%, filled with calcite

**Calcite:** coarse spar – veins

**Fluorescence:** vein associated dolomite with high organics is very bright with no zones.

**General description:** Highly bioturbated or brecciated. Very large clasts are subangular to rounded, 2-3cm in size. Highly fractured vertical to subvertical. At least 2 veining events, those which penetrate only the clasts and those that cross both the clasts and the matrix. These are filled with calcite. Clasts are dolomite and chert, see some dolomite rhombs that are larger than others. This is very dirty dolomudstone. Several stylolites and quartz crystals associated with

these. The matrix between the clasts is lighter and finer clay or dolomite. Geopetal fabric is apparent in some brachiopods in clasts. Some fossils are filled with megaquartz.

**Paragenesis:** deposition, fracturing, chert, brecciation, dissolution, calcite cement, stylolite, dolomitization (?).

---

**TS #:** 5-6-7-1

**Name:** crinoidal grainstone (sparstone)

**Dolomite:** selective – 25-30%, 20-110 $\mu$ m, an-eu, replacing interparticle pores

**Porosity:** moldic – 5%

interparticle – 30-35%, mostly dolomitized

**Calcite:** coarse spar – intergranular matrix and in molds

blocky – in molds

**Fluorescence:** no zoning, slight fluorescence of dolomite

**General description:** Several large calcite crystals 500  $\mu$ m with inclusion rich cores.

Dedolomitization is occurred by calcite. This is now a sparstone but was a coarse grained crinoidal grainstone, but is very messy. Know it may be crinoidal from unit extinction of large calcite crystals. There are also several round and oval shapes filled with a coarse calcite spar. The interparticle spaces around these are mainly microcrystalline dolomite. Fracturing (subvertical) occurred after calcite cement and prior to dolomitization followed by very large calcite crystals that are highly fractured, inclusion rich cores (dolomite and fluid), twinned and causing dedolomitization. This is all followed by silicification by chert in crystals.

**Paragenesis:** deposition, interparticle calcite cement, dissolution, dolomitization, blocky calcite, dedolomitization, chert.

---

**TS #:** 5-6-8-1

**Name:** grainstone with cherty collapse structure

**Dolomite:** selective – 10-20%, <5-25 $\mu$ m, eu-an, interparticle porosity, micro in crinoids

**Porosity:** fracture – 1-2%, filled with calcite

moldic - <1%, of brachiopods.

**Calcite:** micrite – throughout

sparry – matrix

syntaxial – on crinoids

blocky – in vein

**Fluorescence:** organics are very bright with no zones in muddy facies.

**General description:** This is a grainstone with a cherty collapse looking structure. The crinoidal-peloidal grainstone has 15% dedolomitization of eu-sub rhombs replaced by calcite spar 40-60  $\mu$ m. There is a fine anhedral dolomite replacing crinoid centers. Syntaxial calcite cement on crinoids makes up 75-60% of slide. Very dirty and messy. High micrite, allochems include, peloids, crinoids and brachiopods. All is micritized with crinoids micritized partially. The siliceous grainstone is crinoidal and peloidal and silicified 85%. Calcite vein within this section, vertical and made up of blocky calcite. Crosscuts chert. The vein is crosscut by the stylolite. The contact between the 2 is abrupt with stretches that have a stylolite (grains affected). Chert structure is in layers, alternating chert layers with fossiliferous chert layers. Fossils include ostracods and crinoids, see point contacts with fewer sutured and concave. Fossils are replaced by chert and megaquartz. Some calcite still in matrix intermixed with chert. Evidence of broken fossils.

---

**TS #:** 5-6-9-1

**Name:** crinoidal grainstone

**Dolomite:** selective – 10%, <2-10 $\mu$ m, an-eu, selectively replacing fossils

**Porosity:** intraparticle – 5%, filled with fibrous calcite

interparticle – 10-15%, filled with sparry calcite

**Calcite:** syntaxial – crinoids

blocky – all over, interparticles

bladed – along brachiopods

**Fluorescence:** organics associated with allochems are bright green.

**General description:** Very coarse grainstone, fossils are up to 1cm. 10% silicification of allochems. Highly calcite cemented, very dirty and inclusion rich. Allochems are fractured, aligned indicating mechanical compaction. There is blocky calcite cement all over, sometimes making it difficult to distinguish where the allochems are. Some of this may be syntaxial cement. Many broken fossils and sutured contacts. Some horizontal microstylolites. Fossils include crinoids, brachiopods, bryozoans and algae (strange structured fossils). Blocky calcite is twinned.  
**Paragenesis:** deposition, bladed calcite, blocky and syntaxial calcite, mechanical compaction, neomorphism (?), chemical compaction, dolomitization, silicification

---

## **Well 6**

**TS #:** 6-1-1-1

**Name:** breccia

**Dolomite:** pervasive – 60-65%, <5-25 $\mu$ m, eu-sub, selectively replacing center of calcite crystals and scattered throughout rock

**Porosity:** fracture – 15-20%, filled with calcite cement

**Calcite:** sparry – all over  
blocky – in larger veins

**Fluorescence:** Fine matrix dolomite fluoresces yellow to orange and bright green.

**General description:** Highly fractured sparstone that is brecciated into clasts that are still fitted. Dolomite occurs in calcite crystal cores, these may have been fossils that were neomorphosed. Vertical fractures or veins 1-2 mm wide contain calcite spar. These are crosscut by horizontal hairline fractures. Some clastic areas are completely dolomitized others are half calcite half dolomite. Calcite is fractured and twinned. In the bottom corner of the slide there are calcite (possibly quartz before) crystals floating in one large calcite crystal. These have quartz like terminations or may be anhydrite or gypsum. Blocky calcite filling larger fractures. Neomorphism of original limestone. Bitumen is scattered only in the original rock.

**Paragenesis:** deposition, brecciation, neomorphism, sparry calcite, dolomitization, blocky calcite, anhydritization or silicification.

---

**TS #:** 6-1-2-1

**Name:** mudstone

**Dolomite:** none

**Porosity:** vuggy – 20%, seams associated with them  
interparticle – 5-7%

moldic – 3%, brachiopod molds mainly

**Calcite:** sparry – in some interstices

micrite – makes up all of matrix

blocky – filling some pores

**Fluorescence:** none

**General description:** A mudstone with very large features 1-6mm filled with calcite cement. Blocky calcite that fills these is associated with bitumen, it is fractured and twinned. Also molds of fossils (round and arc shaped) filled with calcite cement. Gypsum or quartz crystals scattered throughout, very tiny. Pores filled with bitumen and blocky calcite. Several calcispheres scattered throughout.

**Paragenesis:** deposition, micritization, bitumen, blocky calcite, sparry calcite, vertical fracture, horizontal fracture, stylolites and quartz.

---

**TS #:** 6-1-3-1

**Name:** wackestone

**Dolomite:** pervasive – <1%, 10-30 $\mu$ m, sub-an, replacing matrix, scattered

dsa – 1-2%, 10-40 $\mu$ m, an, along seams

**Porosity:** fracture – 1-2%

interparticle – 20-25%



**Calcite:** sparry – in some interstices

micrite – makes up all of matrix

**Fluorescence:** stylolites fluoresces, organic rich

**General description:** Wispy laminated wackestone with microstylolites and associated microdolomite. Bitumen specs occur throughout the rock. 10-15% quartz grains 20-40 $\mu$ m. Vertical fracture filled with sparry calcite and crosscut by a horizontal clay or dolomite filled fracture. The rock is highly micritized and peloids exist surrounded by sparry calcite cement. Very fossiliferous, includes brachiopods. Many small dissolution seams.

**Paragenesis:** deposition, micritization, sparry calcite, vertical fracture, horizontal fracture, stylolites and quartz.

---

**TS #:** 6-2-8-1

**Name:** dolostone

**Dolomite:** pervasive – 55-60%, 10-40 $\mu$ m, eu-sub, rock not completely dolomitized

**Porosity:** vuggy – 30-35%, filled with blocky calcite

intercrystalline – 10-15%, filled with bitumen

**Calcite:** blocky – may be coarse spar, what is not dolomitized

**Fluorescence:** bituminous regions highly fluoresces, dolomite fluoresces slightly a dull green

**General description:** Almost completely dolomitized, the rest is calcite cement. Sediments look disturbed, many swirls with dissolution seams everywhere. There is a vertical fracture filled with calcite cement partially dolomitized. White card reveals circular shapes, possibly ooids or crinoids with dark centers. Original rock fabric has been almost completely destroyed.

**Paragenesis:** deposition, calcite cement, neomorphism, fracturing, dolomitization.

---

**TS #:** 6-2-11-1

**Name:** dolostone

**Dolomite:** pervasive – 95%, 10-70 $\mu$ m, eu-an

void filling – 2%, 20-60 $\mu$ m, eu, lines vugs

**Porosity:** vuggy – 10-15%, filled with blocky calcite, lined with dolomite

intercrystalline – 10-15%, filled with bitumen

**Calcite:** blocky – fills vugs

**Fluorescence:** Half of dolomite fluoresces bright green the rest is dull with no zoning.

**General description:** Completely dolomitized with scattered specs of bitumen.

**Paragenesis:** deposition, dolomitization, dissolution, void filling dolomite, blocky calcite cement, bitumen.

---

**TS #:** 6-2-11-2

**Name:** dolostone

**Dolomite:** pervasive – 100%, 10-35 $\mu$ m, eu-an, mainly an to sub microdolomite

**Porosity:** vuggy – <1%, filled with blocky calcite

intercrystalline – 5%, filled with bitumen

fracture – one very large vein filled with a single crystal of calcite

**Calcite:** blocky – fills vugs and vein(?), twinned, fractured

**Fluorescence:** Zones exist within the large vein with bright green cores and overgrowths are dull, many strained fabrics in the vein.

**General description:** Completely dolomitized with scattered specs of bitumen. A large vein filled calcite cement cuts vertically through dolomite, contact is stylolitized. It is twinned, fractured and inclusion rich.

**Paragenesis:** deposition, dolomitization, dissolution, blocky calcite cement in vein, bitumen, stylolite.

---

**TS #:** 6-2-12-1

**Name:** crinoidal grainstone

**Dolomite:** none

**Porosity:** intraparticle – 1-2%, filled with bladed and sparry calcite

interparticle – 10-15%, filled with bitumen and calcite cement

**Calcite:** syntaxial – on crinoids

drusy mosaic – in brachiopods

blocky – fills interparticle pores

bladed equant – lines grains in interparticle pores

**Fluorescence:** organics fluoresces

**General description:** Allochems include crinoids, brachiopods, ostracods, peloids and fossil fragments. Many fossils are broken, slide is messy. Most fossils are rimmed with bitumen. Bladed equant calcite cement around many fossils that are filled with blocky calcite. Syntaxial overgrowth on crinoids. Concave and sutured contacts exist between grains. This limestone is overcompacted and many edges of grains are oil stained. Drusy mosaic fabric is seen in some brachiopods. Was likely not well cemented prior to compaction.

**Paragenesis:** deposition, micritization, drusy mosaic, syntaxial cement, mechanical compaction, hydrocarbons, bladed, blocky, chemical compaction.

---

**TS #:** 6-2-15-1

**Name:** grainstone (cementstone)/ dolostone

**Dolomite:** dsa – 2-4%, 30-50 $\mu$ m, eu-an, along bituminous seams

selective – 20-25%, 10-50 $\mu$ m, eu-an, scattered patches, centers of previous fossils (?)

**Porosity:** fracture – 1-2%, filled with bladed and sparry calcite

interparticle – 10-15%, filled with bitumen and calcite cement

**Calcite:** coarse sparry – matrix

**Fluorescence:** organics fluoresces associated with dolomite, dolomite fluoresces slightly.

**General description:** This is a very complex sample that may have been a grainstone with outlines of fossils (crinoids or ooids) still apparent. It has largely been neomorphosed by coarse sparry calcite. Some selective dolomite throughout as well as scattered bitumen. Edges of dolomite rhombs are etched. Peloids are replaced by dolomite. Crinoids are completely obliterated by calcite cement. Sample is very heavily oil stained as well.

**Paragenesis:** deposition, neomorphism to coarse sparry calcite, dolomitization, chemical compaction/dissolution seams, dissolution seam associated dolomite, bitumen, dedolomitization.

---

**TS #:** 6-3-17-1

**Name:** ooid grainstone

**Dolomite:** selective – 2-5%, microdolomite replacing rims of ooids

**Porosity:** intraparticle – 5%, filled with calcite

interparticle – 40-45%, filled with syntaxial and blocky calcite cement

moldic – 2%, crinoids dissolved out and filled with calcite

**Calcite:** blocky – matrix

syntaxial – matrix on crinoids

isopachous – surrounds grains

**Fluorescence:** rims of ooids fluoresces brightly, associated to organics

**General description:** This grainstone was cemented early and shows no mechanical or chemical compaction. Blocky calcite cement fills the interparticle pores and it is fractured and inclusion free. Some larger crystals have inclusion rich cores. Many grains are lined with isopachous radial fibrous cement. Few grains are touching and none are deformed. A few crinoids occur as ghost in cement, possibly syntaxial has completely replaced them. There is a possible hardground because fossils are cut off. Syntaxial calcite cement is very early. Ooid rims are very oil or bitumen rich. Allochems include peloids, crinoids and ooids.

**Paragenesis:** deposition, micritized, isopachous, syntaxial, blocky, bitumen and dolomitization.

---

**TS #:** 6-3-18-1

**Name:** ooid grainstone

**Dolomite:** selective – 5-10%, microdolomite in crinoids and along edges of fossils

**Porosity:** intraparticle – crinoids or ooids dissolved out and filled with spar

interparticle – filled with calcite cement and bitumen

**Calcite:** blocky – matrix (very little)

syntaxial – matrix on crinoids

sparry – in ostracods

drusy mosaic – in brachiopods

**Fluorescence:** rims of ooids fluoresces brightly, associated to organics

**General description:** This fossiliferous grainstone includes ooids, crinoids, peloids, brachiopods, bryozoans and ostracods. Contacts are concave and sutured and there is 4% silicification of crinoids. Syntaxial cement is seen on some crinoids. Most allochems are in contacts and in interparticle spaces blocky calcite cement occurs. Some fossils are broken and very dirty micritized. All fossils have micrite envelopes, most are ooids with fossils as nuclei. Sparry calcite which fills ostracods has sweeping extinction. This rock is very dirty and oil stained. Brachiopods are filled with drusy mosaic calcite (early). Syntaxial overgrowths on crinoids are pre-compaction. Flat fossils are aligned. There are very few pore spaces left except where filled by syntaxial overgrowths.

**Paragenesis:** deposition, sparry, drusy mosaic, micritized, syntaxial, mechanical compaction, chemical compaction, blocky, bitumen and dolomitization.

---

**TS #:** 6-3-19-1

**Name:** crinoidal grainstone

**Dolomite:** selective – 2-5%, microdolomite in crinoids and along edges of fossils

**Porosity:** intraparticle –1-2%

interparticle – 20-25%, filled with calcite cement and bitumen

**Calcite:** syntaxial – matrix on crinoids

pendant and meniscus – edges of fossils

bladed – in molds of fossils dissolved out

**Fluorescence:** rims of ooids fluoresces brightly, associated to organics

**General description:** As per previous crinoidal grainstone but much dirtier and less cement. It is fossiliferous but mostly made up of crinoids (60-65%). It is also highly compacted with little to no matrix, highly micritized and has many broken fossils. Bitumen fills many pore spaces. Isopachous bladed cements in dissolved out ooids. Heavily oil stained. Sustained both mechanical and chemical compaction with sutured contacts. Mostly syntaxial overgrowth cement that is twinned. The microdolomite is mainly replacing ooid rims. Some stylolites throughout. Crinoids and other fossils have pendant and meniscus cements that predate syntaxial overgrowths.

**Paragenesis:** deposition, micritized, pendant/meniscus, syntaxial, mechanical compaction, chemical compaction, dissolution, bladed, bitumen and dolomitization.

---

**TS #:** 6-3-19-2

**Name:** crinoidal grainstone

**Dolomite:** selective – 15%, microdolomite on rims of ooids

**Porosity:** interparticle – 5-10%, associated with bitumen

**Calcite:** syntaxial – matrix on crinoids, twinned

drusy mosaic – in fossils

**Fluorescence:** rims of ooids fluoresces brightly, associated to organics

**General description:** Includes many ooids and crinoids and a matrix that is highly altered. Dolomite is selective to ooid rims. Interparticle pores lined with bitumen, possibly formed secondarily. Syntaxial cements on crinoids. Some ostracods are filled with drusy mosaic calcite. Most fossils are broken and most are not touching or point contacts. Matrix is mainly syntaxial overgrowths and blocky calcite. Pores are lined with oil residues. Possible anhydrite replacing syntaxial cement. Some crinoids have dissolved edges.

**Paragenesis:** deposition, micritized, drusy mosaic, syntaxial, mechanical compaction, chemical compaction, dissolution, bitumen/oil, dolomitization and anhydritization.

---

**TS #:** 6-3-20-1

**Name:** crinoidal grainstone

**Dolomite:** selective – 1-2%

**Porosity:** interparticle – 50%, filled with syntaxial and bitumen  
intraparticle – 10%, drusy mosaic in fossils

**Calcite:** syntaxial – matrix on crinoids, twinned  
drusy mosaic – in fossils

**Fluorescence:** organics fluoresces brightly and are associated with micrite

**General description:** A very messy crinoidal grainstone with very large fossils up to half a cm wide. Highly brecciated with several broken fossils. Syntaxial cement on crinoids and some crinoids' centers are dissolved out and filled with sparry. Calcite cement in this slide are more fractured and twinned. Early bladed calcite lines brachiopods. Some brachiopods are filled with drusy mosaic calcite. Some dissolved edges on crinoids are apparent. Very similar to previous sample but with larger crinoids and less bitumen and porosity.

**Paragenesis:** deposition, micritized, drusy mosaic, syntaxial, mechanical compaction, chemical compaction, dissolution, bitumen/oil, dolomitization and anhydritization.

---

## Well 7

**TS #:** 7-1-1-1

**Name:** dolostone

**Dolomite:** pervasive – 95%, ~10 $\mu$ m, an  
void filling – 2-3%, 30-300 $\mu$ m, eu, lining pores

**Porosity:** vuggy/moldic – 5-10%, lined with dolomite, some molds  
fractures – 1-2%, vertical filled with calcite

**Calcite:** blocky – fills fracture and pores

**Fluorescence:** dull to bright fluorescence in pervasive dolomite, void filling is dull

**General description:** completely dolomitized. Under white card see ostracod ghost fossils and geopodal fabric in one vug that is eye shaped. Horizontal stylolite with some quartz crystals associated with it. One hairline fracture filled with blocky calcite, vertical, pyrite associated with it. Calcite filling some pores. The vertical vein crosscuts molds lined with void filling dolomite. Pyrite is also in some pores. The horizontal stylolite crosscuts the vein.

**Paragenesis:** deposition, pervasive dolomitization, dissolution (vugs and molds), void lining, fracturing, blocky calcite, pyrite and chemical compaction (stylolite).

---

**TS #:** 7-1-2-1

**Name:** dolostone

**Dolomite:** pervasive – 90-95%, 5-20 $\mu$ m, eu-an  
void filling – 5%, 40-100 $\mu$ m, eu, lining pores

**Porosity:** vuggy – 20%, large ones filled and small ones unfilled, some lined with dolomite

**Calcite:** blocky – fills vugs, fractured, few inclusions, clear, twinned

**Fluorescence:** pervasive dolomite is dull to bright, no zoning

**General description:** completely dolomitized and porous. Under white card faint circular shapes are seen, could be crinoids or ooids. 15-20% porosity. Bitumen spots associated with calcite in vugs. Some brecciation occurs between this sample and the above.

**Paragenesis:** deposition, pervasive dolomitization, dissolution (vugs), void lining, blocky calcite, bitumen.

---

**TS #:** 7-1-3-1

**Name:** dolostone

**Dolomite:** pervasive – 90%, 5-20 $\mu$ m, eu-an

void filling – 10%, 20-100 $\mu$ m, eu, lining pores

**Porosity:** vuggy – 25-30% unfilled

**Calcite:** none

**Fluorescence:** pervasive dolomite is dull, no zoning  
**General description:** completely dolomitized and porous. Under white card faint circular shapes are seen, could be crinoids or ooids. Some vugs lined with oil residue, laminated.  
**Paragenesis:** deposition, pervasive dolomitization, dissolution (vugs), void lining, bitumen.

---

**TS #:** 7-2-4-1

**Name:** dolostone

**Dolomite:** pervasive – 90%, 10-20 $\mu$ m, sub-an  
void filling – 10%, 30-70 $\mu$ m, eu, lining pores

**Porosity:** vuggy – 20-30% unfilled, some lined with dolomite

**Calcite:** none

**Fluorescence:** little to no fluorescence

**General description:** completely dolomitized and very porous. Some pores also filled with quartz and bitumen by < 1%. Slightly coarser and dirtier than previous. Possibly fenestral originally. Oil residue after void filling dolomite. Microfractures every which way after dolomitization.

**Paragenesis:** deposition, pervasive dolomitization, dissolution (vugs), void lining, fracturing, bitumen.

---

**TS #:** 7-2-4-2

**Name:** dolostone

**Dolomite:** pervasive – 90%, 40-80 $\mu$ m, eu-an  
void filling – 10%, 30-100 $\mu$ m, eu, lining pores

**Porosity:** vuggy – 25-30% unfilled, some lined with dolomite

**Calcite:** none

**Fluorescence:** little to no fluorescence

**General description:** completely dolomitized and very porous. This sample is finer than previous, more like 7-1-3-1. Some vugs could be molds (look like brachiopods), some lined with bitumen after void filling, laminated again.

**Paragenesis:** deposition, pervasive dolomitization, dissolution (vugs), void lining, bitumen.

---

## **Well 8**

**TS #:** 8-2-6-1

**Name:** dolostone

**Dolomite:** pervasive – 75-80%, 40-100 $\mu$ m, eu-sub, unimodal distribution

**Porosity:** intercrystalline – 20-25%, filled with blocky calcite or unfilled

**Calcite:** blocky – 20-25%, fills intercrystalline porosity

**Fluorescence:** some dull fluorescence of the dolomite matrix with faint brighter rims on many rhombs.

**General description:** The rock has been almost completely dolomitized. White card studies show no fabrics. Intercrystalline pores have been filled by calcite cement.

**Paragenesis:** deposition, blocky, pervasive dolomitization.

---

**TS #:** 8-2-7-1

**Name:** dolostone

**Dolomite:** pervasive – 98%, 40-80 $\mu$ m, eu-an, bimodal distribution  
void filling – 2%, 100-140 $\mu$ m, eu, lining pores

**Porosity:** vuggy – 3-5% unfilled, some lined with dolomite and bitumen  
intercrystalline – 15-17%, filled with bitumen

**Calcite:** none

**Fluorescence:** some dull fluorescence of the dolomite matrix and void filling dolomite

**General description:** Pervasive dolomite has a bimodal distribution where coarser dolomite is euhedral and finer stuff is subhedral to anhedral. The larger dolomite displays some sweeping

extinction. The coarsening of dolomite may be from recrystallization. Bitumen fills intercrystalline pores. Few dissolution seams.

**Paragenesis:** deposition, pervasive dolomitization, dissolution seams, dissolution (vugs), void lining, bitumen.

---

**TS #:** 8-2-7-2

**Name:** dolostone

**Dolomite:** pervasive – 70-80%, 40-100 $\mu$ m, eu-an

void filling – 20-25%, 80-120 $\mu$ m, eu, lining pores

**Porosity:** vuggy/moldic – 2%, filled with calcite, some look like brachiopods

intercrystalline – 20-30%, filled with bitumen

**Calcite:** blocky – fills pores

**Fluorescence:** dull fluorescence of dolomite with slight zonations.

**General description:** Almost completely dolomitized. White card again shows no precursor fabric. Blocky calcite fills all pore types. There is about 5% bitumen that fills pore spaces. Some of these pores lined with bitumen have no void filling dolomite.

**Paragenesis:** deposition, dissolution, pervasive dolomitization, dissolution (vugs), blocky calcite, bitumen, void lining.

---

**TS #:** 8-2-8-1

**Name:** dolostone

**Dolomite:** pervasive – 75-80%, 40-100 $\mu$ m, eu-sub

void filling – 15-20%, 100-140 $\mu$ m, eu, lining pores

**Porosity:** vuggy – 10%, unfilled to partially filled with calcite

intercrystalline – 45%, filled with bitumen or unfilled

**Calcite:** blocky – 5-10%, fills pores

**Fluorescence:** dull fluorescence of dolomite with slight zonations.

**General description:** Almost completely dolomitized with unimodal distribution. White card again shows no precursor fabric. Blocky calcite fills all pore types. There is some bitumen that fills pore spaces. Void filling dolomite replaces blocky calcite.

**Paragenesis:** deposition, pervasive dolomitization, dissolution (vugs), blocky calcite, bitumen, void lining.

---

**TS #:** 8-2-8-2

**Name:** dolostone

**Dolomite:** pervasive – 90%, 40-200 $\mu$ m, eu-sub

void filling – 10%, 120 $\mu$ m, eu, lining pores

**Porosity:** vuggy – <5%, unfilled to partially filled with calcite

intercrystalline – 15-20%, filled with calcite or unfilled (mostly this)

**Calcite:** blocky – fills pores, inclusion rich

**Fluorescence:** dull fluorescence of dolomite with slight zonations.

**General description:** Almost completely dolomitized with unimodal distribution. White card again shows inclusion rich cores and relatively clear rims in dolomite and may see a ghost fossil. Blocky calcite fills all pore types. There is some bitumen that fills pore spaces. Void filling dolomite replaces blocky calcite.

**Paragenesis:** deposition, pervasive dolomitization, dissolution (vugs), blocky calcite, bitumen, void lining.

---

**TS #:** 8-2-9-1

**Name:** crinoidal grainstone

**Dolomite:** none

**Porosity:** none

**Calcite:** Syntaxial – on crinoids

sparry – fills spaces later

micrite – throughout

**Fluorescence:** slight fluorescence of micritic stuff

**General description:** Several crinoid fragments and spines with syntaxial overgrowths. These are micritized partially and twinned. This cement is early due to affects of chemical compaction (sutured contacts between syntaxials). Some microstylolites throughout that crosscut fossils and syntaxial cement. Spar is scattered throughout, post syntaxial. There is a major diagenetic overprint. Allochems include crinoids, brachiopods, forams. All cements are highly fractured and inclusion rich. Silica or anhydrite replacing centers of crinoids.

**Paragenesis:** deposition, syntaxial cement, micritization, neomorphism to sparry calcite, mechanical compaction (twinning), chemical compaction (sutured contacts), microstylolites, scattered evaporates.

---

**TS #:** 8-2-10-2

**Name:** dolostone

**Dolomite:** pervasive – 65-70%, 140-220 $\mu$ m, eu-sub

void filling/saddle – 5-10%, 200-220 $\mu$ m, curved and sweeping extinction

dsa – 1-2%, <40 $\mu$ m, sub, seam associated

**Porosity:** vuggy – 5%, unfilled to partially filled with calcite  
intercrystalline – 20%, filled with calcite or unfilled (mostly this)

**Calcite:** blocky – 20-25%, fills pores, inclusion rich, twinned

**Fluorescence:** dull fluorescence of dolomite with brighter cores and duller rims.

**General description:** Almost completely dolomitized with pervasive dolomite having cloudy cores and clear rims. Possible recrystallization due to coarse crystal size. Evidence of dedolomitization of saddle dolomite. White card again shows nothing. Blocky calcite fills all pore types. There is some bitumen that fills pore spaces. It occurs before calcite and saddle dolomite. Void filling dolomite replaces blocky calcite. Dolomite is etched. The stylolite is crosscut by pervasive dolomite.

**Paragenesis:** deposition, dsa, pervasive dolomitization, dissolution (vugs), bitumen, blocky calcite, void lining.

---

**TS #:** 8-2-10-3

**Name:** dolostone

**Dolomite:** pervasive – 90-95%, 120-160 $\mu$ m, eu-sub

void filling – 2%, 140-200 $\mu$ m, dedolomitized

**Porosity:** vuggy – 1-2%, unfilled to partially filled with calcite and bitumen

intercrystalline – 20%

**Calcite:** blocky – 20-25%, fills pores, inclusion rich, twinned

**Fluorescence:** dull fluorescence of dolomite with brighter cores and duller rims.

**General description:** Almost completely dolomitized with pervasive dolomite having cloudy cores and clear rims. White card again shows nothing. Blocky calcite fills all pore types. There is some bitumen that fills pore spaces. It occurs before calcite. Much of the pervasive dolomite has sweeping extinction.

**Paragenesis:** deposition, pervasive dolomitization, dissolution (vugs), bitumen, blocky calcite, void lining, dedolomitization(?).

---

**TS #:** 8-2-11-1

**Name:** dolostone

**Dolomite:** pervasive – 98%, 40-80 $\mu$ m, eu-an

void filling – 1-2%, 100-200 $\mu$ m, eu

**Porosity:** vuggy – <1-2%, filled with calcite

intercrystalline – 5-8%

**Calcite:** blocky – 20-25%, fills pores, inclusion rich, twinned

**Fluorescence:** Zoning in void filling dolomite with duller rims and brighter cores.

**General description:** Almost completely dolomitized with pervasive dolomite having cloudy cores and rims. Void filling dolomite has cloudy cores and clear rims. White card again shows possible ghost fossils. Blocky calcite fills all pore types. There is some bitumen that fills pore

spaces. It occurs before calcite. Some horizontal microfractures that are post pervasive dolomite and void filling dolomite. Some bitumen in intercrystalline pores.

**Paragenesis:** deposition, pervasive dolomitization, dissolution (vugs), bitumen, blocky calcite, void lining.

---

**TS #:** 8-2-11-2

**Name:** crinoidal grainstone

**Dolomite:** selective – 15%, 5-25 $\mu$ m, replaces crinoid centers and fine matrix

**Porosity:** none

**Calcite:** Syntaxial – on crinoids

sparry – fills spaces later, neomorphism ?

micrite – throughout

**Fluorescence:** bright hydrocarbons and organic inclusions, micrite rims of crinoids fluoresces

**General description:** Crinoids are the dominant fossil types many with syntaxial cement that is twinned and inclusion rich. Sutured and concave contacts between crinoids are common. There is a major diagenetic overprint. The rock is micritized all over. Some sparry calcite cement replacing finer grained fossils and matrix (neomorphism?). Cements are fractured and inclusion rich. Few fossils are mechanically broken.

**Paragenesis:** deposition, micrite rims, syntaxial cement, micritization, neomorphism to sparry calcite, mechanical compaction (twinning), chemical compaction (sutured contacts), microstylolites, microdolomite.

---

## **Well 9**

**TS #:** 9-9-1-1A

**Name:** dolostone

**Dolomite:** pervasive – 98%, 50-100 $\mu$ m, eu-an

void filling/saddle – sweeping extinction

**Porosity:** intercrystalline – 2-5%, unfilled and filled with anhydrite

**Calcite:** blocky – in very large dolomite grains

**Fluorescence:** Dolomite is more fluorescent than anhydrite. The dolomite is dark green, some have dark green cores and bright rims.

**General description:** Almost completely dolomitized with pervasive dolomite having cloudy cores and clear rims. Large anhydrite nodule or vein made up of lathes and tiny crystals every which way. Dolomite is replacing anhydrite and calcite. Saddle dolomite is replacing large calcite crystals. See some anhydrite inclusions in dolomite.

**Paragenesis:** deposition, blocky calcite, anhydrite, pervasive dolomitization, saddle dolomite.

---

**TS #:** 9-9-1-1B

**Name:** dolostone

**Dolomite:** pervasive – <20 $\mu$ m, sub-an

void filling/saddle – sweeping extinction

**Porosity:** fenestral (?) – filled with anhydrite, chalcedony and calcite

**Calcite:** blocky – in pores

**Fluorescence:** Pervasive dolomite has dark cores and bright rims.

**General description:** Almost completely dolomitized with pervasive dolomite. Dolomite replaces the original calcite fabric which may have been a fenestral mudstone. Saddle dolomite is replacing calcite. Authigenic quartz is filling fenestral pores and replaces calcite and anhydrite. Anhydrite replaces blocky calcite. Pervasive dolomite replaces all previous mentioned cements. Finer dolomite seems to replace finer precursor fabrics. White card studies show that ghost fossils with micrite rims are present with muddy portions between fenestral cements.

**Paragenesis:** deposition, micritization, fenestral pores, blocky calcite, anhydrite, silicification, pervasive dolomitization, saddle dolomite.

---



**TS #:** 9-9-3-1

**Name:** dolostone

**Dolomite:** pervasive – 70-75%, 80-140 $\mu$ m, sub-eu

void filling/saddle – 2%, 600 $\mu$ m – 1mm, sweeping extinction

**Porosity:** intercrystalline – 25%, anhydrite and calcite filled

**Calcite:** blocky – in pores

**Fluorescence:** Pervasive dolomite has dull fluorescence and saddle dolomite is slightly brighter.

**General description:** Almost completely dolomitized with pervasive dolomite. Microstylolites are pre-dolomite. Anhydrite nodules are replaced by saddle dolomite and anhydrite is also found in intercrystalline pores. Anhydrite is replacing the calcite cement. White card shows definite textures but not distinguishable and dolomite has cloudy cores and clear rims.

**Paragenesis:** deposition, blocky calcite, anhydrite, silicification (<1%), chemical compaction, pervasive dolomitization, saddle dolomite.

---

**TS #:** 9-9-4-1

**Name:** dolostone

**Dolomite:** pervasive – 85-90%, 60-200 $\mu$ m, sub-an

void filling – 5%, 240 $\mu$ m, eu, replacing anhydrite

**Porosity:** intercrystalline – 5-10%, unfilled

**Calcite:** none

**Fluorescence:** Pervasive dolomite has dull cores and brighter yellow rims. Void filling is even brighter and better zoned.

**General description:** Almost completely dolomitized with pervasive dolomite. The anhydrite layer is made up of fine crystals intermixed with large lathes, the contact with dolomite is sharp in some areas with dissolution seams and others gradual showing dolomite replacing the anhydrite (10-15%). There is less than 1% quartz. There are several fine seams of anhydrite throughout the dolomite that may have been calcite before. Dissolution seams occur after dolomite. White card shows nothing.

**Paragenesis:** deposition, anhydrite, silicification (<1%), pervasive dolomitization, chemical compaction, void filling dolomite.

---

**TS #:** 9-9-5-1

**Name:** dolostone

**Dolomite:** pervasive – 95%, 20-50 $\mu$ m, sub-eu

void filling – 5%, 50-60 $\mu$ m, eu

**Porosity:** intercrystalline – 20-25%, unfilled

**Calcite:** none

**Fluorescence:** Pervasive dolomite has dull fluorescence.

**General description:** Almost completely dolomitized with pervasive dolomite. This dolomite is finer than the previous. White card shows nothing.

**Paragenesis:** deposition, pervasive dolomitization, void filling dolomite.

---

**TS #:** 9-9-6-1

**Name:** dolostone

**Dolomite:** pervasive – 85-90%, 60-120 $\mu$ m, eu-an

**Porosity:** intercrystalline – 15-20%, unfilled, 5-10% are calcite filled

vuggy – 2-3%, empty

**Calcite:** sparry or fibrous – strained, as layers, fractured and inclusion rich

**Fluorescence:** Pervasive dolomite has dull fluorescence with slightly brighter cores.

**General description:** Almost completely dolomitized with pervasive dolomite. White card shows nothing. There are 2 generations of chemical compaction, the first is dissolution seams the second crosscuts the first and is made up of stylolites. Horizontal fractures are crosscut by stylolites and is partially healed in areas by pervasive dolomite. Original fabric may have been neomorphosed because pervasive dolomite is replacing highly strained fibrous to sparry calcite. The dolomite is pre-chemical compaction (both). Calcite layers are being replaced by dolomite.

**Paragenesis:** deposition, calcite, mechanical compaction (calcite strain), pervasive dolomitization, early and late chemical compaction.

---

**TS #:** 9-9-7-1

**Name:** dolostone

**Dolomite:** pervasive – 85-90%, 20-70 $\mu$ m, eu-an

**Porosity:** intercrystalline – 20%, unfilled and 5% calcite filled

vuggy – 1-2%, empty

**Calcite:** blocky – in pores and nodules

**Fluorescence:** Pervasive dolomite has dull fluorescence with slightly brighter rims. Can see dissolved edges better.

**General description:** Almost completely dolomitized with pervasive dolomite. This one is finer than the previous. White card shows nothing. Dolomite replaces a calcite nodule and has etched edges. The blocky calcite nodule is twinned, fractured and has several inclusions. There are patches of dolomite replacing it. There is detritus and organics filling empty pores in the calcite nodule. Calcite is being replaced by tiny anhydrite crystals (1-2%). Calcite cement is also in intercrystalline pores.

**Paragenesis:** deposition, blocky calcite, anhydrite, mechanical compaction (calcite strain), pervasive dolomitization, dissolution.

---

**TS #:** 9-9-8-1

**Name:** dolostone

**Dolomite:** pervasive – 100%, 40-100 $\mu$ m, eu-an

**Porosity:** intercrystalline – 2-5%, unfilled

vuggy – 10-15%, empty

**Calcite:** blocky – <1% in a vug

**Fluorescence:** Pervasive anhedral dolomite has dull fluorescence with slightly brighter cores.

**General description:** Completely dolomitized with pervasive dolomite. White card shows cloudy cores and clear rims. Few horizontal fractures partially healed by dolomite.

**Paragenesis:** deposition, fracturing, pervasive dolomitization, dissolution.

---

**TS #:** 9-9-9-1

**Name:** bioclastic wackestone

**Dolomite:** scattered – 15-20%, 20-100 $\mu$ m, eu-an

**Porosity:** none

**Calcite:** fibrous – associated with stylolite

sparry – filled calcispheres

micrite - throughout

**Fluorescence:** Pervasive dolomite has dull fluorescence with slightly brighter cores.

**General description:** A large stylolite crosscuts dolomite and it is high amplitude on a cm scale. It is associated with a fibrous calcite. It also crosscuts dissolution seams. Many fossils have sutured contacts. The dolomite occurs before the dissolution seam and stylolite. Most of the dolomite is etched and dedolomitized. There is <1% anhydrite replacing the fibrous calcite. Fossils include brachiopods, ostracods, few crinoids and many fossil fragments. The matrix is micritic and there are many broken fossils and fossil which are aligned. Fibrous calcite is twinned and strained and is associated with the stylolite. Hairline horizontal fracturing is pre-stylolite and post dolomite. White card shows larger peloidal type clasts and circular (calcispheres?) fossils all over which are filled with sparry calcite.

**Paragenesis:** deposition, sparry calcite fills fossils, mechanical compaction, scattered dolomite, early (dissolution seams) and late (stylolite) chemical compaction, anhydrite.

---

**TS #:** 9-9-9-2

**Name:** dolostone

**Dolomite:** pervasive – 95%, 30-60 $\mu$ m, eu-an

void filling – 2%, 130-230 $\mu$ m, eu, zoned with clear, then cloudy than clear rim.

**Porosity:** intercrystalline – 5-10%, unfilled  
vuggy – filled with calcite, anhydrite and dolomite

**Calcite:** blocky – 1-2% in vugs

**Fluorescence:** Pervasive dolomite has dull fluorescence with slightly brighter rims. Void filling has brighter green cores and duller yellow brown rims.

**General description:** Completely dolomitized with pervasive dolomite. Few fractures are pre-dolomite and calcite. Blocky calcite is replaced by dolomite and anhydrite.

**Paragenesis:** deposition, fracturing, pervasive dolomitization, dissolution, blocky calcite, anhydrite and void filling dolomite.

---

**TS #:** 9-9-10-1

**Name:** dolostone

**Dolomite:** pervasive – 75-80%, 60-360 $\mu$ m, eu-sub

**Porosity:** intercrystalline – 2%

vuggy – 2-3%, unfilled

**Calcite:** blocky – 20-25% in pores

**Fluorescence:** very dull

**General description:** Completely dolomitized with pervasive dolomite. Dolomite has cloudy cores and clear rims. Blocky calcite is replaced by dolomite and anhydrite. It is fractured and twinned. <1% anhydrite replaces calcite. White card shows nothing. There is a high amplitude stylolite that is post dolomite.

**Paragenesis:** deposition, blocky calcite, anhydrite, pervasive dolomitization, dissolution, chemical compaction.

**APPENDIX III  
GEOCHEMICAL RESULTS**

**Oxygen, carbon and strontium isotopes**

	<b>Sample</b>	<b>Phase</b>	<b>Depth (meters)</b>	$\delta^{18}\text{O}$ (‰) (VPDB)	$\delta^{13}\text{C}$ (‰) (VPDB)	$^{87}\text{Sr}/^{86}\text{Sr}$
<b>Well 1</b>	1-2-3-1-a	PD	2080.35	-4.79	2.67	
	1-2-3-1-b	SCD	2080.35	-5.07	2.17	0.708795
	1-2-3-1-c	BC	2080.35	-7.29	-0.02	
	1-2-5-1-a	PD	2081.65	-4.41	3.17	
	1-2-5-2-a	PD	2081.75	-5.01	2.95	
	1-3-6-1-a	PD	2083	-5.84	2.71	
	1-3-6-2-a	PD	2083.5	-4.76	2.88	
	1-3-11-1-a	PD	2085.8	-2.34	3.46	
	1-3-13-1-a	VFD	2088.4	-1.53	2.63	
	1-3-13-1-b	PD	2088.4	0.43	3.09	0.708574
	1-3-14-1-a	PD	2089.5	1.09	3.32	
	1-3-14-1-b	PD	2089.5	0.43	3.23	
	<b>Well 2</b>	2-2-3-1-a	BC	2046.58	-10.40	9.36
2-2-3-1-b		MC	2046.58	-6.48	2.15	
2-2-4-1-a		BC	2046.76	-14.76	-9.24	
2-2-4-1-c		MC	2046.76	-9.23	1.46	
2-2-5-1-a		BC	2048.87	-10.90	3.64	
2-2-5-1-b		DMC	2048.87	-5.56	1.29	
2-2-5-1-c		MC	2048.87	-9.79	1.33	
2-2-5-2-a		BC	2050	-10.77	8.37	0.708789
2-2-5-2-b		MC	2050	-10.02	1.62	
2-2-5-2-c		NSC	2050	-11.30	5.41	
2-2-6-1-a		BC	2050.08	-13.45	-3.56	
2-2-6-1-b		MC	2050.08	-7.97	1.94	
2-2-6-1-c		brachs	2050.08	-11.33	-2.08	
2-2-7-1-a		NSC	2050.62	-13.22	1.07	
2-2-7-1-b		BC	2050.62	-10.50	9.36	
2-2-7-1-c		BC	2050.62	-13.92	-2.37	
2-2-9-1-a		MC	2051.46	-13.21	0.96	
2-2-9-1-b		NSC	2051.46	-13.14	0.75	
2-2-10-1-a		NSC	2053	-13.09	1.86	
2-2-12-1-a		PD	2054.89	-8.66	0.49	0.709646
2-2-12-1-a		NSC	2054.89	-8.60	0.90	
2-2-14-1-a	NSC	2056	-9.25	1.19		
<b>Well 3</b>	3-1-1-1-a	BC	4752	-4.79	-4.32	
	3-1-1-1-b	MC	4752	-4.47	1.16	
	3-1-1-1-c	CRC	4752	-5.17	0.99	
	3-1-2-1-a	PD	4753.59	-3.91	3.69	0.708738
	3-1-2-1-b	FC	4753.59	-5.06	-0.62	0.708481
	3-1-2-2-a	DSAD	4754.88	-3.97	3.15	
	3-1-2-2-a	CRC	4754.88	-4.00	2.33	
	3-1-2-2-b	BC	4754.88	-4.82	0.80	

	Sample	Phase	Depth (meters)	$\delta^{18}\text{O}$ (‰) (VPDB)	$\delta^{13}\text{C}$ (‰) (VPDB)	$^{87}\text{Sr}/^{86}\text{Sr}$
	3-1-2-2-b	VFD	4754.88	-6.26	1.67	
	3-1-2-2-c	PD	4754.88	-5.47	2.66	
	3-1-7-1-a	CRC	4768.75	-3.93	2.49	
	3-2-8-1-a	FC	4770.65	-4.46	2.12	
	3-2-8-1-b	CRC	4770.65	-3.97	2.36	
	3-2-9-1-a	VFD	4776.5	-3.78	2.99	0.708613
	3-2-9-1-b	VFD	4776.5	-5.09	2.43	
	3-2-9-1-b	BC	4776.5	-4.32	1.93	
	3-2-9-1-c	PD	4776.5	-3.44	3.06	
	3-2-10-1-a	CRC	4783.9	-5.12	2.53	
<b>Well 4</b>	4-19-2-1-a	PD	3569.38	-3.89	3.36	
	4-19-2-1-c	MC	3569.38	-5.15	2.15	
	4-19-5-1-a	PD	3569.57	0.50	4.54	
	4-19-5-1-b	BC	3569.57	-6.88	2.29	
	4-19-7-1-a	PD	3570.93	-5.95	4.01	0.708805
	4-19-7-1-b	PD	3570.93	-7.04	3.97	
	4-19-7-1-b	BC	3570.93	-5.61	3.61	
	4-19-7-1-c	NSC	3570.93	-11.12	0.36	
	4-19-7-1-c	SD	3570.93	-12.53	-0.55	
<b>Well 5</b>	5-5-1-1-a	PD	3109.11	-1.17	1.32	
	5-5-1-1-b	NSC	3109.11	-11.20	-1.34	
	5-5-2-1-a	PD	3109.87	-5.06	2.54	0.709589
	5-5-3-1-a	PD	3110.94	-1.92	3.20	
	5-5-3-1-a	MC	3110.94	-1.79	3.07	
	5-5-3-1-b	BC	3110.94	-5.71	0.46	
	5-5-3-1-b	SCD	3110.94	-5.12	0.92	0.709499
	5-5-3-1-c	BC	3110.94	-10.65	-0.83	
	5-5-3-2-a	PD	3111.4	-3.22	2.72	
	5-5-3-2-b	PD	3111.4	-1.06	3.00	
	5-6-4-1-a	PD	3111.6	-4.34	2.51	
	5-6-4-1-a	BC	3111.6	-5.68	1.36	
	5-6-4-1-b	SCD	3111.6	-6.32	0.05	0.709185
	5-6-4-1-b	BC	3111.6	-7.36	-0.23	
	5-6-4-1-c	BC	3111.6	-15.90	0.16	
	5-6-5-1-a	PD	3111.83	-0.80	1.76	
	5-6-5-1-a	NSC	3111.83	-10.02	-1.34	
	5-6-6-1-a	NSC	3113.08	-10.41	-1.10	
	5-6-6-2-a	PD	3113.23	-10.08	2.59	
	5-6-6-2-a	MC	3113.23	-8.33	1.88	
	5-6-6-2-b	BC	3113.23	-14.24	-0.11	
	5-6-7-1-a	CRC	3117.65	-9.97	2.11	
	5-6-7-1-b	NSC	3117.65	-10.67	0.12	
	5-6-7-1-b	SCD	3117.65	-9.73	1.15	
	5-6-8-1-a	NSC	3118.69	-8.13	1.01	
	5-6-9-1-a	CRC	3123.9	-9.23	1.71	
	5-6-9-1-b	BC	3123.9	-10.62	1.92	

	Sample	Phase	Depth (meters)	$\delta^{18}\text{O}$ (‰) (VPDB)	$\delta^{13}\text{C}$ (‰) (VPDB)	$^{87}\text{Sr}/^{86}\text{Sr}$
<b>Well 6</b>	6-1-1-1-a	PD	2290.35	-3.10	2.89	
	6-1-1-1-a	BC	2290.35	-5.00	-0.40	
	6-1-1-1-b	BC	2290.35	-13.88	-1.58	
	6-1-1-1-c	NSC	2290.35	-10.07	-3.24	0.708941
	6-1-2-1-b	BC	2291.8	-13.74	-0.38	
	6-1-3-1-a	MC	2291.9	-4.89	1.42	
	6-2-8-1-a	BC	2298	-9.77	-0.98	
	6-2-8-1-a	PD	2298	-8.09	1.93	
	6-2-11-1-a	PD	2298.58	-5.07	2.49	
	6-2-11-1-a	BC	2298.58	-4.15	2.04	
	6-2-11-2-a	PD	2299	-5.93	2.18	0.709628
	6-2-11-2-b	BC	2299	-13.54	-1.57	0.709957
	6-2-15-1-a	SCD	2304.7	-8.09	1.92	
	6-2-15-1-a	NSC	2304.7	-12.51	-2.24	
	6-2-15-1-b	BC	2304.7	-15.89	0.30	
	6-3-17-1-a	BC	2304.8	-15.49	0.39	
	6-3-17-1-b	CRC	2304.8	-7.02	0.35	
	6-3-18-1-a	CRC	2305.25	-7.33	0.69	
6-3-19-1-a	CRC	2308	-5.78	1.18		
6-3-19-2-a	CRC	2310.95	-5.96	0.82		
<b>Well 7</b>	7-1-1-1-a	BC	2037.69	-4.08	1.61	
	7-1-1-1-b	PD	2037.69	-4.32	2.67	
	7-1-2-1-a	PD	2041.27	-2.63	2.86	
	7-1-3-1-a	PD	2042.62	-5.35	1.86	
	7-2-4-2-a	VFD	2047.8	-1.99	2.56	
	7-2-4-2-b	PD	2047.8	-0.08	2.87	0.708448
<b>Well 8</b>	8-2-7-2-a	PD	2935.4	-4.03	2.82	
	8-2-7-2-c	BC	2935.41	-16.31	1.51	
	8-2-10-3-a	PD	2939.9	-10.44	2.72	
<b>Well 9</b>	9-9-1-1-Ba	PD	2895.4	-8.82	2.41	
	9-9-1-1-Bd	BC	2895.4	-10.82	1.61	
	9-9-4-1-a	PD	2897.3	-7.72	3.67	
	9-9-5-1-a	PD	2898.2	-1.00	4.45	
	9-9-6-1-a	PD	2898.95	-6.43	4.61	
	9-9-6-1-b	FC	2898.95	-5.46	-8.07	
	9-9-7-1-a	PD	2899.35	-6.09	3.55	
	9-9-7-1-b	BC	2899.35	-4.34	-0.29	
	9-9-9-1-b	BC	2900.6	-4.19	-4.74	

**ICP-OES results for carbonate components**

<b>Sample</b>	<b>Phase</b>	<b>CaCO<sub>3</sub> (mole %)</b>	<b>Mg (ppm)</b>	<b>Fe (ppm)</b>	<b>Mn (ppm)</b>	<b>Sr (ppm)</b>	<b>K (ppm)</b>
1-2-3- 1-a	PD	51.51	84670	920.6	149.2	81.05	634.3
1-2-3- 1-c	BC	90.94	19390	291.1	163.1	343.4	325.9
1-3-11-1-a	PD	56.52	71430	358.1	122.5	108.6	185.8
1-3-13-1-b	PD	50.34	87750	366.3	94.13	77.35	107.7
2-2-5-2-a	BC	99.60	641.6	3.787	86.25	205.0	23.51
2-2-12- 1-a	PD	97.95	3333	153.5	36.44	211.9	144.0
3-1-1-1-a	BC	98.99	1980	20.67	11.34	628.0	< DL
3-1-2-1-a	PD	55.42	66940	39.08	36.67	114.3	61.38
3-1-2-1-b	FC	97.64	4545	40.46	15.23	490.1	< DL
3-1-2-2-d	FC	89.87	21320	< DL	16.08	430.1	< DL
3-2-8-1-a	FC	97.87	4230	54.75	13.71	512.6	163.8
3-2-9-1-c	PD	58.16	49520	139.3	35.02	126.6	261.9
4-19-5-1-b	BC	98.43	2959	14.42	36.62	1382	78.73
4-19-7-1-a	PD	58.45	44900	72.77	51.90	159.5	99.99
5-5-2-1-a	PD	61.47	42210	301.4	147.3	775.4	90.73
5-6-9-1-b	BC	99.33	1370	24.50	29.39	256.0	< DL
6-2-11-2-a	PD	53.38	50360	112.3	55.78	78.72	45.07
6-2-11-2-b	BC	98.60	2150	< DL	18.01	202.2	< DL
7-1-1-1-b	PD	55.45	56350	661.5	174.7	144.6	281.0
7-1-2-1-b	BC	97.60	4602	21.57	90.56	756.8	< DL
7-2-4-2-b	PD	51.70	62850	171.1	60.12	58.78	87.30
8-2-7- 2-a	PD	56.23	54840	376.4	36.61	129.4	248.8
8-2-7- 2-c	BC	97.45	4699	87.25	26.96	414.8	< DL
8-2-10- 3-a	PD	57.06	32360	327.6	21.68	100.8	43.90
9-9-6- 1-a	PD	56.27	65380	460.0	63.25	96.78	75.51
9-9-6-1-b	FC	97.77	3961	45.45	24.56	549.8	< DL
9-9-7-1-a	PD	65.70	42490	272.0	38.14	198.0	92.67
9-9-7-1-b	BC	98.22	2341	13.17	22.15	326.3	< DL

## VITA AUCTORIS

NAME: JoAnn Marie Lise Adam

PLACE OF BIRTH: Windsor, Ontario, Canada

YEAR OF BIRTH: 1975

EDUCATION: Ecole Secondaire L'Essor, Windsor, Ontario  
1989-1994

University of Windsor, Windsor, Ontario  
1996-2001 Honours B. Sc. (Geology)

University of Windsor, Windsor, Ontario  
2003-2005 M. Sc. (Geology)